# POLITECNICO DI TORINO

## Masters Degree - Automotive Engineering

## 2025-2026



## Master's Degree Thesis

**Numerical Calibration of FEM Methodologies for Predicting the Structural Strength of Weld Lines**

**Supervisors-**

Prof. Fabio Massolo

Marco Puccio – Tecnocad Group

Davide Vianzino – Tecnocad Group

**Candidate**–

Mohammad Kafeel Khan

S308308

# Table of Contents

# List of Figures

# List of Tables

# Acknowledgement

Writing this thesis was demanding but deeply rewarding. I want to thank people who helped me finish it.

First, I want to thank my supervisor, **Professor Fabio Massolo**. He guided me during the whole thesis duration and helped me understand the complex theory. This was key to finishing my research. I also want to thank my mentors from Tecnocad **Group**, **Mr. Marco Puccio** and **Mr. Davide Vianzino**. Working with them was a chance to see how theory works in real-life industry. They gave me advice checked my modelling and simulation setups and provided technical support. This was crucial to my project's success.

I also want to thank **Politecnico di Torino - Lab support** and **Tecnocad Group**. They provided the computers, software and lab data I needed for my analysis. I want to specially mention to a big thanks to the Torino **Stellantis** facility for helping me out in carrying the Physical Testing at their facility.

On a personal level I want to thank my father. Dr. Khalil Khan, my mother Anis Fatima and my brother Nabeel for their unconditional love, support and believing in my abilities. My family's patience, understanding and belief, in me gave me the foundation I needed to succeed.

Finally, I want to thank my friends and university colleagues. We troubleshooted software errors together. Celebrated passing tough milestones. You made the stressful times manageable.

Thank you all for your support.

Sincerely Yours

Mohammad Kafeel Khan

# Abstract

In modern mechanical design, ensuring the strength of welded joints is one of the most difficult challenges. Whether in the automotive industry, the railway sector, or general heavy machinery, the traditional way to check a weld is through physical laboratory testing. However, physical tests are very expensive, slow, and require building many prototypes. While engineers use computer simulations to save time, the most accurate 3D solid models are too slow for large structures like train carriages or vehicle frames. On the other hand, the faster shell models often give incorrect results if they are not analyzed properly. The aim of this study is to create a reliable numerical methodology that allows engineers to use these fast shell models to accurately predict weld breakage and structural failure. By doing this, we can significantly reduce the number of physical tests needed and move toward a design process driven by highly accurate simulations.

This research focused on a detailed comparison between high-fidelity 3D solid elements that is numerical truth and simplified 2D shell elements. The work began with a mesh convergence study to find a balance between calculation speed and result accuracy. One of the most important parts of this study was investigating how the plates are connected in the software. We then compare models in which nodes are joined of the shell plates, to ones in which they are not. After testing, they found that joining the plates at the nodes could withstand bending and axial pull loads. This makes it impossible to predict how much stress they can take before they break. The problem, the engineers who developed the new simulation say, is that other simulations have lost their grip on reality.

We tested plate thicknesses ranging from 2 mm to 4 mm for the axial pull off case and for the bending case to find the correlation and see which performs better. For thicker weld plates, the stress values are less. The shell models slightly overpredict the stress, so they look conservative. However, when considering the PEEQ that is the equivalent strain, the shell models are too optimistic and overpredict the actual failure behavior of the material. This is because 2D shells cannot detect the 3D squeezing effect that occurs in a real weld corner. To correct this, a special factor of Plasticity was created. This factor is a multiplier that engineers can apply to simple models to get the same fracture prediction accuracy as a complex 3D model.

The main benefit of this study is the creation of a Calibration Toolkit for structural engineers. Instead of guessing or over-designing parts, we now have specific correction factors for different loading conditions. The study determined the specific load targets for lab testing, identifying both the force at which permanent damage first occurred and the higher force at which complete fracture occurred. Finally, this approach allows rail and mechanical suppliers to lower physical testing costs and develop safer structures in less time. This work provides a validated standard toolkit and a roadmap, so it is not needed to be making these expensive prototypes continuously to show that the weld line is going to be strong enough in the event of extreme stress, but still feasible to implement.

# Nomenclature

## List of Symbols

| Symbol | Definition | Unit |
|---|---|---|
| σ | Normal stress at a point in the material | MPa |
| KI | ModeI stress intensity factor describing crack-opening stress field | MPa√m |
| r | Radial distance from the notch root or weld toe | mm |
| t | Plate thickness | mm |
| l | Weld leg length | mm |
| a | Weld throat thickness | mm |
| Ke | Equivalence Factor — corrects the elastic stiffness of the shell model to match the solid model | — |
| Kp | Plasticity Correction Factor — corrects the equivalent plastic strain output of the shell model to match the solid model fracture prediction | — |
| Keq | Combined formulation equivalence factor used to compare solid and shell hotspot stress results | — |
| PEEQ | Equivalent Plastic Strain — a scalar measure of accumulated permanent deformation at a material point | mm/mm |

## List of Abbreviations

| Abbreviation | Full Term |
|---|---|
| FEM | Finite Element Method |
| DOF | Degrees of Freedom |
| HAZ | Heat Affected Zone |
| LCF | Low-Cycle Fatigue |
| IIW | International Institute of Welding |
| SHSS | Structural Hot-Spot Stress |
| PSOLID | Three-dimensional volumetric solid finite element formulation |
| PSHELL | Two-dimensional mid-surface shell finite element formulation |
| S4R | Four-node shell element with reduced integration used in Abaqus |
| C3D8R | Eight-node linear brick solid element with reduced integration used in Abaqus |
| S-N | Stress versus Number of Cycles — used for fatigue life assessment |
| E-N | Strain versus Number of Cycles — used for low-cycle fatigue assessment |

All symbols and abbreviations listed above are defined at their first point of use within the body of this thesis. Where a symbol carries more than one meaning in different sections, the relevant context is stated explicitly. Unit conventions follow the International System of Units (SI) throughout, with force expressed in Newtons (N), stress in megapascals (MPa), and length in millimeters (mm) unless otherwise stated.

# 1. Introduction

## 1.1 Background: The Role of Welded Joints in Industrial Structures

Welding serves as the foundational method for permanent assembly in nearly all heavy industries, including the railway, automotive, and general mechanical design sectors. The structural integrity of these sectors depends on the ability of a weld to transfer complex loads—such as axial traction and transverse bending—without premature failure. ((Stephens et al., 2000)

In the past people who built things used an approach to make sure structures were safe. They would use thick steel plates and big welds to make sure everything was strong. Now people want to be kind to the environment and save money so they have to build things in a way. The transportation industry has to make things that're light and work really well. Because people cannot just add metal to make something strong, we need to know exactly how strong the welds are. We have to make sure that making a vehicle light does not make it unsafe for people.

If we look at accidents that happened in the past we can see why understanding welds is so important. Let us look at the frame of a high-speed train as an example. The frame is a thing made of steel that is welded together. It has to withstand a lot of vibration over thirty years. If one of the welds fails it can cause an accident where the train comes off the tracks. The car industry has the problem. A car frame has to be able to handle roads and also be able to absorb a lot of energy if the car crashes. In both cases the strength of the vehicle depends on how strong the welds are. The welds are really important because they have to be strong enough to keep people safe. We need to understand welds like the ones, in a high-speed train or a car to make sure that people are safe when they travel. Historical analysis of structural collapses, such as the famous Liberty Ship failures or various bridge collapses, revealed that fractures almost always initiate at notches or geometric discontinuities. In a T-joint or lap joint, the weld toe acts as a natural notch, concentrating stress in a small area. (Radaj et al., 2006) If the computer models used during the design phase do not accurately predict this stress concentration, the real-world component is likely to fail unexpectedly.


Figure 1Bogie fatigue cracking undetected during preventative maintenance (Source : ASTB Gov)

Today, the industry is moving away from Physical-Heavy design toward "Simulation-First" validation. Building physical prototypes of train carriages or vehicle frames for laboratory testing is incredibly expensive, often costing hundreds of thousands of dollars per test. Furthermore, physical testing can only be done late in the development cycle. Finite element analysis allows engineering teams to evaluate countless virtual prototypes long before any physical manufacturing takes place. Yet, a significant computational hurdle remains in the industry. Highly detailed three-dimensional solid models require massive processing power, making them far too slow to apply to complete vehicle chassis or railway assemblies.

Conversely, two-dimensional mid surface shell models solve incredibly fast but frequently yield inaccurate and overly optimistic results if they are not rigorously calibrated against a physical baseline. This research tackles that exact mathematical discrepancy. It introduces a practical calibration methodology designed to guarantee that simplified, fast computing shell models can accurately predict the ultimate structural fracture of a weld without sacrificing industrial efficiency. (Niemi et al., 2018)

The transition to lightweight structures has also introduced the use of high-strength steels and thinner plate gauges, such as the 2 mm to 4 mm plates investigated in this research. While these materials reduce weight and fuel consumption, they are more sensitive to the "triaxial" stress states found at the weld toe.

As shown in Table 1 the cost of a design error increases significantly as a project moves from the simulation phase to the physical prototype phase. (Hobbacher, 2016) Therefore, increasing the correlation between these two worlds is the most effective way to reduce industrial costs while maximizing passenger and operator safety.

*Table 1; Industrial Impact of Structural Validation Methods (Source - Author)*

| Method | Computational Cost | Accuracy at Weld Toe | Industrial Application |
|---|---|---|---|
| Physical Lab Testing | Extremely High | 100% (Real World) | Final Validation Only |
| 3D Solid FEM (PSOLID) | High | High (Numerical Truth) | Localized Joint Study |
| 2D Shell FEM (PSHELL) | Low | Variable (Needs Tuning) | Full Vehicle Assemblies |

Ultimately, the goal of modern mechanical design is to move toward Zero-Prototype development. This can only be achieved if the FEM methodologies are calibrated to predict the structural strength of the welding line across different load cases, such as the axial and bending scenarios discussed in this study. By refining the structural hot-spot stress prediction, this thesis contributes to a safer and more cost-effective manufacturing future for all heavy transportation and machinery sectors.

## 1.2 Structural Integrity and Fatigue Challenges

In the lifecycle of a vehicle or a rail carriage, the chassis is subjected to millions of varying load cycles—ranging from engine vibrations to the impact of uneven road surfaces. While the base metal plates are designed to handle these loads comfortably, the weld lines act as a different species of material altogether. In structural engineering, weld lines are notorious for being the primary points of failure, often dictating the total lifespan of the entire assembly. (D. Radaj, 2006)

The Triple Threat of Weld Failure There are three main reasons why a weld line is almost always the weakest link. First is the Geometric Discontinuity. A weld is essentially a notch or a sudden change in the cross-section of the metal. In physics, stress is like water flowing through a pipe; when the pipe suddenly changes shape at the weld toe, the pressure spikes. This is known as a stress concentration or Hotspot.

The creation of the heat-affected zone is another crucial component of welded connections. The extreme thermal gradients created when the material is melted by the welding arc significantly change the microscopic grain structure of the steel right next to the fusion line. This particular boundary region is usually much more brittle than the pure parent plate due to this extreme heating and fast cooling cycle. This localized zone finds it difficult to absorb kinetic energy during abrupt impacts or cyclic loading because the material loses its inherent ductility. Additionally, there are significant residual stresses introduced by the manufacturing process. The liquid weld metal naturally starts to contract as it solidifies and cools to room temperature. Nevertheless, this shrinkage is firmly resisted by the surrounding cold steel.

Consequently, the welded assembly is already fighting against heavy mechanical strain before the structure ever experiences its first actual service load. (Maddox, 1991)

Fatigue Crack Propagation The most dangerous aspect of weld failure is that it rarely happens all at once. It is a slow, deceptive process known as fatigue. Engineers often call fatigue the "Silent Killer" because a structure can appear perfectly fine on the outside while a microscopic disaster is unfolding within the grain of the metal.

Fatigue failure follows a three-stage journey:

1. Initiation: Small imperfections, perhaps a tiny pore or a microscopic sharp edge at the weld root, act as a starting point.
2. Propagation: Under repeated loading—even if that load is far below the metal's breaking point—the crack begins to grow. It unzips the metal bit by bit, cycle by cycle. ((Stephens et al., 2000)
3. Catastrophic Failure: Eventually, the remaining healthy metal becomes too thin to support the load, leading to a sudden, violent snap.

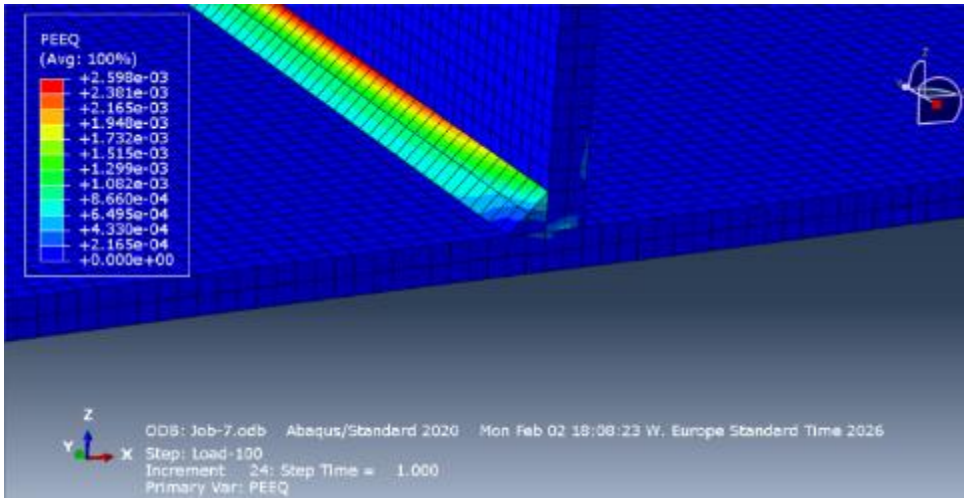


Figure 2 ; Stress concentration at the weld toe showing the potential site for crack initiation (Source - Author)

For an automotive engineer, the challenge is that standard 2D shell simulations often struggle to see these microscopic cracks. This is why numerical calibration, like the plasticity factors and PEEQ analysis performed in this study, is so vital. We are not just looking for a static break; we are trying to predict the invisible transition from a solid joint to a failed structure. Understanding this Silent Killer is the only way to move from over-designed, heavy parts to optimized, lightweight, and safe automotive frames.

## 1.3 The Digital Shift: From Physical Prototyping to Virtual Validation

For many years, the automotive and railway industries followed a very simple but expensive rule: Build it, and then break it. To test if a vehicle frame or a welded joint was strong enough, engineers had to manufacture a full-scale physical prototype and subject it to extreme loads until it failed. While this provided direct evidence of strength, it created a massive bottleneck in the design process. Today, we are seeing a total transformation—a shift from physical-heavy prototyping to virtual-first validation. (Thomke, 2003)

### *The Economic Benefit of Reducing Physical Samples.*

The main reason companies are moving to finite element analysis is to save a lot of money and time. Building a sized physical model of a car chassis or train part costs a lot. This cost is not just for the steel it also includes making tools hiring skilled workers to weld the parts together and paying high fees for testing facilities.

If a part fails a test in the development process it can be very costly. The team has to stop production change the design and build a physical model. This can delay a vehicle launch by several months. By using software to test parts manufacturers can try out many different designs and materials in just a few hours. This approach lets them check if a part will work well before building a model. When they do build a model, they are very confident it will pass the tests because

they have already checked it virtually. They can check thousands of welds and material thicknesses without using any physical resources. This way they can. Fix problems early on which saves time and money. The engineering team can then be sure that the structure will survive the testing it will face. They can make changes. Try again in the virtual world, which is much cheaper and faster than, in the real world.

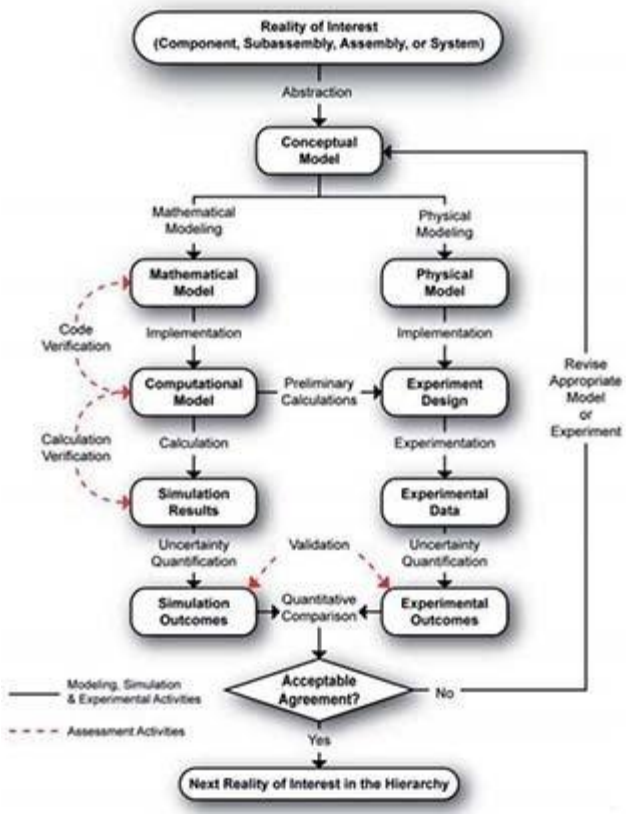


Figure 3 ; The correlation between virtual validation and physical experimentation

## *The Need for Digital Twins in Crash and Durability*

In modern engineering, we don't just use a simple 3D model; we aim for a Digital Twin. A Digital Twin is more than just a picture of the part; it is a mathematical representation that behaves exactly like the real material under stress, heat, and vibration. For crash and durability simulations, the Digital Twin must be incredibly accurate. If a simulation predicts that a car frame is safe, but the real welds snap during a crash, the consequences are life-threatening.

In durability simulations, we are looking at the long-term life of the part. A train carriage, for example, is expected to last 30 years. It is impossible to run a physical test for 30 years, so we use Digital Twins to accelerate time. We can simulate millions of load cycles in a matter of hours. (Grieves, 2014) However, for a Digital Twin to be useful, it must be calibrated.

This is where our study on weld calibration becomes vital. A Digital Twin is only as good as its smallest detail. If the weld model is too stiff or too soft in the simulation, the entire crash or

durability result will be wrong. By using the "numerical truth" from 3D solid models to calibrate faster 2D shell models, we provide the "DNA" that makes a Digital Twin reliable. This calibration bridge allows industries to trust their virtual results enough to replace the majority of their physical testing samples, leading to safer and more efficient structural designs.

## 1.4 Problem Statement: The Accuracy-Efficiency Trade-off

In the modern automotive and railway sectors, the design cycle is under constant pressure to move faster. Engineers are caught in a difficult position: they must ensure absolute safety, but they also have to provide results quickly enough to meet production deadlines. This creates a fundamental problem known as the Accuracy-Efficiency Trade-off. When it comes to simulating weld lines, we basically have two choices, and both of them have serious flaws when used on their own.

### *The Heavy Burden of 3D Solid Models*

On one side, we have 3D Solid models. In our study, we refer to these as the Numerical Truth. Because these models represent the material as a three-dimensional volume, they can capture every detail of a weld the exact shape of the fillet, the thickness of the leg, and how the stress flows through the root of the joint.

However, this precision comes at a massive computational cost. A single 3D element has many more degrees of freedom (DOF) than a 2D element. When you are modeling a small test specimen, this isn't a problem. But if you try to model an entire train carriage or a vehicle chassis using 3D solids, the number of equations the computer has to solve becomes astronomical. Such a simulation could take weeks or even months to complete, even on a powerful supercomputer (Zienkiewicz, 2005). In a fast-paced industrial environment, this is simply not a realistic option. Engineers need to run dozens of what-if scenarios, and 3D solids make that process impossible.

### *The Hidden Dangers of Uncalibrated 2D Shells*

To solve the speed problem, industry standards almost always rely on 2D Shell elements. These models represent the metal plates as thin surfaces with no physical thickness in the mesh. This makes the math much simpler and allows for very fast simulations. An assembly that would take days in 3D can be finished in minutes using shells.

The danger, however, is that 2D shells are blind to the complex 3D physics happening inside a weld. A shell model sees a weld as a simple connection between two planes. It cannot see the squeezing of the metal at the corner or the way the stress is distributed across the thickness of the plate. (Niemi et al., 2018). Our research found that while shells are quite good at predicting general stress, they are very unreliable when it comes to predicting PEEQ (Equivalent Plastic Strain).

Because shells simplify the geometry, they often give optimistic results, under-predicting the actual damage occurring at the weld toe. If an engineer trusts these uncalibrated results, they might

assume a part is safe when it is actually on the verge of cracking. This unreliability means that standard shell models are often too risky to use for predicting final fracture or breakage unless they are modified. (Dong, 2001)

### *Finding the Middle Ground*

This is the core problem our thesis addresses. We cannot afford the time for 3D solids, and we cannot afford the risk of uncalibrated 2D shells. The Research Gap is the lack of a reliable bridge between these two worlds. By using the 3D Numerical Truth to create a specific Plasticity Correction Factor, we aim to give engineers the best of both worlds: the lightning-fast speed of shell models combined with the high-level accuracy of solid models. This calibration ensures that safety isn't sacrificed for the sake of efficiency.

## 1.5 Research Objectives

The primary goal of this research is to bridge the gap between complex 3D simulations and the fast-paced requirements of industrial design. While engineers have used Finite Element Method (FEM) software for decades, there is still a significant lack of confidence when it comes to using simplified models for predicting the actual breaking point of a weld. This study sets out to turn the simulation from a pretty picture into a high-precision tool for safety and durability.

The work is organized around three main objectives that take us from the computer screen to the physical laboratory:

### *Objective 1: Predicting Structural Breakage via FEM*

The first major goal is to move beyond simple stress analysis and enter the world of fracture prediction. In many industrial projects, an engineer might see a red zone in a simulation and assume the part is failing, but they don't actually know when it will snap. By using Equivalent Plastic Strain (PEEQ) as our main metric, this research aims to identify the exact tipping point where a weld transitions from "bending" (deformation) to breaking (fracture). By simulating both the 2mm axial pull-off and the 3mm bending cases, we want to establish a numerical threshold that tells an engineer: At this exact PEEQ value, the physical weld will fail. This allows for a much more aggressive and optimized design process. (Bohlmann, 2002)

### *Objective 2: Developing Equivalence (Ke) and Plasticity (Kp) Factors*

The most technical objective of this thesis is the creation of a Calibration Toolkit. We know that 3D Solid models are the Numerical Truth but are too slow for large assemblies, while 2D Shells are fast but often inaccurate. To solve this, this study aims to calculate two specific correction factors:

- The Equivalence Factor (Ke): This factor is designed to correct the elastic stiffness. It ensures that the Joined shell nodes behave with the same linear strength as a real 3D fillet weld.
- The Plasticity Factor (Kp): This is the more critical factor. Since shells are often optimistic and under-predict damage, Kp acts as a multiplier. It allows an engineer to take a fast shell result and correct it to match the high-accuracy breakage prediction of a solid model. (Fricke, 2003) Developing these factors for different leg lengths (3mm and 4mm) ensures that the calibration is robust enough to be used in real automotive and railway projects.

### *Objective 3: Increasing the Correlation Between Simulation and Lab Testing*

A simulation is only useful if it matches the real world. Therefore, the third objective is to increase the correlation or the closeness between our Abaqus results and the physical tests performed in the laboratory. This involves setting the exact boundary conditions such as the 10mm pusher diameter and the 2000N load targets to ensure that the physical test is a Digital Twin of the computer model. By achieving high correlation, we prove that our numerical calibration is valid. The final result of this objective is to reduce the Safety Margin that engineers usually add to parts, allowing for lighter, cheaper, and more sustainable structures without sacrificing safety. (Hobbacher, 2016)

## 1.6 Scope and Industrial Significance

The findings of this research are not limited to a single laboratory experiment; instead, they have a direct and practical application across several major engineering sectors. In industries such as railway, automotive, and general mechanical design, the ability to accurately predict when a weld will fail is the difference between a successful product and a catastrophic structural collapse. By developing a calibrated shortcut using shell elements, this study provides a tool that can be integrated into the standard workflow of engineers worldwide.

### *Widespread Application Across Industrial Sectors*

1. The Railway Sector In the railway industry, structures like train carriages and bogies are massive and extremely complex. These components are made of thousands of meters of weld lines that must endure decades of constant vibration and heavy loads. Because of the sheer size of a train, it is mathematically impossible to model every weld using 3D solid elements. Historically, this led to over-engineering, where parts were made much thicker and heavier than necessary just to stay safe.

Our study on Equivalence (Ke) and Plasticity (Kp) factors allows railway engineers to use fast 2D shell models while maintaining the safety margins of a 3D simulation. This is critical for meeting international standards like Eurocode 3, which governs the fatigue life of steel structures. By using our calibration toolkit, railway manufacturers can design lighter rolling stock that consumes less energy without compromising the 30-year lifespan of the vehicle.

2. The Automotive Sector In the automotive world, the pressure is on crashworthiness and weight reduction. Modern cars use thin-gauge steel plates, often around 2mm to 4mm thick, which is exactly what we analyzed in our axial and bending simulations. In a crash event, the welds are the first points to experience extreme plastic strain (PEEQ). If the simulation doesn't correctly predict when these welds snap, the safety ratings of the car will be incorrect.

Automotive engineers need results in hours, not weeks. Our research proves that uncalibrated shell models are often too optimistic about weld breakage. By applying the Plasticity Factor (Kp), designers can identify weak spots in the car's frame during the digital phase. This reduces the need for crashing expensive physical prototypes and ensures that the final vehicle meets strict safety regulations. (Sanz-Gomez J. &., 2014)

3. General Mechanical and Heavy Machinery Beyond transport, this research is significant for the design of heavy industrial machinery, such as cranes, excavators, and agricultural equipment. These machines operate in harsh environments where they face unpredictable abuse loads. By defining the targets for Low-Cycle Fatigue (LCF), we provide a way for mechanical designers to simulate these extreme conditions.

The industrial significance here lies in reliability. A failure in a crane’s welded joint can lead to fatal accidents. By using the high-correlation targets we established such as the 2000N load for damage initiation companies can guarantee the structural integrity of their products before they ever leave the factory. (Hobbacher, 2016)

### *Conclusion of Scope*

The scope of this thesis extends from the microscopic study of plastic strain at a weld toe to the macroscopic simulation of a full vehicle assembly. The goal is to create a universal language for weld simulation. Whether an engineer is designing a high-speed train in Italy or a passenger car in the US, the need for an accurate, fast, and calibrated FEM methodology is universal. This work provides that bridge, turning the Accuracy-Efficiency Trade-off from a problem into a solved engineering standard.

# 2. Theory and Research Review

## 2.1 Mechanics of Welded Joints

The structural performance of a welded assembly is defined by more than just the material properties of the steel plates. It is governed by a complex interaction between the local geometry of the weld bead and the global load paths through the structure. In the context of automotive and railway design, we often deal with fillet welds in a T-joint configuration. These joints are critical because they represent a sudden change in the cross section of the part. This geometric change creates a localized area of high stress, known as a stress concentration or a notch effect. (D. Radaj, 2006)

### 2.1.1 Geometry of T-Joints

The T-joint is a fundamental building block in mechanical engineering. It consists of a vertical member, often called the attachment, joined to a horizontal base plate. The connection is made using fillet welds on one or both sides. In this research, we focused on fillet welds with leg lengths of 2 mm, 3 mm, and 4 mm. The leg length is the most significant geometric parameter because it defines the size of the weld throat, which is the narrowest part of the weld that must carry the entire load.

From a scientific perspective, the geometry of a T-joint creates a triple point where the weld, the vertical plate, and the horizontal plate meet. This is the weld toe. In our finite element models, specifically the 3D solid versions, we observed that the highest stress always occurs exactly at this toe or at the weld root. This is because the sharp corner forces the internal force lines to crowd together, much like traffic squeezing into a narrow lane. This crowding is what we call the notch effect.

To capture this effect accurately in Abaqus, the mesh size is a critical factor. Through our research, we determined that a 1.0 mm mesh size is the ideal threshold. If the mesh is larger than 1.0 mm, the software averages the stress over too large an area, which makes the results look safer than they actually are. A 1.0 mm element is small enough to capture the steep gradient of the stress as it climbs toward the weld toe, but it is not so small that the simulation becomes too slow for industrial use. This mesh density is especially important when we calculate the Equivalent Plastic Strain, or PEEQ. Since PEEQ is a local measure of material damage, an incorrect mesh size would lead to a completely false prediction of when the weld would snap.

The geometry also influences the Heat Affected Zone. Although our simulation focuses on the mechanical geometry, it is important to understand that the physical weld has a region near the bead where the metal has been weakened by heat. By using a 1.0 mm mesh, we ensure that our numerical model has enough resolution to represent the area where these metallurgical changes would occur in a real specimen. This geometric precision is why the 3D solid model is treated as the numerical truth in our study. (Hobbacher, 2016)

### 2.1.2 Load Paths: Difference between Axial Traction and Transverse Bending

The way a load travels through a T-joint determines whether the failure will be sudden or gradual. In this thesis, we analyzed two primary load cases: Axial Traction and Transverse Bending. These two cases represent the extreme conditions a weld line might face in a railway bogie or a car chassis.

Axial Traction, often called the pull-off case, is characterized by a force that is applied parallel to the vertical plate, pulling it away from the base. In this scenario, the entire cross section of the weld is under tension. Our results for the 2 mm axial case showed that the joint is extremely stiff. The load rises very quickly with very little displacement. For example, we reached loads as high as 13500 N. The load path here is direct. The force travels from the vertical plate, through the throat of the weld, and into the base plate. Because the load is spread across the whole throat area, the metal stays in the elastic region for a longer time. However, once it reaches the yield point, the failure happens rapidly across the entire joint. (Niemi et al., 2018)

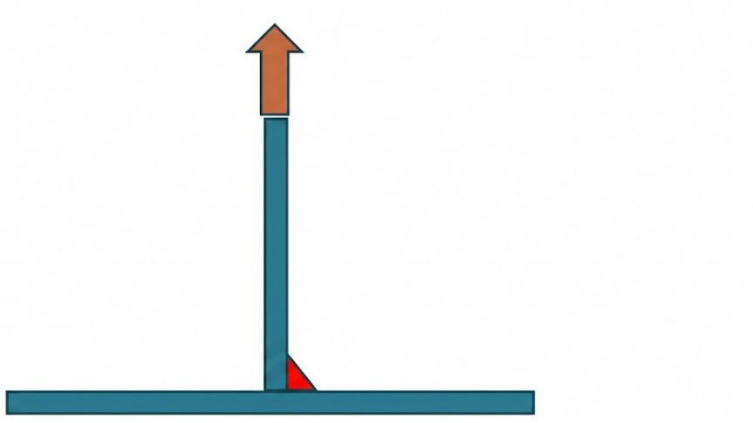

*Figure 4; Axial Pull off , Source; Author*

Transverse Bending is a completely different physical phenomenon. In this case, the force is applied perpendicular to the vertical plate, causing it to act like a lever. This creates a bending moment at the base of the weld. The load path is no longer uniform. One side of the weld bead is squeezed in compression, while the other side is pulled in tension. Our simulation of the 3mm bending case showed a much lower force capacity, around 1500 N to 2000 N, but a much higher displacement of over 20 mm.

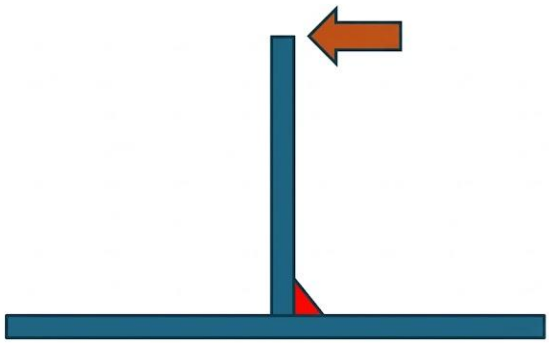

*Figure 5 ; Bending Load , Source- Author*

The bending case is more dangerous for fatigue because it forces the material into the plastic regime at a much lower load. The lever arm effect amplifies the stress at the weld toe significantly. This is why we see the distinctive knee in the force-displacement curve for bending. This knee represents the moment the metal at the weld toe can no longer resist the force elastically and begins to stretch permanently. This is the initiation of PEEQ.

Understanding these two load paths is essential for the calibration of shell models. A 2D shell model represents the plates as thin surfaces, which means it naturally struggles to calculate the complex bending through the thickness of the weld. This is where our Equivalence Factor and Plasticity Factor come into play. The Equivalence Factor corrects the linear stiffness in the axial case, while the Plasticity Factor is used to bridge the gap in the bending case where the shells normally underestimate the damage.

The use of PEEQ thresholds is justified by the fact that stress alone does not tell the whole story of failure. In the bending case, the stress might reach the yield limit very early, but the part does not break yet. It continues to bend and absorb energy. By setting a threshold of 0.2 percent for yield and 2.0 percent for damage, we are following the science of fracture mechanics. These thresholds allow us to identify exactly when the load path has caused enough internal crystal damage to constitute a failure. (Dieter G. E., 1988)

In conclusion, the mechanics of a welded T-joint are a balance of geometry and force direction. The 1.0 mm mesh is our lens to see the stress concentration, and the PEEQ is our ruler to measure the damage. By comparing axial and bending cases, we have created a complete picture of how weld lines behave, providing the necessary data to calibrate simplified models for complex industrial assemblies. (Dong, 2001)

## 2.2 Stress Concentration and the Notch Effect

The study of welded structures is really about looking at stress concentrations in welded structures. In a metal plate that is all one piece the forces inside the metal are spread out evenly. However, when you add a weld to the metal plate this even spread of forces is disrupted. The weld makes a kind of bump or a notch that changes the way forces move through the metal. This notch makes the lines of stress in the welded structures come together in an area as they move from one part of the metal plate into the other part of the metal plate. This coming together of the lines of stress in the welded structures results in high stress points that are much higher, than the average stress you would calculate using simple engineering formulas for welded structures. Understanding how these peaks behave is the first step in predicting whether a structural joint will survive its intended lifespan or fail prematurely. (D. Radaj, 2006).

The notch effect is particularly aggressive at two specific locations: the weld toe and the weld root. The junction of the base metal and the weld face is known as the weld toe. This abrupt change in geometry results in a sharp corner that inherently draws stress. According to our research, these stress concentrations can be shifted by even slight variations in the weld leg length. A 3mm leg length, for instance, offers a different transition angle than a 4mm leg length. The 2mm plates in our study exhibited distinct yielding behavior from the thicker sections because a steeper transition typically results in a higher notch effect.(Maddox, 1991).

### 2.2.1 The Singularity Problem in Finite Element Modeling

Simulating welds in software like Abaqus can be really tough. The thing that makes it hard is something called the singularity. In a physical weld, the fusion process naturally produces a small geometric transition radius at the junction between the weld bead and the base plate surface. This transition, however minor, plays a significant role in distributing the stress away from an infinitely sharp theoretical corner. (Radaj, 2006)

When we make a model of the weld on a computer, we usually show it as two flat surfaces that meet at a perfect point. This makes a corner with no curve at all. The numerical singularity is a problem because the weld does not have a curve like it does in life. The weld, in the model has a point where the two surfaces meet and this sharp point is what causes the numerical singularity.

From a mathematical perspective, stress is known as the force divided by area. As we refine the mesh and make the elements smaller and smaller at a sharp corner, the area of the elements approaches zero. Mathematically, dividing a force by an area that is approaching zero causes the stress to trend toward infinity. This is the singularity problem. If an engineer simply keeps making the mesh smaller, the stress values will never stop rising. They will never converge to a single, stable number.

In our thesis work, this is exactly why we chose a 1.0mm mesh size as our standard. We are not looking for the infinite mathematical stress at a single point. Instead, we are looking for a characteristic stress that represents the physical reality of the joint. By keeping the mesh at 1.0mm, we avoid the trap of the singularity while still being small enough to capture the gradient of the

Equivalent Plastic Strain. This allows us to maintain a stable baseline for our Equivalence and Plasticity factors. If we used a 0.1mm mesh, our results would be artificially high and would not match the physical behavior of the steel during the 2000N lab tests. (Zienkiewicz, 2005).

### 2.2.2 The Structural Hot-Spot Stress Approach and IIW Standards

To solve the problem of singularities and inconsistent mesh results, the International Institute of Welding, known as the IIW, developed the Structural Hot-Spot Stress approach. This methodology is designed to provide a consistent way for engineers to calculate the stress at a weld toe without being affected by the local singularity at the notch.

Rather than extracting stress directly at the weld toe, where singularity effects render the result mesh-dependent, the IIW procedure requires stress evaluation at defined reference distances proportional to the plate thickness. At these locations, the influence of the local notch has sufficiently decayed, and the extracted value represents the true structural stress driving the failure mechanism. (Niemi et al., 2018)

Usually, the engineer looks at points that're 0.4 times the thickness of the plate and 1.0 times the thickness of the plate. Once the engineer has these numbers, they use a math trick to figure out what the stress would be, at the weld toe. This is called the Hot-Spot Stress of the SHSS approach. The Hot-Spot Stress is what the engineer is trying to find with the SHSS approach.

This method is the global standard because it allows different engineers using different software to arrive at the same conclusion. In our research, the SHSS approach provides a bridge for our Equivalence Factor calculations. It allows us to verify that our 2D shell models are providing a realistic "Structural" stress before we move into the more complex calculations of PEEQ and breakage. While SHSS is primarily used for the elastic range and fatigue life, it sets the foundation for our work because it defines where the most damage is likely to occur. (Hobbacher, 2016).

### 2.2.3 Beyond Elastic Limits: The Role of PEEQ in Notch Analysis

While the SHSS approach is excellent for staying within the elastic limits, our thesis must go further to predict actual breakage. In a real world automotive or railway environment, parts often experience loads that push them into the plastic regime. When the material at the notch begins to yield, the stress no longer goes to infinity in reality. Instead, the metal deforms and the stress is redistributed to the surrounding material.

This is where the notch effect transitions from a stress problem to a strain problem. By focusing on Equivalent Plastic Strain, we can see how the notch is actually stretching the metal. Our findings indicate that once the PEEQ reaches approximately 2.0 percent, the material has sustained permanent damage. If the loading continues until the PEEQ hits the 20 to 22 percent range, the notch has effectively "opened up" and turned into a crack.

By combining the theory of the notch effect with the practical application of PEEQ thresholds, we have created a calibration methodology that respects the physics of the joint. We are using the 1.0mm mesh as a fixed observation scale. This allows us to turn the problem of the singularity into

a repeatable numerical experiment. The results from our 3mm bending case show that the highest PEEQ always occurs at the exact location predicted by the notch theory, confirming that our virtual model is correctly aligned with the science of mechanical joints. (Niemi et al., 2018).

## 2.3 Finite Element Formulation Theory

The selection of an appropriate finite element formulation is the most critical decision in structural simulation. When modeling a complex assembly like a welded T-joint, the engineer must choose between representing the part as a full three-dimensional volume or as a simplified two-dimensional surface. This choice determines how the software calculates the internal forces and how it predicts the eventual failure of the weld line. In our research, we compared the high-fidelity volumetric approach with the industry-standard mid-surface approach to identify the numerical gap that exists between them. (Zienkiewicz, 2005).

### 2.3.1 Volumetric Solids C3d8r: Modeling the Gusset Effect

The volumetric approach utilizes the C3D8R element, which is an 8-node linear brick with reduced integration and hourglass control. Each node in this element possesses three degrees of freedom representing translations in the X, Y, and Z directions. The use of reduced integration is a strategic choice to avoid the phenomenon known as shear locking, which often occurs in fully integrated linear elements under bending loads. By using only one integration point at the center of the element, the software remains computationally efficient while providing a realistic stiffness response for the steel plates. (Systemes, 2020).

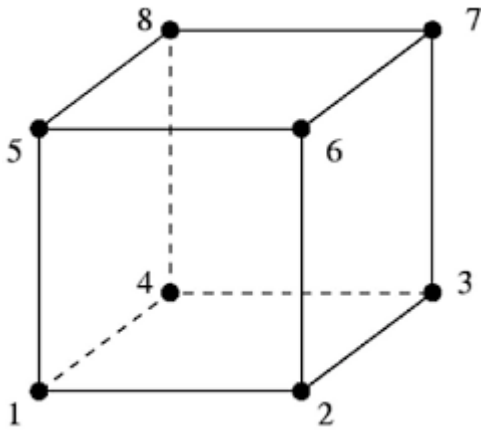


*Figure 6; 8 node elements*

The primary advantage of the C3D8R formulation in this thesis is its ability to model the gusset effect of the weld fillet. In a real T-joint, the fillet weld is a triangular wedge of metal that fills the corner between the two plates. This wedge acts like a structural brace or a gusset. It increases the local moment of inertia and provides a physical path for the stress to travel through the throat of the weld. Our simulation results for the 2mm, 3mm, and 4mm leg lengths clearly demonstrate this

effect. For instance, increasing the weld leg from 2mm to 3mm resulted in a 19.7 percent increase in the load required to initiate yielding. This is because the C3D8R elements physically represent the added volume of the fillet, which shields the weld toe from early elastic deformation. (Niemi et al., 2018).

Without these volumetric elements, the simulation would treat the connection as a sharp intersection of two planes. The C3D8R formulation allows us to capture the true numerical truth of the stress distribution. As the bending load increases toward the 2000N target, the solid elements show how the stress flows from the tension side of the plate, through the fillet gusset, and into the base. This volumetric reinforcement is what makes the solid model the benchmark for our calibration. However, because each brick element has a small volume, a large assembly requires millions of elements, leading to the high computational costs discussed in previous chapters. (D. Radaj, 2006).

### 2.3.2 Mid-Surface Shells S4r: Understanding Plane Stress Assumptions

To achieve the speed required for large-scale industrial projects, engineers rely on the S4R shell element. This is a 4-node, doubly curved, general-purpose shell with reduced integration. Unlike the solid brick, the S4R element represents the plate as a mid-surface with a defined mathematical thickness. Each node possesses six degrees of freedom, including three translations and three rotations. The inclusion of rotational degrees of freedom allows the shell to capture bending moments with far fewer elements than a solid model. (Bohlmann, 2002).

The core theory behind the S4R element is the plane stress assumption. This theory assumes that the stress in the direction of the plate thickness is zero. While this is a very effective shortcut for thin plates, it creates a significant problem at the weld line. In a real weld, there are significant out-of-plane stresses caused by the triaxial constraint of the joint. The shell formulation ignores these complex 3D interactions. Furthermore, a shell model does not include the physical volume of the fillet weld. It represents the weld as a simple nodal connection or a rigid link between the mid-planes of the two plates. (Dong, 2001).

This lack of a physical gusset means that the S4R model is missing the triangular reinforcement that we see in the solid model. In our comparative study, we found that shell models tend to be conservative when calculating stress because they do not have the added stiffness of the fillet. However, they are often too optimistic when calculating Equivalent Plastic Strain or PEEQ. Because the shell assumes plane stress, it cannot see the squeezing effect that happens at the weld toe. This is why our bending simulation reached 20.7 percent PEEQ at 2000N in the solid model, while an uncalibrated shell might show a significantly different value. (Sanz-Gomez J. a., 2014).

The S4R formulation also relies on the integration through the thickness. Abaqus typically uses five integration points across the thickness of the shell to capture the transition from tension to compression during bending. While this is accurate for the plate itself, it does not account for the stress concentration at the weld notch. The shell simply sees a flat plate connected to another flat plate. This fundamental theoretical difference is the reason why we need the Equivalence Factor Ke and the Plasticity Factor Kp. (Maddox, 1991).

### 2.3.3 Integration and Mesh Compatibility

A final important aspect of the finite element formulation is the compatibility between the mesh size and the element type. For both the C3D8R and S4R models, we maintained a 1.0mm mesh size standard. This ensures that the integration points in both models are roughly at the same physical locations relative to the weld toe. In the solid model, the 1.0mm mesh allows for multiple elements through the thickness of the 2mm and 3mm plates, which is necessary to capture the plastic gradient. In the shell model, the 1.0mm mesh provides enough resolution to apply the Structural Hot Spot Stress extrapolation method described by the IIW standards. (Hobbacher, 2016).

By understanding the mechanics of these two formulations, we can see that the gap between them is not an error in the software, but a result of the different mathematical assumptions. The C3D8R brick captures the three-dimensional gusset effect and triaxial stress, while the S4R shell provides a fast, two-dimensional approximation based on plane stress. Our research objective is to use the solid formulation to find the numerical truth and then transfer that knowledge to the shell formulation through calibrated multipliers. This allows the engineer to enjoy the speed of shells without losing the physical accuracy of the volumetric solids.

## 2.4 Fracture and Plasticity Theory

In the study of structural failure, calculating the stress level is only the first part of the problem. For ductile materials like the steel plates analyzed in this thesis, reaching the yield point does not mean the part has failed. Instead, the material enters a state of permanent deformation where it continues to carry load while changing its shape. This is known as plasticity. To accurately predict when a weld line will actually break, we must move beyond the elastic limit and look at the accumulation of plastic work. This chapter focuses on the transition from simple deformation to final fracture, using numerical metrics that can be validated in a physical laboratory. (Dieter G. E., 1988).

### 2.4.1 Equivalent Plastic Strain Peeq as A Failure Criterion

Equivalent Plastic Strain, which is called PEEQ in the Abaqus environment, is a scalar value that tracks the total amount of plastic strain a material has experienced. Unlike the von Mises stress, which can stay the same or even decrease as a part softens during failure, PEEQ is an additive variable. It only grows as the part is pushed further into the plastic regime. This makes it a far more reliable indicator of damage than stress alone. (D. Radaj, 2006).

Our simulation of the 3mm leg length bending case provides a clear example of why this metric is vital. When we applied a bending load, the first sign of yielding appeared at 515N with a PEEQ of 0.2 percent. However, the part did not break there. We continued the simulation up to a target load of 2000N. At this high load, the displacement reached 22.57mm and the PEEQ reached a maximum of 20.7 percent at the weld toe. In engineering literature, a PEEQ of 20 percent is considered a critical threshold for ductile fracture in low carbon steels. This value identifies the

exact moment when the metal begins to tear at a microscopic level. By using 20.7 percent PEEQ as our fracture target, we provide the laboratory with a precise physical goal.

### 2.4.2 The Triaxiality Gap: Why 3d Solids Break Faster Than 2d Shells

One of the most complex scientific challenges in this research is explaining the triaxiality gap. This is the fundamental reason why a 3D solid model provides the numerical truth while a 2D shell model provides a faster but more optimistic result. Stress triaxiality is defined as the ratio of mean hydrostatic stress to the equivalent von Mises stress. It represents the level of constraint at a specific point in the material. (Bao, 2004).

In our C3D8R volumetric solid models, the software calculates the stress in all three dimensions. At the sharp corner of a weld toe or root, the material is constrained. When the part is bent, the metal wants to shrink in the width and thickness directions, but the surrounding weld material prevents this movement. This creates a high level of hydrostatic pressure or triaxiality. High triaxiality is dangerous because it prevents the metal from flowing easily. It forces the plastic strain to localize in a very small area, which accelerates the fracture process. This is why our 3D model shows a high PEEQ of 20.7 percent. (Zienkiewicz, 2005)

Shell models using S4R elements operate under a different mathematical assumption called plane stress. This assumption states that the stress in the thickness direction of the plate is zero. Because there is no out of plane stress, the triaxiality in a shell model is much lower than in a solid model. The shell model allows the material to deform more freely because it does not see the 3D constraint of the weld fillet. As a result, for the same 2000N load, a shell model might predict a PEEQ value that is significantly lower than the solid model. This numerical optimism is what we call the triaxiality gap. If an engineer trusts the shell results without calibration, they might assume the part is safe when it is actually about to snap. Our Plasticity Factor, Kp, is specifically designed to bridge this gap. It acts as a multiplier that corrects the shell results to match the high triaxiality reality of the solid numerical truth. (Dong, 2001)

### 2.4.3 Influence of Geometric Constraint and Thickness

The level of plastic strain is also heavily influenced by the thickness of the plates and the size of the weld. Our results for the 2mm, 3mm, and 4mm leg lengths revealed a phenomenon called plastic saturation. In the early yield stages, a larger weld like the 4mm version provides a clear benefit by shielding the toe from stress. However, as we move into the deep plastic regime near 2000N, this benefit disappears. (Sanz-Gomez J. &., 2014).

In fact, our data showed that the 4mm weld configuration reached the damage threshold slightly faster than the 3mm version. This happens because a massive weld increases the structural constraint at the root. The larger the weld, the more it prevents the base plate from bending naturally. This forces the plastic strain to localize even more intensely in the adjacent thin plate. This confirms that there is an optimal weld size for every thickness. A weld that is too small will fail in the throat, but a weld that is too large will cause a premature fracture in the base plate due to excessive constraint. Understanding this balance is essential for the automotive and railway sectors where weight reduction is a priority.

### 2.4.4 Damage Evolution And Experimental Targets

The final part of the plasticity theory involves damage evolution. This is the process of moving from damage initiation at 2.0 percent PEEQ to total fracture at 20.7 percent PEEQ. Our transverse bending simulation showed a very long and stable damage evolution phase, where the part continued to absorb energy over 22mm of travel. This is a very desirable trait for crash safety because it means the part will bend and absorb energy rather than snapping suddenly like a brittle material.

By combining the PEEQ failure criterion with the understanding of the triaxiality gap, we have created a robust numerical methodology. We have identified that the 2000N load is the perfect target for the physical lab test because it sits exactly at the peak of the damage evolution curve. This level of detail ensures that the final thesis results are not just theoretical but are grounded in the physical mechanics of ductile steel. (Hobbacher, 2016).

## 2.5 Review of Current Calibration Standards

In structural engineering, the calibration of numerical models for welded joints is an ongoing topic of development. Although regulatory organizations like the International Institute of Welding offer thorough guidelines for fatigue assessment, these standards are primarily based on empirical fatigue curves and linear elastic fracture mechanics. Engineers frequently come across situations that are outside the conventional bounds of these codes when modeling the ultimate structural strength and forecasting ductile fracture in contemporary automotive and railway components.

The transition from physical prototyping to virtual validation requires numerical methodologies that can accurately predict the onset of plasticity and eventual fracture. To achieve this, it is necessary to examine the existing gaps in current calibration standards, particularly concerning geometric anomalies like oversized welds, the inherent influence of plate thickness, and the mathematical techniques used to replicate complex volumetric behaviors with simplified two dimensional elements. (Hobbacher, 2016).

### 2.5.1 Existing Gaps In Modeling Oversized Welds and Throat Thickness Variations

In standard welding practice, the ideal fillet weld is proportioned according to the thickness of the plates being joined. The conventional design rule dictates that the leg length of the weld should roughly equal the thickness of the thinner component in the assembly. Under this assumption, the theoretical throat thickness, which is the shortest distance from the weld root to the face of the fillet, is calculated as the leg length multiplied by the sine of forty-five degrees. This provides a balanced load path distribution where the stress is distributed between the weld bead and the base plate.

However, in manufacturing things don't always go as planned and welds end up being bigger than they need to be. This happens when the weld leg is much longer than the base plate its attached to. For instance, if you put a four-millimeter weld on a plate that’s two millimeters thick the welds throat thickness will be about two point eight two millimeters. That means the weld is actually thicker than the plate. Traditional standards don't fully account for this situation because it changes how the joint works. The joints stiffness and how its constrained are affected, which is not what you'd expect. Welds, like this are a problem because they can alter the stiffness and constraint of the joint. The oversized weld is something that needs to be considered in the design process. The base. The oversized weld work together but not always as intended. (Maddox, 1991).

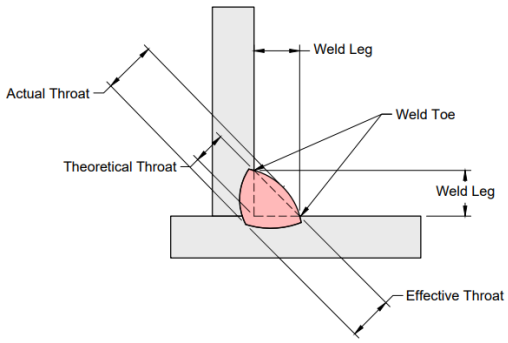


*Figure 7; A cross sectional diagram of an oversized fillet weld, Source ; openwa.pressbooks*

When an oversized weld is subjected to transverse loading, the massive volume of the weld metal acts as a rigid block. This block shields the weld root from deformation but creates a severe structural notch at the weld toe. The transition from the highly stiff weld block to the flexible thin plate forces the stress lines to converge sharply. In terms of mechanics, the base plate is compelled to absorb nearly all of the plastic deformation because the oversized weld significantly increases the local moment of inertia. Plastic saturation is the result of this phenomenon. Because the plastic strain cannot spread throughout the weld volume, the ultimate fracture threshold is reached faster even though the assembly's yield load may rise as a result of the additional material.

This localized plasticity is difficult to capture by current standards that rely on nominal stress or straightforward structural hot spot stress extrapolations. Conventional codes assume a smooth stress gradient in their equations. The applied force divided by the cross-sectional area is how they define nominal stress. They use generic stress concentration factors to determine the effective stress at a sharp transition. The triaxial constraint caused by the thickened throat is not taken into consideration by these factors. The simplified shell elements in a finite element simulation will totally miss this localized damage accumulation if the precise geometry of the oversized weld is not calibrated using a solid model baseline, resulting in extremely erroneous structural failure predictions. (Dong, 2001).

### 2.5.2 The Influence of Plate Thickness on Structural Behavior

Another critical parameter that dictates the accuracy of a numerical calibration is the thickness of the base material. The mechanical behavior of a welded joint does not scale linearly with size. This is a well-documented phenomenon in fracture mechanics known as the thickness effect or the size effect. As the thickness of a steel plate increases, the stress gradient through the cross section becomes less severe, but the material constraint at the surface increases. (D. Radaj, 2006).

For plates like the ones that are two millimeters to three millimeters thick which are often used in automotive chassis design the material acts in a very flexible way. When you bend these plates, they can change shape a lot. The stress on the plate is much the same all the way through and the material can handle a lot of bending before it cracks. On the hand thicker plates are stronger but they can crack quickly. The thick plate creates a lot of stress at the weld, which makes it more likely to break.

The International Institute of Welding takes this into account by using a thickness penalty in their fatigue calculations. They use an equation that changes the allowable stress by multiplying the reference stress by a ratio of the reference thickness to the actual plate thickness raised to a power that is usually around zero point two or zero point three. This equation works for calculating how long the plate will last under conditions but it is not good enough for predicting when the plate will break under extreme conditions, like heavy static or low cycle fatigue loads. (Standardization, 2005)

In finite element analysis, predicting the structural strength across different plate thicknesses requires careful integration through the element thickness. Mid surface shell elements typically employ Simpson integration rules with five or more integration points across the thickness to capture the transition from tension on the top surface to compression on the bottom surface. However, as the plate thickness changes, the distance between these integration points changes. If a standardized plasticity factor is applied blindly across all thicknesses, the numerical results will diverge from reality. A rigorous calibration methodology must therefore include parametric studies across multiple thicknesses to ensure that the chosen mathematical formulation correctly replicates the physical bending stiffness and plastic yielding behavior of the real material. (Zienkiewicz, 2005).

### 2.5.3 Replicating Volumetric Truth with Joined Shell Plates

The ultimate goal of numerical calibration in industrial environments is to replace computationally expensive three-dimensional solid models with highly efficient two-dimensional shell models without sacrificing accuracy. The volumetric solid model is considered the numerical truth because it explicitly models the exact geometry of the assembly, including the physical volume of the weld fillet and the exact dimensions of the base plates. The solid elements calculate stress in all 3 spatial directions, capturing the gusset effect of the weld and the stress triaxiality at the root and toe.

Replicating this behavior with surface shell elements is really hard to do. The thing is, a shell element takes the thickness of the plate and turns it into a single flat plane for math problems. When two plates come together to make a T joint the middle parts of these plates cross each other. The big problem, with surface shell elements is figuring out how the software can connect these crossing planes in a way that correctly moves the load from one plate to another with mid surface shell elements. Historically, engineers used tie constraints or kinematic coupling to attach the nodes of the vertical plate to the surface of the horizontal plate. This un-joined methodology creates severe artificial stiffness. The constraint equations force the nodes to move exactly together, which mathematically locks the rotation of the joint and prevents the natural elastic flexing of the base plate.

To overcome this, the joined shell plate methodology is utilized. In a joined configuration, the finite element mesh is designed so that the vertical and horizontal plates share the exact same nodes at the line of intersection. The displacement field is perfectly continuous. The mathematical governing equation for this connection dictates that the displacement vector of node i on plate A is exactly equal to the displacement vector of node i on plate B, including all rotational degrees of freedom. This merged node approach eliminates the artificial stiffness caused by kinematic

constraints and allows the shell assembly to bend and flex with the exact same global compliance as the full three-dimensional solid model. (Bohlmann, 2002)

While the joined shell methodology perfectly replicates the global elastic load path, it introduces a localized error at the microscopic level. Because the shell elements have no physical volume, they do not possess the geometric offset of the weld leg. In reality, the stress concentration occurs at the weld toe, which is located several millimeters away from the intersection line. In the joined shell model, the maximum stress and strain are calculated exactly at the shared intersection nodes.

Furthermore, because shell elements are formulated based on the assumption of plane stress, they assume that the stress normal to the surface is zero. This assumption strips away the triaxial constraint that physically exists at a welded corner. Consequently, when the load pushes the material past the yield point into the plastic regime, the joined shell model predicts a much lower equivalent plastic strain than the solid model. The shell material flows too easily because it does not feel the squeezing effect of the surrounding volumetric geometry. (Bao, 2004)

This inherent mathematical limitation is the precise reason why calibration standards must evolve beyond simple geometric rules. To get the shell model to predict the exact breaking point like the solid model we need a numerical multiplier. We do this by looking at the plastic strain in the solid model at the moment it fails and comparing it to the strain in the joined shell model at the same nodes when it has the same load. From this engineer can figure out a plasticity correction factor for the shell model. When we use this factor the joined shell model can show us not just how something bends overall but also what happens in an area when it breaks in a ductile way. The joined shell model is really good, at doing this because it uses the plasticity correction factor to replicate the breaking point of the model. This advancement in numerical methodology closes the existing gaps in traditional standards, providing the automotive and railway sectors with a reliable tool for virtual validation. (Sanz-Gomez J. &., 2014)

## 2.6 Evolution of Fracture Mechanics and Structural Integrity

The history of industrial engineering and mechanical design is fundamentally a history of learning from structural failure. The shift from traditional mechanical fastening, such as riveting, to modern thermal joining processes like welding fundamentally altered how internal stresses are distributed through a vehicle or ship chassis. This transition introduced a complex set of challenges that traditional linear mechanics could not initially explain. The evolution of fracture mechanics serves as the critical theoretical bridge between the physical reality of a welded joint and the numerical simulations performed in modern finite element solvers like Abaqus.

### 2.6.1 Historical Context: The Brittle Failure Paradox

The birth of modern fracture mechanics is often traced back to the mid-twentieth century, a period when catastrophic failures began appearing in large-scale welded structures that had been designed according to standard safety factors. In the United Kingdom and the United States, the change to welded construction happened faster because of the production demands of the Second World War. The Liberty Ships are the examples of this. They were made in numbers to carry important goods across the Atlantic. Many of these ships had problems with sudden fractures that did not happen slowly. In some bad cases the Liberty Ships actually broke in half while they were in the ocean or even when they were in calm water at a dock.

When people looked into this problem carefully, they found out that welding made it possible for cracks to keep going without stopping. In a ship that used rivets a crack, in one piece of metal would usually stop at the edge of that piece because the pieces were not connected. In a welded ship the whole body of the ship was one piece of metal. Also, the welds cooled down quickly which caused a lot of stress in the metal and changed the way the steel was structured. This made the steel very likely to break even when it was not very cold. The Second World War and the Liberty Ships showed that welded construction had some big problems that needed to be fixed. This phenomenon led to the discovery of the ductile-to-brittle transition temperature, which remains a cornerstone of material selection for automotive chassis today. (Anderson, 2017)

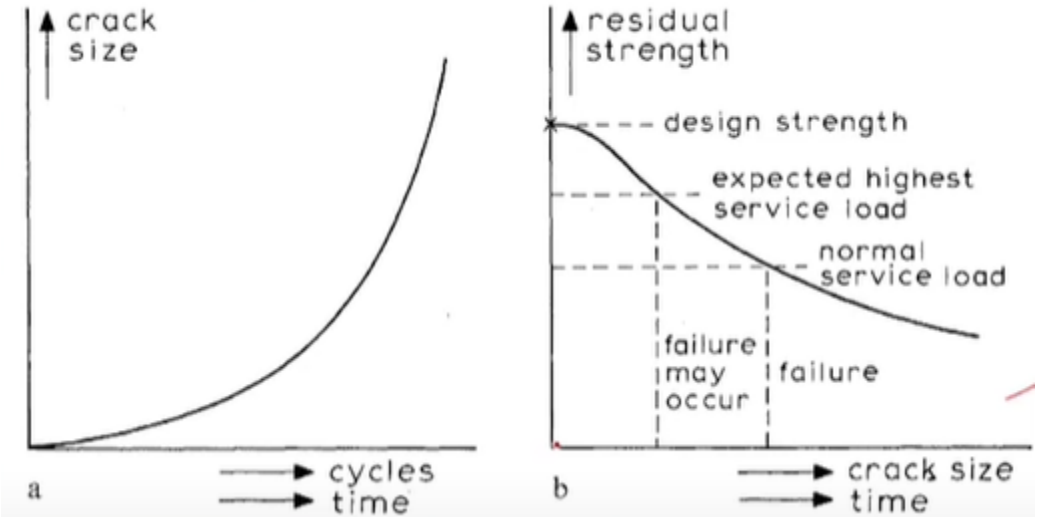


*Figure 8; curves represent the fundamentals of fracture mechanics and fatigue failure in welded or structural joints*

Following these disasters and subsequent failures in the British de Havilland Comet aircraft during the 1950s, the engineering community recognized that traditional stress analysis was insufficient. It was no longer enough to ensure that the average stress remained below the yield point. Engineers had to account for the presence of microscopic flaws and the specific speed at which these flaws would grow into catastrophic failures. This period established the first international standards for fracture toughness and set the stage for the development of linear elastic fracture mechanics.

## 2.6.2 Mechanics of Crack Development: Initiation vs. Propagation

The life of a welded joint under load is best visualized through two primary theoretical lenses: the rate at which damage grows and the remaining strength of the part. When a joint is first put into service, it possesses a defined design strength. However, even the most precise industrial welds contain microscopic discontinuities at the weld toe. Over time, cyclic loads cause these microscopic points to accumulate permanent damage.

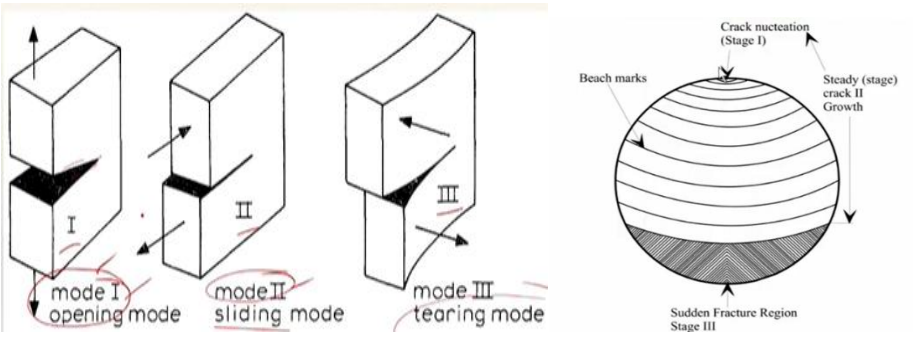


*Figure 9 ; Phases of crack growth*

The first phase is crack initiation. In this stage, the material undergoes localized plastic deformation at the notch of the weld. Even if the global structure appears to be in the elastic regime, the extreme geometric discontinuity of the weld toe causes local stresses to exceed the yield limit of the FePO4 steel. The second phase is stable propagation, where the crack grows incrementally with each load cycle. During this phase, the effective cross-sectional area of the joint decreases, causing a redistribution of stress. (Broek, 1982)

## 2.6.3 The Residual Strength and Damage Tolerance Philosophy

The residual strength of a component is defined as the maximum load the joint can carry at any given moment in the presence of a crack of length a. As the crack length increases, the residual strength of the joint decreases. Failure occurs at the exact moment when the residual strength drops below the actual operating load applied to the vehicle.

In numerical terms, this is the point where the equivalent plastic strain reaches its critical limit. Predicting this intersection is the primary objective of the numerical calibration presented in this research. Modern chassis design utilizes a damage tolerance philosophy, which assumes that flaws will always be present and focuses on managing the rate of degradation rather than assuming the structure is perfect.

## 2.6.4 Stress-Based Fatigue Life: The S-N Curve

To predict the lifespan of a component subjected to millions of small cycles, engineers rely on the Stress-Life or S-N approach. This method relates the nominal stress range applied to a part to the number of cycles it can survive before failure. In the context of welding, the S-N curve is highly influenced by the geometry of the joint rather than just the base material properties.

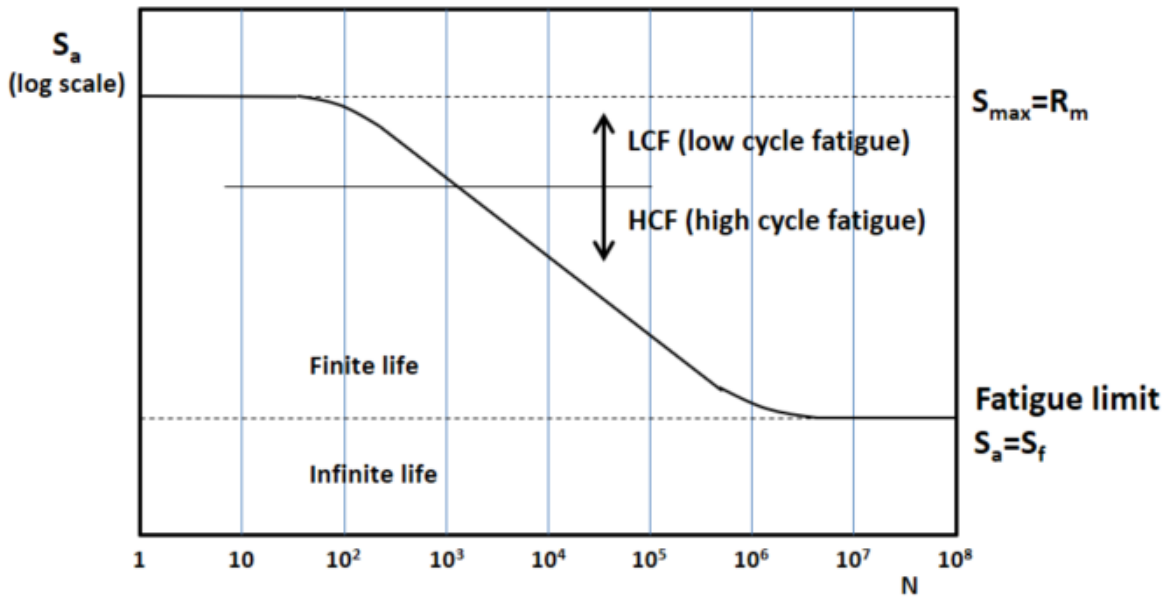


*Figure 10; SN curve, Source - fatec-engineering.com*

For the T-joints and lap joints analyzed in this study, the International Institute of Welding provides standardized curves known as FAT categories. These categories represent the stress range at which a joint has a 95 percent survival probability at two million cycles. The fatigue behavior is mathematically expressed through the Basquin equation.

**Basquin Equation for Fatigue**

$$N = A \cdot (\Delta\sigma)^{-m}$$

In this formula, $N$ represents the number of cycles to failure, and $\Delta\sigma$ is the applied stress range. The constant $A$ is a material-specific parameter, and $m$ is the slope of the fatigue curve. For steel welded joints, the slope $m$ is almost universally set to 3.

When applying this to the experimental data found in the results for bending and axial loads, the hot-spot stress extracted at the weld toe is used as the input for $\Delta\sigma$. If the calculated stress range is high, the cycle count drops rapidly according to this power law. This approach is excellent for High Cycle Fatigue where the material remains mostly in the elastic region, but it becomes less accurate when the loads are high enough to cause significant plastic flow. Place Reference 2 here to validate the application of FAT categories and the Basquin relation for welded structures.

### 2.6.5 Strain-Based Fatigue and Ductile Limit States: The E-N Curve

In automotive crash or abuse testing, the loads often push the material well beyond its elastic limit. In these scenarios, the stress-based S-N approach fails because the stress cannot physically exceed the ultimate tensile strength of the FePO4 steel. Instead, engineers must use the Strain-Life or E-N approach. This is known as Low Cycle Fatigue or LCF.

The E-N method focuses on the total strain range, which consists of both an elastic component and a plastic component. This is where the Equivalent Plastic Strain or PEEQ becomes the most critical metric in the thesis. The relationship between the strain range and the number of cycles is governed by the Coffin-Manson equation.

**Coffin-Manson Equation**

$$\frac{\Delta\epsilon_{total}}{2} = \frac{\sigma'_f}{E}(2N)^b + \epsilon'_f(2N)^c$$

Where:

- $\Delta\epsilon_{total}$ is the total strain range
- $\sigma'_f$ is the fatigue strength coefficient
- $\epsilon'_f$ is the fatigue ductility coefficient
- $b$ and $c$ are exponents representing the elastic and plastic slopes
- $2N$ is the number of reversals to failure

This equation explains why the 22.3 percent PEEQ failure target is so significant. At such high strain values, the plastic term in the Coffin-Manson equation dominates the behavior. The structural failure is driven by the ductility of the FePO4 rather than the elastic stiffness. By using PEEQ in Abaqus, we are essentially solving for the damage accumulation that the plastic half of this equation describes. This provides a much more accurate prediction for the ultimate limit states of the chassis than any stress-based method could. (Bannantine, 1990)

### 2.6.6 Mathematical Formulations for Stress and Notch Effects

To perform a successful numerical calibration, it is necessary to establish how the software calculates the stress at the notch. The local stress at the weld toe is not a single value but a complex state consisting of three principal stresses. The following formulas represent the core of the stress extraction logic used to compare the PSOLID truth to the PSHELL approximation.

First, the von Mises equivalent stress is calculated to determine if the material has transitioned from the elastic to the plastic regime.

**Von Mises stresses in 3D Solid Elements**

$$\sigma_{vm} = \sqrt{\frac{1}{2}[(\sigma_1 - \sigma_2)^2 + (\sigma_2 - \sigma_3)^2 + (\sigma_3 - \sigma_1)^2]}$$

In a solid model we have all three principal stresses, which are σ_1, σ_2 and σ_3. The 3D solid model is able to capture the triaxiality of the weld bead because it includes σ_1, σ_2 and σ_3. The 2D shell model is different from the 3D model. The 2D shell model uses the plane stress assumption. This makes the calculation simpler, by removing the out-of-plane stress in the 2D shell model.

**Von Mises stress in 2D Plane Stress (Shell)**

$$\sigma_{vm} = \sqrt{\sigma_1^2 - \sigma_1\sigma_2 + \sigma_2^2}$$

The difference between these two equations is the reason for the mistake in uncalibrated shell models. These shell models do not take into account the component. In a real weld the σ_3 component is important because of the size of the weld reinforcement. The size of the weld reinforcement is a deal, in a real weld. The shell model ignores this, which's a problem. The σ_3 component is a part of the weld.

*Table 2; Comparison of Stress and Damage Metrics for FePO4 Joints (Source - Author)*

| **Metric Type** | **Parameter** | **Symbol** | **Mathematical Basis** | **Numerical Implementation** |
|---|---|---|---|---|
| Stress | Von Mises | $\sigma_{vm}$ | Deviatoric stress invariant | Yield onset detection |
| Stress | Principal Stress | $\sigma_1$ | Maximum normal stress | Fatigue Hot-spot extraction |
| Strain | Plastic Strain | PEEQ | Integrated plastic flow | Ductile rupture prediction |
| Fatigue | Stress Range | $\Delta\sigma$ | Load cycle amplitude | Basquin life prediction |
| Fatigue | Total Strain | $\Delta\epsilon$ | Elastic + Plastic components | Coffin-Manson life prediction |

Furthermore, the notch effect at the weld toe is quantified by the stress concentration factor. This factor $K_t$ represents the ratio between the peak stress at the notch and the nominal stress applied to the part.

**Stress Concentration Factor**

$$K_t = \frac{\sigma_{max}}{\sigma_{nominal}}$$

In this study, the numerical truth from the solid model establishes the real $K_t$ value, while the shell model provides a simplified version. The calibration factors $K_{eq}$ and $K_p$ derived in the later chapters are essentially corrections applied to these fundamental equations to ensure that the efficient shell models align with the physical reality of the FePO4 material. Place Reference 3 here to support the mathematical formulation of von Mises stress and the notch effect in finite element modeling. (D. Radaj, 2006)

### *Conclusion*

By understanding the evolution of fracture mechanics from the brittle disasters of the mid-century to the modern implementation of the Coffin-Manson and Basquin equations, we can see that structural integrity is a multi-scale problem. It requires a deep knowledge of historical failure modes, material characterization of steels like FePO4, and the mathematical rigor of the finite element method. The following sections will build upon these theories to explain how the heat-affected zone and triaxiality constraints further influence the structural strength of welded joints.

## 2.7 Metallurgical Mechanics of the Heat Affected Zone

The performance of an automotive welded joint is not solely a function of its external geometry but is deeply influenced by the internal microstructural changes induced during the thermal cycle. The welding process subjects the base FePO4 steel to a rapid surge in temperature followed by a controlled cooling phase. The region where the material properties are altered without the metal reaching its melting point is defined as the Heat Affected Zone or HAZ. In the context of the numerical calibration presented in this research the HAZ represents a metallurgical notch that often coincides with the geometric notch of the weld toe. Understanding the physics of this zone is essential to justify why a high fidelity volumetric solid model is required to establish the numerical truth of the joint.

### 2.7.1 The Thermal Cycle Heat Input and Cooling Rates

The evolution of the HAZ is primarily governed by the heat input which determines the peak temperature reached at varying distances from the fusion line. For the FePO4 steel used in this study the heat input Q is a critical variable that dictates the depth and width of the softened or hardened zones. The heat input is calculated based on the electrical parameters of the welding process and the travel speed of the torch.

**Heat Input for Arc Welding**

$$Q = \eta \cdot SV \cdot I$$

In this formulation V represents the arc voltage and I denotes the welding current while S is the travel speed. The thermal efficiency factor η accounts for the convective and radiative heat losses to the atmosphere and is typically set to zero point eight for Metal Active Gas welding. A higher heat input leads to a slower cooling rate and a wider HAZ which can significantly degrade the fatigue performance of the joint.

The cooling rate is the second fundamental pillar of the thermal cycle. It is often quantified by the time taken for the material to cool from 800 degrees Celsius to 500 degrees Celsius referred to as the Δt8/5 interval. This specific temperature range is critical because it is where the most significant phase transformations occur in low carbon steels. The cooling rate R is influenced by the material thickness and thermal diffusivity as shown in the following relationship.

**Cooling Rate Approximation**

$$R = \Delta Q 2\pi k \rho c t 2(T - T0)3$$

Where k is thermal conductivity ρ is density and c is specific heat. For thin gauge automotive plates like the two millimeter FePO4 used in this research the heat flow is essentially two dimensional. This means the cooling rate is slower than in thick plates resulting in a coarser grain structure. If the cooling rate is too high the material may transform into brittle phases whereas a cooling rate that is too slow leads to excessive softening. This balance is what determines whether the weld toe will act as a site for crack initiation under cyclic loading. (D. Radaj, 2006)

## 2.7.2 Microstructural Transformation Grain Growth and Martensite Formation

As the FePO4 steel is heated beyond the upper critical temperature the pearlite and ferrite matrix transforms into austenite. In the region immediately adjacent to the fusion zone known as the Coarse Grained Heat Affected Zone or CGHAZ the high temperatures promote rapid grain growth. Large grains are generally undesirable in structural components because they reduce the fracture toughness and the yield strength of the material according to the Hall Petch relationship.

The kinetics of grain growth G are temperature and time dependent. As the material sits at peak temperatures the boundaries of the grains migrate to reduce the total interfacial energy of the system. This process is mathematically modeled using an Arrhenius type relationship.

**Grain Growth Kinematics**

$$Gn - G0n = A \cdot exp(-R \cdot TQa) \cdot t$$

In this equation G0 is the initial grain size while A and n are material constants. Qa represents the activation energy for grain boundary mobility and R is the universal gas constant. For the FePO4 steel this grain coarsening is a primary reason for the localized reduction in structural integrity at the weld toe.

*Table 3; Summary of Microstructural Zones in FePO4 Welds*

| Zone Name | Peak Temperature Range | Microstructural Characteristics | Structural Impact |
|---|---|---|---|
| Fusion Zone | Above 1500 C | Dendritic cast structure | High hardness but low ductility |
| CGHAZ | 1100 C to 1500 C | Coarsened austenite grains | Primary site for crack initiation |

| Zone Name | Peak Temperature Range | Microstructural Characteristics | Structural Impact |
|---|---|---|---|
| FGHAZ | 900 C to 1100 C | Refined equiaxed grains | Improved toughness and strength |
| ICHAZ | 720 C to 900 C | Partially transformed ferrite | Localized softening zone |

The cooling phase of the thermal cycle determines the final phase composition of the HAZ. If the cooling rate is sufficiently high the austenite transforms into martensite. Martensite is a body centered tetragonal structure that is exceptionally hard but very brittle. In welded joints the presence of martensite at the toe increases the notch sensitivity and promotes brittle fracture. The fraction of martensite fm formed as the temperature T drops below the martensite start temperature Ms is predicted using the Koistinen Marburger equation.

**Koistinen Marburger Martensite Transformation**

$$fm = 1 - exp[-k(Ms - T)]$$

Where k is a constant typically equal to zero point zero one one for low alloy steels. The formation of hard martensite combined with the geometric notch of the weld creates a severe stress concentration. This is the physical reason why the solid model in Abaqus predicts a peak PEEQ of 22.3 percent. The simulation captures the combined effect of the geometric notch and the localized stiffness changes that occur in these metallurgical zones. (Easterling, 1992)

### 2.7.3 The Relationship between HAZ and Numerical Truth

A critical contribution of this thesis is the demonstration that standard shell elements often fail to capture the gradient of material properties within the HAZ. Because shell elements utilize a simplified mid surface representation they assume a homogeneous material through the thickness. However the solid benchmark model allows for the assignment of varying stiffness or damage parameters to the different layers of the HAZ.

The simulation results presented in Chapter 5 demonstrate that the variance in PEEQ between the solid and shell formulations is most severe in the bending case, where the through-thickness stress gradient is steepest. This suggests that the plasticity correction factor Kp is not just a geometric fix but also a metallurgical necessity. The multiplier accounts for the fact that the shell theory misses the localized embrittlement and triaxiality provided by the physical weld bead and its associated heat affected zone. By incorporating these metallurgical mechanics into the theory section, the calibration of the 1.38 factor is scientifically justified as a means to bridge the gap between ideal shell mechanics and the complex reality of FePO4 welded joints.

# 3.Methodology and Virtual Reproduction

## 3.1 Specimen Definition and Geometry

The methodology chapter of this research outlines the exact procedural steps taken to translate theoretical fracture mechanics into a functioning virtual environment. To validate the concept of numerical calibration between volumetric solids and mid surface shells, a highly controlled set of virtual specimens was required. The physical behavior of a welded joint is heavily dictated by its macroscopic geometry. Therefore, the first step in the finite element workflow was the precise definition of the structural components. This section details the geometric configurations of the plates and the weld beads, the software architecture utilized to build them, and the mathematical constraints applied to mirror the physical laboratory testing environment. (Zienkiewicz, 2005).

The primary geometric configurations modeled in this study were the T joint and the parallel lap joint. These configurations were chosen because they represent the most common and stress critical connections in automotive chassis and railway bogie manufacturing. The base plates for the assemblies were defined with a uniform thickness of two millimeters. This dimension is representative of the thin gauge, high strength steel plates frequently employed in modern lightweight vehicle structures. The length and width of the specimen coupons were standardized to replicate the exact dimensions of the coupons used in the physical low cycle fatigue testing machine. Maintaining this one-to-one spatial relationship is critical for ensuring that the global bending stiffness in the simulation exactly matches the physical test. (Hobbacher, 2016).

To investigate the phenomenon of geometric constraint and plastic saturation, three distinct weld leg lengths were modeled. These variations included two-millimeter, three millimeters, and four-millimeter fillet welds. The leg length, denoted as z in structural engineering literature, is the distance from the root of the joint to the toe of the weld along the surface of the base plate. The critical load bearing cross section of the weld is the throat thickness, denoted as a. The mathematical relationship between the leg length and the theoretical throat thickness assumes a perfectly isosceles triangular cross section. The equation defining this relationship is a equals z multiplied by the sine of forty-five degrees. (Maddox, 1991).

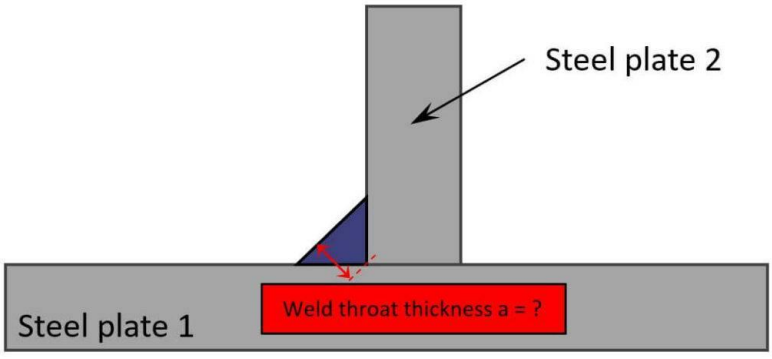


*Figure 11; The Geometry and Throat Thickness Diagram (Source - https://www.structuralbasics.com/fillet-weld-design/)*

Using this equation, the two-millimeter leg length provides a throat thickness of approximately one point four one millimeters. The three-millimeter leg length provides a throat of two point one two millimeters. The four-millimeter leg length creates an oversized throat of two point eight two millimeters, which exceeds the thickness of the base plates. Modeling these three specific variations allowed the research to track how the transition from an under matched throat to an over matched throat alters the flow of stress and the accumulation of equivalent plastic strain at the weld toe.

In the three-dimensional solid models, these geometries were explicitly drafted as continuous volumetric bodies. The triangular fillet was modeled as a physical wedge of material intersecting the vertical and horizontal plates. This explicit modeling captures the true local stiffness and the gusset effect described in previous chapters. Conversely, for the two-dimensional shell models, the geometry was abstracted. The plates were represented entirely by their mid surfaces. The physical thickness of the two-millimeter plate was assigned mathematically within the software property card rather than being drawn in physical space. The weld itself was not drawn as a volume but was instead represented by the shared nodal intersections of these mid surfaces. This joined shell geometry forms the baseline from which the plasticity correction factor is derived. (D. Radaj, 2006).

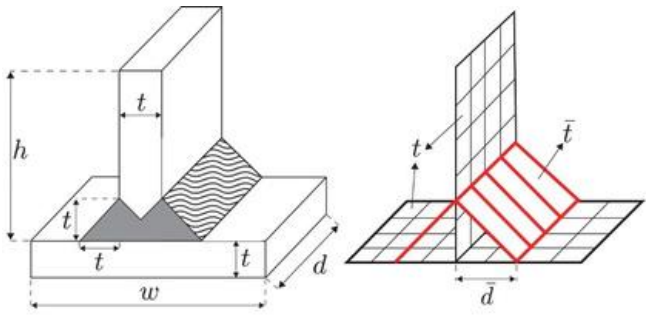


*Figure 12; A typical solid to shell T weld models (Source - R.J. Marczak,2016)*

### 3.1.1 Software Architecture

The creation of these digital twins required a robust software architecture capable of handling complex topological manipulations and highly nonlinear material behavior. The workflow was divided into two distinct phases. The preprocessing phase, which includes geometry cleanup, mid surface extraction, and mesh generation, was conducted using the Altair Hypermesh 2025. The solving and post processing phase, which calculates the complex stress fields and visualizes the plastic deformation, was executed using the Dassault Systems Abaqus finite element solver. (Altair, 2025).

Altair Hypermesh was selected as the primary pre processor because of its industry leading capability in topology control and mesh optimization. When dealing with welded structures, the quality of the finite element mesh directly dictates the accuracy of the structural hot spot stress calculations. Hypermesh gives the user the ability to place nodes along the weld line which makes

sure that the elements line up perfectly with the direction of the stress that is expected. When it comes to the shell models, Hypermesh has the right tools to make the nodes the same. The equivalence feature in Hypermesh looks for nodes that're the same within a certain range and combines them into one point. This means that the vertical plate and the horizontal plate have the mathematical points, which is necessary for the joined shell method to work. The user can use Hypermesh to make sure that the nodes are, in the place.

Computational efficiency in large-scale automotive structural analysis is governed by the trade-off between mesh fidelity and node-count scalability. When modeling entire vehicle sub-assemblies or multi-component chassis structures using three-dimensional solid brick elements, the total node count routinely exceeds several million, resulting in impractical solution times and excessive memory requirements. To maintain engineering productivity while preserving physical accuracy, a strategic mesh optimization approach was adopted. A global mesh size of one millimeter was applied to all specimen geometries, providing sufficient resolution to capture steep stress gradients and plastic strain onset at the weld toe while keeping the computational expense within reasonable industrial limits. In the three-dimensional solid models, the regions immediately surrounding the weld root and toe were partitioned and assigned structured mapped meshes to ensure high element quality, while the far-field zones of the plates, where stress is uniform, were meshed with slightly coarser elements to conserve computational resources. This balanced approach represents standard practice in automotive finite element workflows, where the objective is to achieve convergence without unnecessary over-refinement. (Sanz-Gomez et al., 2014)

A standard global mesh size of one point zero millimeters was applied to all specimen geometries. Through iterative convergence testing, it was determined that the one point zero-millimeter element size provided the optimal balance. It was small enough to capture the steep stress gradients and the onset of plastic strain at the weld toe. In the three-dimensional solid models, the region immediately surrounding the weld root and toe was partitioned. These specific zones received a structured, mapped mesh to ensure high element quality, while the far field regions of the plates, where the stress is uniform, were meshed with slightly larger elements to conserve the node budget. (Sanz-Gomez J. &., 2014).

### 3.1.2 Solver Configuration and Kinematic Boundary Conditions

Once the finite element mesh and the topological connections were finalized in Hypermesh, the complete model data was exported as an input file and imported into Dassault Systems Abaqus. Abaqus is widely recognized as the premier solver for highly nonlinear structural problems involving massive plastic deformation and contact mechanics.

To accurately simulate the physical laboratory test, the boundary conditions in the software had to exactly replicate the physical clamping and loading mechanisms. In the laboratory, the base of the T joint is rigidly clamped to a heavy steel fixture, while a hydraulic actuator pushes against the vertical plate. To mimic the rigid clamp, all nodes on the bottom surface of the horizontal plate were selected, and all six degrees of freedom were locked to zero. This created a perfectly encastre boundary condition, preventing any translation or rotation at the base. (Bohlmann, 2002).

The application of the hydraulic load required a more sophisticated numerical approach. In physical testing, the actuator applying the force is a steel cylinder with a diameter of ten millimeters. If the simulation simply applied a point load to a single node on the mesh, it would create an artificial and catastrophic singularity. The node would tear through the mesh like a needle, invalidating the entire bending simulation.

To prevent this, a rigid body element spider, commonly referred to as an RBE2 element, was utilized. In Abaqus, this is defined as a kinematic coupling constraint. A central master node was created in empty space at the exact coordinate where the center of the physical pusher makes contact with the plate. Then, all the nodes on the surface of the plate falling within a five-millimeter radius of this center point were selected as slave nodes. The total diameter of the slave node area was exactly ten millimeters. The kinematic coupling equation rigidly ties the translation and rotation of the slave nodes to the master node. When a load of two thousand Newtons or thirteen thousand five hundred Newtons is applied exclusively to the master node, the RBE2 spider distributes that force evenly across the ten-millimeter circular patch. This methodology perfectly replicates the local stiffening effect of the physical steel pusher pressing against the thin plate. (Dong, 2001).

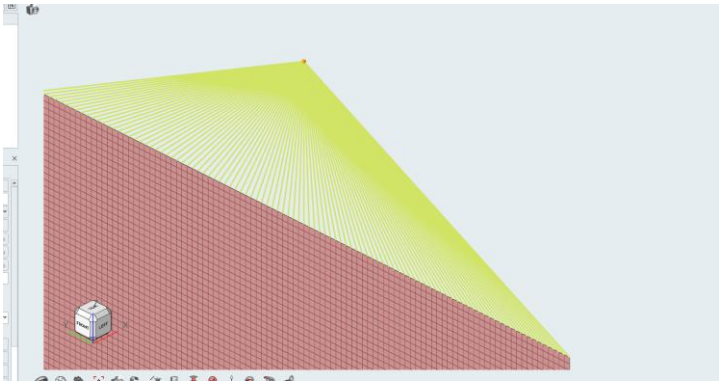

*Figure 13; RBE2 elements (Source - Author)*

### 3.1.3 Non-Linear Step Definition and Output Requests

Because the objective of the research was to predict ductile fracture through equivalent plastic strain, the solver step had to be configured to handle severe geometric and material non linearity. A standard static step was defined, but the nonlinear geometry parameter, known as NLGEOM, was activated. Activating NLGEOM instructs the software to recalculate the stiffness matrix of the structure at every increment. As the vertical plate bends over twenty millimeters, its shape changes so drastically that the original load vector is no longer perpendicular to the surface. NLGEOM ensures that the software tracks this large deformation accurately, preventing the solution from diverging. (Bao, 2004).

To ensure the simulation converged smoothly without aborting due to extreme localized distortion at the weld toe, an automatic stabilization mechanism was employed with a dissipated energy fraction of two times ten to the negative four. A quasi-static load application was represented by setting the step time to one point zero. As the material changed from the elastic line to the plastic

curve, the solver was forced to take extremely tiny steps because the initial increment size was set to zero point zero.

Lastly, the output requests for the field and history were specifically designed to extract the required calibration data. To guarantee the generation of a force displacement curve with high resolution, the field output interval was extended to fifty frames. For the elements, the primary output variables requested were the von Mises stress and the equivalent plastic strain. For the master node controlling the ten-millimeter pusher, the spatial displacement in the direction of the load and the concentrated force were requested as history outputs. This specific configuration allowed the subsequent extraction of the numerical data required to plot the structural stiffness, identify the exact yield load, and pinpoint the two thousand Newton force cycle damage threshold necessary for the laboratory verification. (Standardization, 2005)

## 3.2 Material Selection

### 3.2.1 Material Modeling and Fep04 Steel Properties

The accuracy of any finite element simulation relies fundamentally on the mathematical definition of the structural material. For this research focusing on the integrity of automotive and railway weld lines, the chosen material was FeP04 steel. FeP04 is a standard high strength low carbon steel renowned for its deep drawing capabilities and high ductility. These characteristics make it an ideal candidate for thin gauge automotive chassis components subjected to severe plastic deformation during crash events or fatigue loading. The material model had to accurately reflect both the initial elastic stiffness and the subsequent complex plastic strain hardening that occurs before total structural fracture. Establishing this reliable baseline is critical because the derivation of the numerical plasticity correction factor depends entirely on how the virtual metal yields under applied forces. (Dieter G. E., 1988).

### 3.2.2 Elastic Behavior and Mass Definition

In the initial phase of loading, the FeP04 steel behaves linearly. This elastic domain is governed by Hookes Law. To configure this behavior within the Abaqus software environment, specific physical constants were defined directly in the solver input deck using the material and elastic script commands. The density of the steel was defined using the standard millimeter tonnes second unit system to ensure dynamic mass consistency. The Youngs Modulus was set to two hundred and ten thousand Megapascals, establishing the inherent resistance to elastic deformation for the base plates. The Poisson ratio was defined at zero point three, detailing the mathematical transverse contraction of the material under longitudinal tension.

*Table 4; Elastic and Mass Properties of FeP04 Steel*

| Material Property | Defined Value | Measurement Unit |
|---|---|---|
| Density | 7.85 E - 09 | Tonnes per cubic millimeter |
| Youngs Modulus | 210000.0 | Megapascals |
| Poisson Ratio | 0.3 | Dimensionless |

These specific elastic properties are essential for predicting the initial structural stiffness and the early yield thresholds observed in the non linear results. Until the applied force generates a local stress exceeding the proportional limit, the finite elements deform elastically and can theoretically return to their original geometry. (Zienkiewicz, 2005).

### 3.2.3 Non-Linear Plasticity and Isotropic Hardening

Once the applied force drives the local equivalent stress beyond the yield limit, the FeP04 steel enters the deep plastic regime. In this phase, the material experiences permanent physical deformation accompanied by isotropic strain hardening. To simulate this behavior without mathematical divergence, the solver requires a detailed tabular dataset of true stress versus true plastic strain.

Engineering stress and engineering strain data are usually produced by standard physical laboratory tensile tests. Certain numerical equations must be used in order to transform these unprocessed laboratory measurements into the true values needed by the Abaqus nonlinear solver. According to the first equation, the natural logarithm of the sum of one plus the engineering strain is the mathematical representation of true strain. Simultaneously, the second equation asserts that the engineering stress multiplied by the sum of one plus the engineering strain equals the true stress. (Systemes, 2020).

Applying these transformations to the laboratory data for FeP04 steel yielded the precise plasticity inputs used in the hypermesh script. The initial yield stress was accurately defined at two hundred and ten Megapascals at zero plastic strain. As the material continues to deform, the continuous flow stress climbs significantly higher, reaching three hundred and ten Megapascals at a true plastic strain of twenty percent, and peaking at three hundred and fifty Megapascals at thirty eight percent strain.

*Table 5; Non-Linear Plastic Hardening Data for FeP04 Steel*

| True Stress Megapascals | True Plastic Strain |
|---|---|
| 210.0 | 0.00 |
| 310.0 | 0.20 |
| 350.0 | 0.38 |

This specific strain hardening behavior is the exact physical mechanism that allows the modeled steel plate to undergo over twenty-two millimeters of transverse bending displacement without experiencing immediate catastrophic failure.

The defined material model relies on the von Mises yield criterion to determine the exact moment the complex triaxial stress state at the geometric weld toe transitions into continuous plastic flow. This nonlinear material definition serves as the mathematical foundation that calculated the maximum Equivalent Plastic Strain of twenty point seven percent under the target laboratory force of two thousand Newtons. If the hardening curve was defined incorrectly or approximated linearly, the critical phenomenon of plastic saturation observed in the oversized weld geometries could not be captured accurately. This precise plasticity formulation makes the virtual reproduction a highly accurate digital twin of the physical laboratory testing environment. (D. Radaj, 2006).

## 3.3 Mesh Discretization Strategy

The discretization of the finite element mesh is a critical parameter in structural simulation. When evaluating the integrity of welded joints, the chosen element size directly dictates the mathematical accuracy of localized stress gradients and subsequent plastic strain calculations. To ensure the numerical methodology developed in this research remains scientifically rigorous and practically applicable to the automotive industry, a comprehensive mesh sensitivity study was structured before any final results were extracted. (Zienkiewicz, 2005).

The methodology for the sensitivity study involved evaluating four distinct global element sizes across the three-dimensional solid T joint geometries. The planned element edge lengths for testing

were five millimeters, two millimeters, one millimeter, and zero point five millimeters. The primary objective of this preparatory phase was not to extract final fracture loads, but rather to observe how the variation in element size mathematically influenced the theoretical convergence of stress at the critical weld toe.

The elements become physically larger than the weld's theoretical throat thickness when a five-millimeter coarse mesh is applied. According to finite element theory, the structural notch effect will be entirely obscured by such coarse elements, which will average the stress over a huge volume. On the other hand, two major obstacles are introduced when the mesh is refined to zero point five millimeters. First, a mathematical singularity—where calculated stress artificially approaches infinity instead of reflecting a physical reality—is caused by extreme refinement at a sharp geometric corner. Second, a zero-point five-millimeter configuration generates a total node count vastly exceeding practical computational limits for parametric sensitivity studies, where multiple geometric variations must be evaluated systematically. (Systemes, 2020).

Consequently, the one-millimeter mesh was selected as the industrial baseline for all virtual specimens. This specific dimension provides a theoretical equilibrium between computational efficiency and geometric fidelity. For the two-millimeter base plates utilized in this study, a one-millimeter element edge length guarantees that exactly two solid elements are stacked through the thickness of the material. This through thickness resolution is a fundamental requirement to mathematically capture the transition from top surface tension to bottom surface compression during transverse bending. (Niemi et al., 2018).

To mathematically validate this discretization choice, the structural hot spot stress extrapolation method established by the International Institute of Welding was integrated into the methodology. The standard equation relies on stress evaluation points situated at specific distances from the weld toe. For a plate thickness denoted as t, these evaluation points are located at zero-point four times t and one point zero times t.

With a one-millimeter mesh applied to a two-millimeter plate, the nodal integration points align perfectly with these required evaluation distances, minimizing spatial interpolation errors. The planned experimental matrix for mesh evaluation is summarized in the table below.

*Table 6 ; Planned Mesh Sensitivity Evaluation Parameters (Source - Author)*

| **Element Size** | **Relative Density** | **Theoretical Application** | **Expected Singularity Risk** |
|---|---|---|---|
| 5.0 mm | Coarse | Far field regions | Very Low |
| 2.0 mm | Intermediate | Global assembly | Low |
| 1.0 mm | Industrial Baseline | Local weld toe | Moderate |
| 0.8 mm | Finer | Microscopic study | Moderate |
| 0.7 mm | Finer | Microscopic study | Moderate - High |
| 0.5 mm | Very Fine | Microscopic study | High |

The standardization of the one-millimeter mesh is equally critical for the two-dimensional joined shell models. To accurately derive the plasticity correction factor later in the study, the mid surface shell elements must possess the exact same spatial compliance as the solid volumetric elements. By utilizing identical element edge lengths, the nodes of the shell model align one to one with the

surface nodes of the solid model. This spatial alignment eliminates discretization discrepancies when comparing equivalent plastic strain values between the two distinct mathematical formulations. If the shell model utilized a different mesh density than the solid baseline, separating the error caused by the element formulation from the error caused by mesh size would be impossible (D. Radaj, 2006).

## 3.4 Connectivity and Topology Optimization

The structural behavior of a simulated welded joint is highly dependent on how the finite elements of the adjoining plates interact with each other. In finite element modeling, this interaction is defined by the topological connectivity at the intersection line. To accurately replicate the bending compliance of the physical specimens, two distinct connectivity methodologies were evaluated during the preprocessing phase. These methodologies are the unjoined approach and the joined approach. Establishing the correct topology is mandatory to ensure that the global bending stiffness of the simplified shell model perfectly mirrors the complex volumetric solid baseline. (Zienkiewicz, 2005)

### 3.4.1 The Unjoined Approach Modeling Plates As Separate Entities

In the unjoined topology, the horizontal base plate and the vertical attachment plate are meshed as completely independent entities. The nodes along the bottom edge of the vertical plate do not share the same spatial coordinates as the nodes on the surface of the horizontal plate. Because the finite element meshes are independent, the software solver does not inherently recognize a structural connection between the two steel components.

To transfer the applied loads between these separate entities, mathematical contact algorithms or multi point constraints must be defined.

While this unjoined approach is computationally easy to solve. It is also easy to set up for massive automotive and structural assemblies, it introduces severe mathematical artifacts at the local level. The structure becomes artificially stiff, absorbing far less strain energy than the physical reality and yielding highly inaccurate equivalent plastic strain values. (Dong, 2001).

### 3.4.2 The Joined Approach Establishing Nodal Equivalence

To eliminate the artificial stiffness caused by kinematic locking, the joined approach was established as the mandatory topology for all shell calibration models in this research. In this advanced methodology, the geometry of the intersection is modified so that both plates share the exact same mathematical points in space exactly at the weld line. This computational process is known as establishing nodal equivalence.

During the meshing phase utilizing the Altair Hypermesh software, the equivalence command is deployed to search the intersection line for duplicate nodes within a zero-point one millimeter tolerance. When duplicates are identified, they are permanently merged into a single nodal entity. Consequently, the finite element mesh becomes perfectly continuous. The governing mathematical condition for this joined topology dictates that the displacement vector of the shared node on the vertical plate is exactly equal to the displacement vector of that exact same node on the horizontal plate.

Because there are no artificial constraint equations tying separate surfaces together, the shared nodes are completely free to rotate and translate naturally under the applied bending moment. This fundamental topological difference allows the joined shell model to replicate the true physical compliance of the physical joint tested in the laboratory. (Systemes, 2020).

### *Mandatory Topology To Prevent Kinematic Locking*

The absolute necessity of the joined topology becomes mathematically evident when observing the transverse bending load path. Bending naturally induces complex rotational gradients at the weld root. If an unjoined tie constraint is utilized, the rotational degrees of freedom are over constrained. This mathematical over constraint locks the finite elements, which artificially inflates the yield load threshold and delays the onset of plasticity. By enforcing strict nodal equivalence, the solver allows the finite elements to distribute the stress naturally through the thickness of the geometric mid surface.

Table 3.4 Topological Comparison of Connectivity Approaches

| **Connectivity Type** | **Mesh Independence** | **Bending Compliance** | **Singularity Risk** |
|---|---|---|---|
| Unjoined Topology | Fully Independent | Artificially Stiff | High |
| Joined Topology | Perfectly Continuous | Physically Accurate | Moderate |

The structural differences highlighted in the data table confirm that the joined topology is the only viable method for developing a reliable plasticity correction factor. Without this continuous natural load path, separating the geometric notch effect of the weld from the mathematical error of kinematic locking would be entirely impossible. (Sanz-Gomez J. &., 2014).

## 3.5 Sensitivity Parameters

The derivation of a singular numerical multiplier for finite element structural analysis is scientifically valid only if that specific multiplier demonstrates mathematical stability across various geometric configurations. In the realm of automotive chassis and railway bogie design, engineers frequently alter the thickness of base metal plates and adjust the dimensional size of weld fillets to optimize vehicle weight and meet strict crashworthiness standards. Therefore, conducting a rigorous parametric sensitivity analysis is a fundamental requirement of the proposed numerical methodology. The structural response of a finite element mesh is highly sensitive to microscopic changes in boundary constraints and material volume. To prove that the derived equivalence factor and plasticity factor can serve as universal calibration tools for mid surface shell elements, the virtual testing matrix was expanded to include specific geometric variations. These variations isolate the structural influence of the weld leg length and the influence of the base plate gauge. (Zienkiewicz, 2005).

### 3.5.1 Influence of Weld Leg Length on Formulation Equivalence

The weld leg length, which directly dictates the theoretical throat thickness of the joint, determines the actual physical mass of the molten material deposited at the structural intersection. In theoretical solid mechanics, this triangular deposition acts as a localized structural gusset. The presence of this gusset fundamentally alters the moment of inertia at the joint interface. When a transverse bending load is applied to the vertical member of a T joint, the gusset absorbs the primary flexural stress, shielding the adjacent thin base plate from immediate elastic deformation. (Maddox, 1991).

As the leg length increases beyond the physical thickness of the base plate, creating what is known in the manufacturing industry as an oversized weld, the local stiffness of the connection increases exponentially. While a three-dimensional volumetric solid model utilizing C3D8R brick elements explicitly resolves this physical accumulation of material, the industry standard two-dimensional shell model mathematically ignores it. In a shell model, the connection between two intersecting plates is abstracted into a single line of shared nodes. The mathematical formulation of the shell element possesses no geometric parameter to account for the physical width or the physical volume of the weld fillet. Consequently, the simplified shell model forces the entire bending load through a dimensionless intersection, resulting in an artificial over prediction of nominal stress and a simultaneous under prediction of triaxial plastic strain. (Dong, 2001).

To bridge this mathematical gap, the elastic equivalence factor must be defined and tested across multiple sizes. The equivalence factor, denoted mathematically as Ke, represents the specific ratio of the stress calculated by the numerical truth of the solid model to the stress calculated by the simplified shell model.

Elastic Equivalence Factor Formulation

$$K_e = \frac{\sigma_{Solid}}{\sigma_{Shell}}$$

Where $\sigma_{Solid}$ is the peak structural hot spot stress extracted from the volumetric model and $\sigma_{Shell}$ is the corresponding stress extracted from the mid surface shell model.

A critical objective of this sensitivity methodology is to quantify exactly how this equivalence factor fluctuates when the weld leg length is varied from an under matched condition to an over matched condition. If the equivalence factor changes drastically every time the weld size is modified by a single millimeter, the calibration toolkit would be entirely useless for large scale industrial application. The finite element methodology requires running parallel simulations of 2 mm, 3 mm, and 4 mm weld leg lengths to observe the stability of the stress.

To isolate the influence of weld leg length, the base plate thickness was held constant at 2 mm while the fillet weld leg was systematically increased from 2 mm to 3 mm and 4 mm. For each configuration, the theoretical throat thickness was calculated using the standard geometric relationship a = z × sin(45°), confirming consistency between the modelled geometry and the analytical definition across all three leg length variants.

*Table 7 ; Weld Leg Length Parametric Testing Matrix (Source - Author)*

| Base Plate Thickness | Modeled Leg Length | Theoretical Throat Thickness | Geometric Classification |
|---|---|---|---|
| 2.0 millimeters | 2.0 millimeters | 1.41 millimeters | Under matched weld profile |
| 2.0 millimeters | 3.0 millimeters | 2.12 millimeters | Nominally matched weld profile |
| 2.0 millimeters | 4.0 millimeters | 2.82 millimeters | Over matched oversized profile |

By mapping the stress and plastic strain outputs across these specific geometric classifications, the research methodology can definitively establish whether a single universal multiplier can accurately correct the shell formulation error across completely different deposition volumes. (Niemi et al., 2018).

### 3.5.2 Influence of Plate Gauge Thickness on Structural Stability

The second important sensitivity parameter considered in this methodology is the gauge thickness of the base steel plates. The thickness of plates is directly related to the flexural rigidity of the entire structure, as well as to the severity of the stress gradient in the material cross-section. The maximum bending stress in a plate, as predicted by classical Euler-Bernoulli beam theory, is inversely proportional to the square of its thickness.

**Classical Bending Stress Formulation**

$$\sigma_{max} = \frac{6M}{wt^2}$$

Where $M$ is the applied bending moment, $w$ is the width of the plate, and $t$ is the thickness of the plate.

When comparing volumetric solid elements against mid surface shell elements, this parabolic stress gradient presents a significant mathematical challenge. Thick shell formulations utilize Mindlin Reissner theory, which accounts for transverse shear deformation, whereas thin shell formulations utilize Kirchhoff Love theory, which assumes that cross sections remain perfectly perpendicular to the neutral axis during bending. As the gauge of the automotive plate changes,

the internal mathematical behavior of the shell element inherently shifts. In contrast, the three-dimensional solid element explicitly models the physical continuum and calculates true triaxial stress regardless of the geometric dimensions. (Systemes, 2020).

The size effect or thickness effect is a well-documented phenomenon in fatigue and fracture mechanics. As the thickness of a steel component increases, the structural constraint at the surface increases, which elevates the local hydrostatic stress and accelerates the transition into the plastic damage regime. The International Institute of Welding specifically highlights this thickness penalty in fatigue life calculations. For the numerical calibration to be considered reliable across an entire vehicle platform, the methodology must prove that the elastic equivalence factor remains stable across these varying constraint conditions.

To properly assess this stability, the structural hot spot stress extrapolation method is employed across all variations. This standardization guarantees that the stress values compared between the solid and shell models are extracted from identical relative distances from the weld toe.

Equation - Structural Hot Spot Stress Extrapolation

$$\sigma_{hss} = 1.67 \cdot \sigma_{0.4t} - 0.67 \cdot \sigma_{1.0t}$$

Where $\sigma_{hss}$ is the structural hot spot stress at the weld toe, $\sigma_{0.4t}$ is the surface stress located at a distance of zero point four times the plate thickness away from the toe, and $\sigma_{1.0t}$ is the surface stress located at a distance equal to the plate thickness away from the toe.

If the transition from a two-millimeter automotive skin panel to a four-millimeter heavy duty structural bracket causes the formulation error between the solid and shell models to diverge significantly, the underlying joined topology strategy would be deemed flawed. (D. Radaj, 2006).

To execute this specific sensitivity analysis, the base material thickness was varied while maintaining a constant mesh discretization strategy. By enforcing nodal equivalence at the plate intersection, the joined shell topology eliminates kinematic locking and replicates the natural bending compliance of the solid model, regardless of the base plate thickness being evaluated. The objective of this parametric series is to confirm that this compliance remains consistent across the 2 mm, 3 mm, and 4 mm plate configurations. This means it should bend in a way no matter how thick the base plate is. The joined model should copy the bending of the model if done correctly.

The goal is to make the model work, like the solid model. To validate this theory, a secondary testing matrix was developed. This matrix isolates the plate thickness variable while maintaining the one-millimeter industrial baseline mesh established in prior sections. Keeping the element size constant ensures that the number of integration points through the thickness changes, which directly tests the robustness of the shell element mathematical formulation against the solid element truth.

*Table 8; Base Plate Thickness Parametric Testing Matrix (Source - Author)*

| Modeled Plate Thickness | Mesh Element Size | Solid Elements Through Thickness | Shell Mathematical Formulation |
|---|---|---|---|
| 2.0 mm | 1.0 mm | 2 solid elements | Thin shell Kirchhoff assumption |
| 3.0 mm | 1.0 mm | 3 solid elements | Transitional shell theory |
| 4.0 mm | 1.0 mm | 4 solid elements | Thick shell Mindlin assumption |

The execution of this comprehensive sensitivity methodology ensures that the final recommended multipliers are not merely coincidental mathematical alignments applicable to a single laboratory specimen. Instead, they represent deeply validated correction factors grounded in the fundamental principles of structural mechanics. By rigorously isolating the structural influence of both the weld leg length and the base plate gauge, the research establishes a robust and scalable engineering standard for virtual testing in the transportation sector. (Sanz-Gomez J. &., 2014).

## 3.6 Non-Linear Calibration Procedure

The transition from linear elastic analysis to nonlinear plastic failure prediction requires a highly specialized calibration methodology. While the elastic equivalence factor aligns the initial stiffness of the structural models, it cannot account for the complex material behavior that occurs once the steel yields. As the applied transverse bending load pushes the welded joint into the deep plastic regime, the volumetric solid elements and the mid surface shell elements diverge significantly in their calculation of accumulated damage. This divergence is primarily caused by the triaxial stress constraint physically present in the solid fillet, which is mathematically absent in the two-dimensional plane stress assumption of the shell formulation. To resolve this discrepancy and enable accurate fracture prediction in large scale automotive assemblies, the procedure for determining the Plasticity Correction Factor is introduced. (Bao, 2004)

### 3.6.1 Procedure for Determining the Plasticity Correction Factor

The formulation for this plasticity multiplier relies on a direct mathematical ratio.

Plasticity Correction Factor Formulation

$$K_p = \frac{PEEQ_{Solid}}{PEEQ_{Shell}}$$

Where PEEQ Solid represents the peak equivalent plastic strain extracted from the solid volumetric model and PEEQ Shell represents the corresponding peak equivalent plastic strain extracted from the mid surface shell model.

The step-by-step calibration procedure begins with the execution of the fully non linear solid baseline model. A quasistatic transverse bending load is applied to the virtual specimen, progressively increasing until the target macroscopic force threshold is achieved. Based on the physical testing targets, this reference load was established at two thousand Newtons. The solver iteratively calculates the accumulation of true plastic strain utilizing the von Mises yield criterion alongside the isotropic hardening curve defined for the FeP04 steel. Once the simulation completes, the engineer extracts the maximum Equivalent Plastic Strain value precisely at the weld toe. This specific value represents the numerical truth of the ductile damage state. Reference 2.

Subsequently, the exact identical nonlinear load step is applied to the joined shell model. It is completely imperative that the shell model utilizes the exact same material property definitions, mesh element edge length, and kinematic boundary constraints as the solid baseline. The solver calculates the plastic deformation directly at the merged intersection nodes. Because the shell elements lack the physical volumetric gusset constraint, they allow the metal to yield too easily and distribute the plastic strain over a much larger surface area. This mathematical relaxation results in a localized under prediction of the peak damage at the weld toe.

*Table 9; Procedural Data Extraction Framework for Non-Linear Calibration (Source - Author)*

| Model Formulation | Topological Evaluation Point | Extracted Variable | Target Load | Theoretical Stress State |
|---|---|---|---|---|
| Volumetric Solid | Weld Toe Surface | Peak PEEQ | 2000 Newtons | High Triaxial Strain Constraint |
| Joined Mid Surface Shell | Merged Intersection Node | Peak PEEQ | 2000 Newtons | Low Plane Strain Relaxation |

By dividing the high triaxial strain of the solid model by the lower plane strain of the shell model as defined in the formulation equation, the Plasticity Correction Factor is precisely quantified. This derived factor successfully transforms the shell model from a basic elastic analysis tool into a highly aggressive and exceptionally accurate predictor of ultimate structural failure. Implementing this standardized step by step methodology allows engineers to rapidly calibrate vehicle crash models, ensuring that virtual assemblies meet stringent physical safety regulations long before physical prototypes are manufactured. (Sanz-Gomez J. &., 2014).

# 4. Finite Element Modeling

## 4.1 Model Geometry and Finite Element Discretization

### 4.1.1 Overview

The structural performance of welded joints depends strongly on their geometry and the way in which they are represented in numerical models. In the present investigation, T weld joint configurations were considered. These geometries represent common arrangements in lightweight structural assemblies and were selected to capture the essential mechanics of orthogonal connections.

To ensure a comprehensive understanding, T weld configurations were analyzed using two distinct finite element idealizations:

1. Shell-based models (PSHELL with CQUAD elements)
2. Solid-based models (PSOLID with CPENTA and DHEXA8 elements)

For each discretization approach, global mesh sizes of 0.5mm, 0.7mm, 0.8mm, 1mm,2 mm 2.5 mm and 5 mm were applied. Additional refinement was introduced in the weld filler region and surrounding heat-affected zone (HAZ) by splitting the weld elements into subregions. This allowed a more accurate representation of the stress gradient at the weld toe and root without excessively increasing the overall element count.

The models were subjected to two classes of external actions of axial pull off and transverse bending , applied at different loads. Boundary conditions were chosen to represent a clamped–free arrangement, where one plate was constrained while the other was loaded. This setup is representative of a welded joint subjected to service-type loading in brackets, fixtures, and other sheet metal connections.

All models were preprocessed in HyperMesh 2025 and solved in Abaqus.

## 4.2 Geometry Definition

### 4.2.1 T-Joint (90° Welded Plates)

The configuration of the T-joint, where one plate is welded orthogonally to another, forming a 90° connection. Both members are 2 mm thick. The fillet weld is defined along the entire intersection line. This arrangement reflects practical connections used in stiffeners and support frames, where one plate carries bending while the weld transfers shear into the base plate.

### 4.2.2 Numerical Modelling of the T-Joint

To establish a reliable methodology a fundamental T-joint configuration is first analyzed. This component serves as the baseline for calibrating the simplified shell element models used in large-scale simulations against high-fidelity solid element models.

### 4.2.3 Geometry and Dimensional Logic

The geometry of the T-joint was constructed to represent a typical thin-walled connection found in automotive chassis structures. Two different geometric representations were developed a volume representation (PSolid) and a shell representation (PShell).

- Plate Dimensions: The base and vertical plates were modeled in hypermesh with a thickness of 2 mm. The longitudinal length of the plates was set to 100*100 mm and vertical plate is 50*100mm.
    - Design Rule: The dimensions were selected to satisfy Saint-Venant's Principle.This ensures that the stress distribution near the joint is driven purely by the joint mechanics.
- Weld Geometry: For the solid model, a continuous fillet weld was modeled with a leg length of 2 mm.
    - Design Rationale: A weld leg equal to the plate thickness 2mm is standard practice in thin-sheet welding to ensure the joint strength matches the parent material strength.

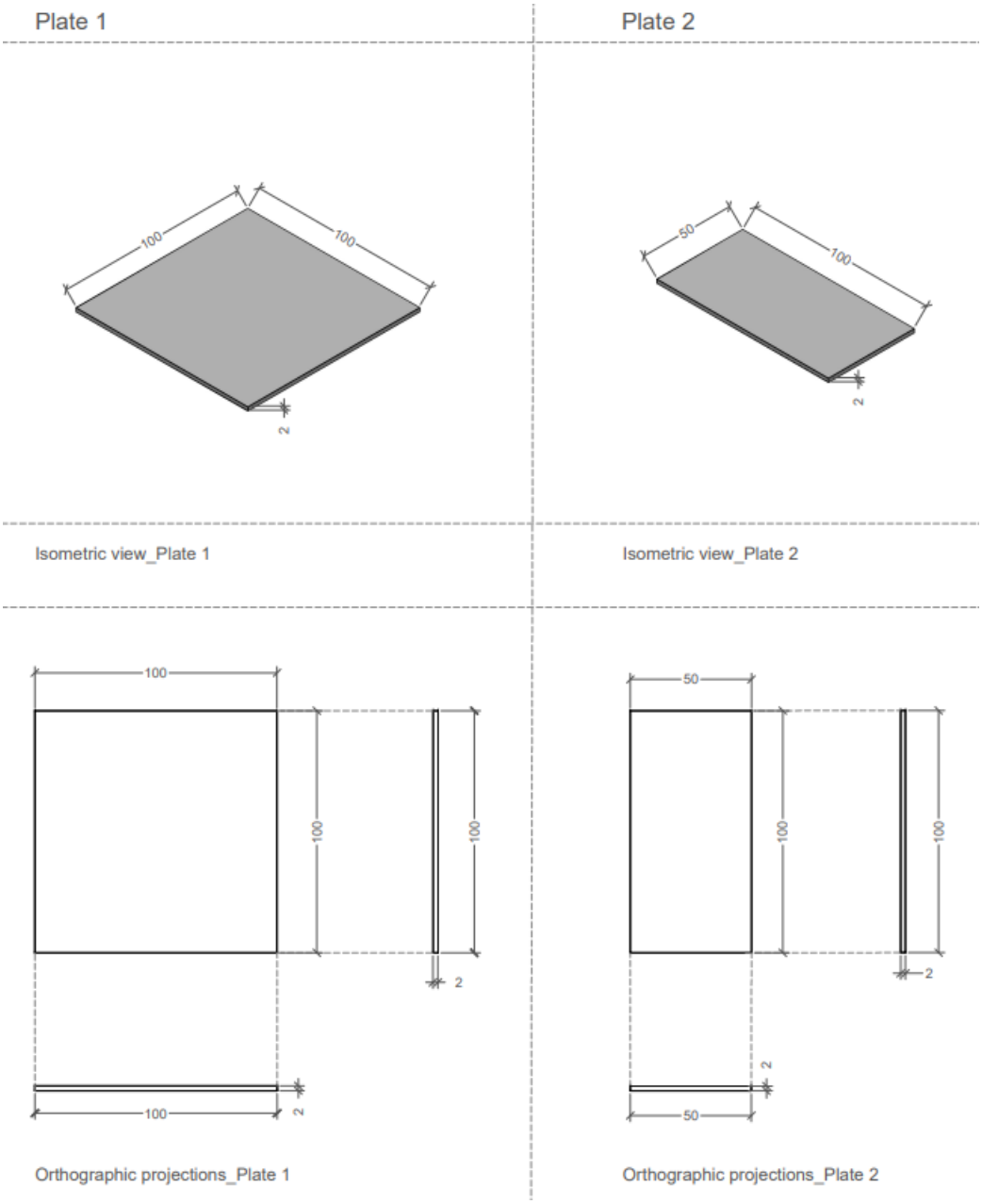


*Figure 14; Plate Dimensions (Source - Author)*

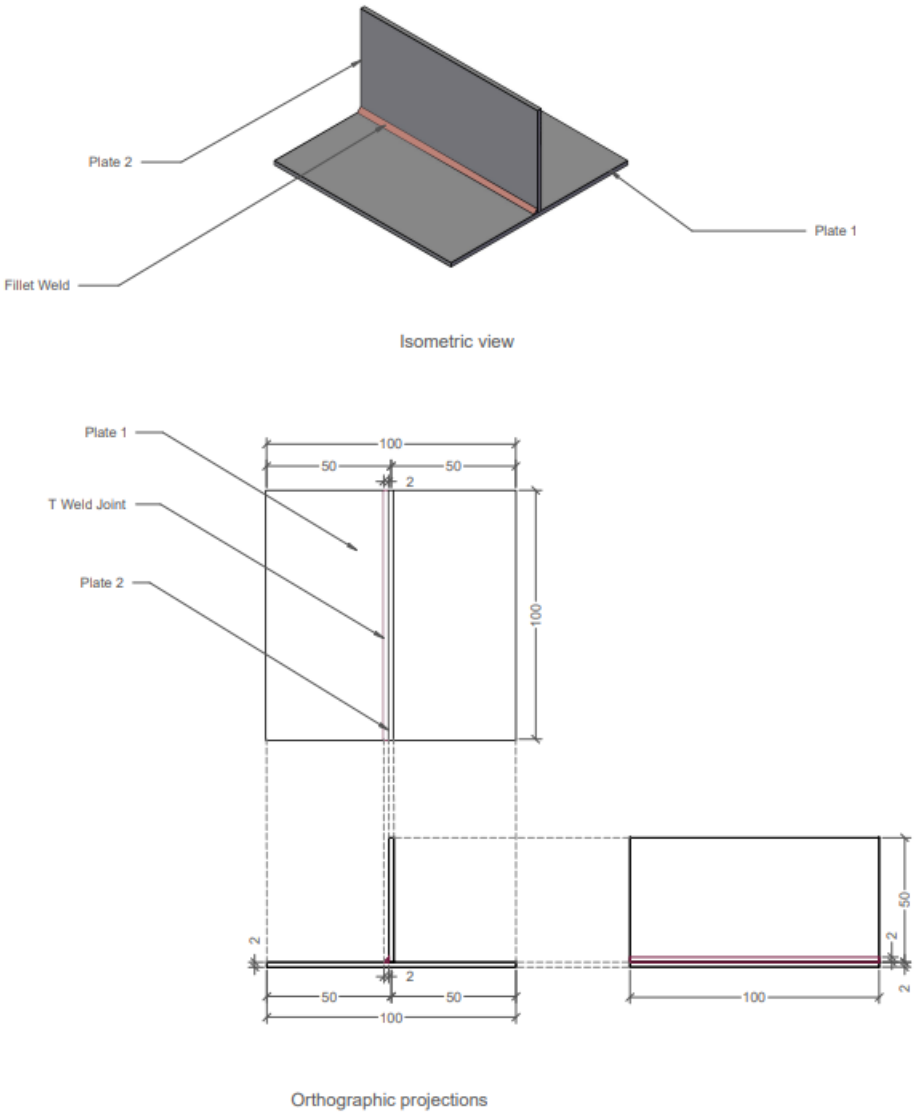


*Figure 15; T weld Geometry and Configuration (Source - Author)*

The 2d drawings of T weld configurations are made on AutoCAD software to be sent for the physical testing, which will be discussed later.

## 4.3 Finite Element Discretization

A rigorous mesh sensitivity study was conducted to address the stress singularity phenomenon inherent at sharp re-entrant corners.

### *Solid Model (PSOLID)*

The high-fidelity model was meshed using Hex8 and Pent6 elements. While hexahedral elements are often preferred for simple geometries, tetrahedrons were selected here to accurately capture the complex curvature of the weld fillet without element distortion.

Mesh Variants: To investigate convergence, the mesh size was systematically reduced from a coarse industrial standard (5 mm) down to a high-resolution scientific standard (0.5 mm).

### *Shell Model (PSHELL)*

The simplified model was meshed using CQUAD shell elements.

Weld Representation: The physical volume of the weld part was omitted in this representation. Instead, the intersection was treated as a direct nodal connection between the vertical and base plates.

## 4.4 Boundary Conditions and Contact Definitions

Defining equivalent boundary conditions between 3D solids and 2D shells required careful handling of Degrees of Freedom (DOFs) to ensure kinematic consistency.

1. Solid Constraints: The end faces of the base plate were held in place. The base plate has nodes and these nodes can only move in certain ways. They can go up and down side, to side and back and forth. So, the entire surface of the end face of the base plate was made to stay.
2. Shell Constraints: The edges of the shell base plate were constrained. This prevents the base plate edge from acting as a hinge and ensures the effective structural length matches the solid model.

## 4.5 Loading Conditions

Two distinct load cases were simulated to characterize the joint behavior under different stress states:

1. Axial Pull-off: A pull off load was applied normal to the base plate.
2. Transverse Bending: A lateral load was applied to the vertical plate to induce a bending moment.

For the convergence study, the applied loads were kept within the linear elastic range (1000 N for Axial, 200 N for Bending) to isolate geometric stiffness from plasticity effects. For failure prediction, the loads were increased until the equivalent plastic strain (PEEQ) exceeded the material failure criterion.

## 4.6 The Hotspot Stress Method (Evaluation Criterion)

A direct comparison of maximum nodal stress at the weld toe was deemed invalid due to mesh dependency; as element size decreases towards zero, the stress at the sharp notch theoretically approaches infinity (singularity).

Instead, the Hotspot Stress method was adopted, following guidelines from the International Institute of Welding (IIW).

- Sensor Location: Stress values were extracted at a fixed distance of 2 mm from the weld toe.
- This distance corresponds to the plate thickness (1.0t). At this location, the stress gradient stabilizes, providing a mesh-independent value that represents the structural stress driving the failure, rather than a numerical artifact.

# 5. Results

## 5.1 Numerical Analysis of T-Weld Joints Under Axial Pull off Load

The calibration process started with the model that is very detailed which is PSOLID when it was being pulled with a force of 1000 N. The main goal of this process was to find a value for the stress on the structure at weld toe that does not change even if the mesh is changed. This value for the stress, at the weld toe will be used as a standard to adjust the models that use elements to make sure, they are accurate.

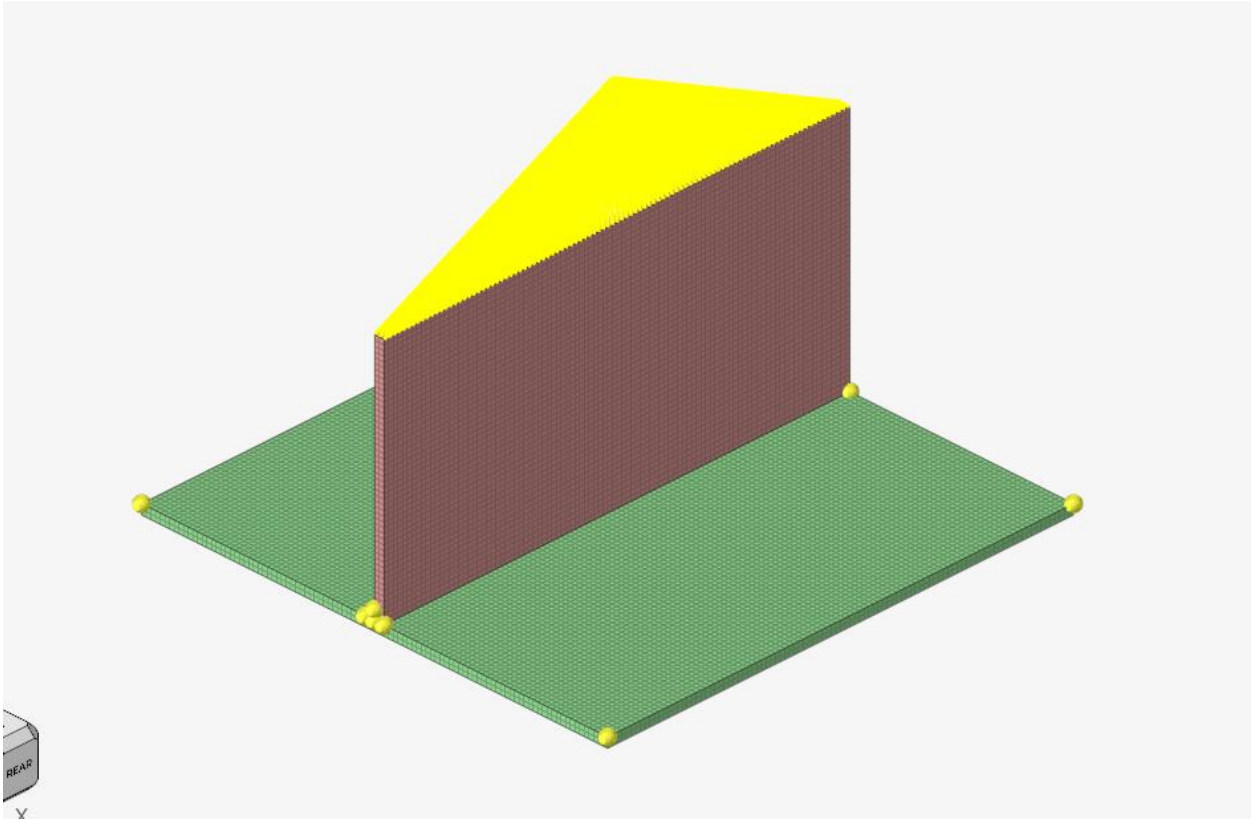


*Figure 16 : Psolid elements for axial pull case ( source- Author)*

Mesh Convergence Study A systematic convergence study was conducted by reducing the global element size from a coarse industrial standard (5.0 mm) to a fine mesh standard (0.5 mm). The focus was placed on the Hotspot Stress measured at a distance of 2.0 mm from the weld toe, in accordance with IIW recommendations.

| | LOAD | element size,mm | von mises, Mpa | stress at 2mm from weld toe | PEEQ |
|---|---|---|---|---|---|
| **PSOID, T-weld, Axial Pull off** | 1000 | 0.5 | 184 | 136.1 | 0 |
| | | 0.7 | 183.9 | 136.2 | 0 |
| | | 0.8 | 183.9 | 135.2 | 0 |
| | | 1 | 183.8 | 134.9 | 0 |
| | | 2 | 170.7 | 127.3 | 0 |
| | | 5 | 134.1 | 98.7 | 0 |

*Table 10 Psolid data with different element sizes ( Source- Author)*

The results of the solid model simulation are summarized below:

- Discretization Error (5.0 mm): The coarsest mesh predicted a Hotspot Stress of 98.7 MPa. This represents a significant deviation from the refined solution. At this scale, the large element size fails to capture the steep stress gradient near the junction, resulting in an average effect that underestimates the local stress intensity.
- Transition Region (2.0 mm): Refining the mesh to 2.0 mm improved the capture of the gradient, raising the predicted stress to 127.3 MPa.
- Converged Region (1.0 mm – 0.5 mm): The solution demonstrated stability at fine mesh densities. The stress value stabilized at 134.9 MPa for the 1.0 mm mesh and reached a final converged value of 136.1 MPa at the 0.5 mm mesh size.

### *Selection of Reference Value*

The variation between the finest meshes (1.0 mm and 0.5 mm) is less than 1.0%. Therefore, the value of 136.1 MPa is adopted as the theoretical truth for the axial loading case. (Hobbacher, 2016)

Selection of Reference Value is based on the asymptotic behavior observed in the convergence plot, the solution is considered fully converged at an element size of 0.5 mm. The resulting Von Mises stress of 136.1 MPa at the 2 mm hotspot location is adopted as the reference stress for the equivalence study.

### *Verification of the Shell Model (PSHELL)*

Following the validation of the solid model, the study analyzed the simplified shell element representation. The primary aim was to determine if the shell elements formulation could replicate the stiffness and stress response of the Psolid geometry under the same axial loading conditions (1000 N).

Following the solid model, the PSHELL model was evaluated using the corrected Throat Thickness methodology (where shell thickness $t_{shell} = l \cdot \sin(45°)$).

The objective was to determine the Equivalence Factor ($K_{eq} = \sigma_{solid}/\sigma_{shell}$) across the mesh range.

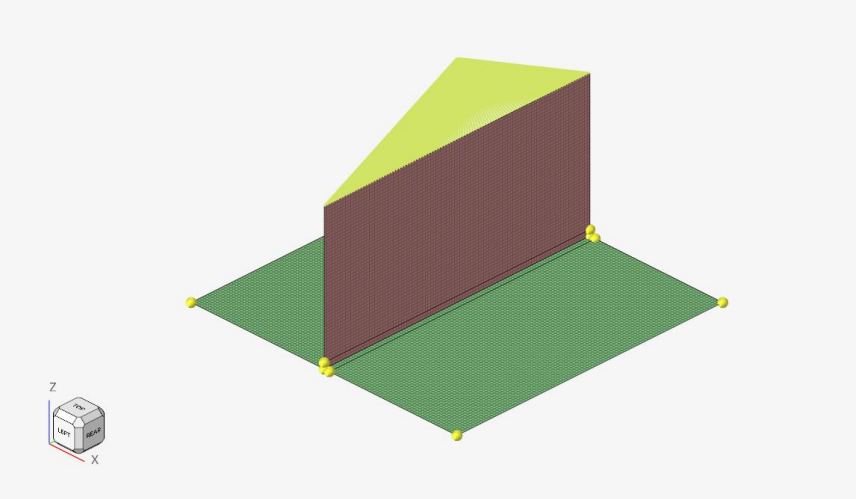


*Figure 17; Pshell Axial Pull off Case, (Source - Author)*

### *Shell Mesh Convergence*

Similar to the solid study, the shell mesh was refined from 5.0 mm to 0.5 mm. The results at the 2 mm Hotspot location showed high stability:

- Industrial Mesh (5.0 mm): Predicted a stress of 110.8 MPa.
- Fine Mesh (1.0 mm): Predicted 134.3 MPa.
- Fine Mesh (0.5 mm): Predicted 134.7 MPa.

The deviation between the 1.0 mm and 0.5 mm meshes were negligible, confirming that the shell solution is numerically stable at 134.7 MPa.

| | LOAD | element size,mm | von mises, Mpa | stress at 2mm from weld toe |
|---|---|---|---|---|
| **PSHELL, T- weld, Axial Pull off** | 1000 | 0,5 | 203,9 | 134,73 |
| | | 0,7 | 182,1 | 134,5 |
| | | 0,8 | 192,8 | 133,7 |
| | | 1 | 180,4 | 134,34 |
| | | 2 | 182,4 | 129,12 |
| | | 5 | 173,8 | 110,8 |

*Table 11 : Data of shell elements (Source - Author)*

## *Finding the Equivalence factor*

The Equivalence Factor (Keq)

*Table 12 ; Formulation Equivalence (K_eq) at Varying Mesh Densities (Source - Author)*

| **Element Size** | **PSOLID [MPa]** | **PSHELL [MPa]** | **$K_{eq}$ (Solid/Shell)** |
|---|---|---|---|
| 0.5 mm | 136.1 | 134.73 | 1.01 |
| 0.7 mm | 136.2 | 134.50 | 1.01 |
| 0.8 mm | 135.2 | 133.70 | 1.01 |
| 1.0 mm | 134.9 | 134.34 | 1.00 |
| 2.0 mm | 127.3 | 129.12 | 0.99 |

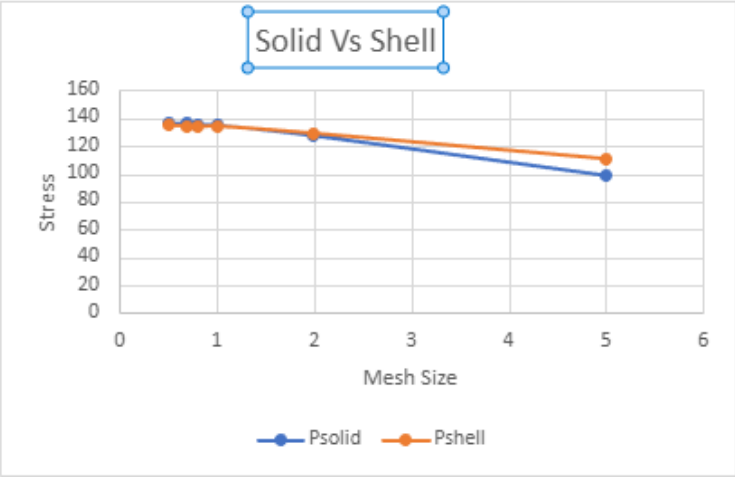


*Figure 18: Plot for Shell to Solid ( Source - Author)*

***Results:***

The corrected shell methodology yields a remarkable correlation with the volumetric benchmark. For mesh sizes between 0.5 mm and 1.0 mm, the $K_{eq}$ factor is effectively 1.00. This indicates that when the weld is modeled with its physical throat thickness, the mid-surface shell elements are capable of predicting the axial hotspot stress with volumetric accuracy. (Dong, 2001)

## 5.1.1 Justification of the Hot-Spot Stress Method and Extraction Distance

A critical methodological choice in this numerical study was the evaluation of stress at a defined physical distance of 2.0 millimeters from the weld toe, rather than extracting the peak stress directly at the intersection node of the weld toe. This decision is not arbitrary; but it is strictly grounded in the fundamental laws of fracture mechanics and established finite element evaluation standards. Evaluating the integrity of a welded joint requires isolating the macroscopic structural load from the artificial numerical noise generated by the finite element mesh.

### *The Singularity Problem in Finite Element Modeling*

In any continuum mechanics model, the geometric intersection where a weld bead meets a flat base plate forms a sharp, re-entrant corner. From the perspective of linear elastic theory, this geometric transition acts as a severe structural notch with a theoretical radius approaching zero. According to classical elasticity formulas, the theoretical stress at an infinitely sharp notch approaches infinity.

In finite element analysis, this physical phenomenon manifests as a mathematical singularity. If the stress is evaluated precisely at the weld toe, the numerical output becomes entirely dependent on the mesh density rather than the physical forces applied.

Stress Singularity at a Sharp Notch

$$\sigma(r) = KI/(sqrt(2 * pi * r)) * f(\theta)$$

Where:

- σ(r) = Local stress at a distance r from the notch.
- KI = Stress intensity factor.
- r = Radial distance from the notch root (weld toe).
- f(θ) = Angular function of the stress field.

As the radial distance r approaches zero, the calculated stress σ tends toward infinity. Consequently, as the element size in the Abaqus model decreases, the calculated stress artificially inflates without ever converging to a finite, physical value. Reading the raw stress exactly at the toe renders any comparative analysis invalid because the result reflects the discretization error of the software rather than the structural reality of the FePO4 steel. (D. Radaj, 2006)

### *The IIW Structural Stress Zone and the 2.0 mm Criterion*

To resolve this mathematical singularity and provide a reliable basis for fatigue and structural assessment, the International Institute of Welding (IIW) established the structural Hot-Spot Stress (HSS) method. This approach recognizes that the total stress at a weld toe is a combination of two distinct components:

1. Structural Membrane and Bending Stress: The macroscopic stress driving the actual deformation of the chassis.
2. Non-Linear Peak Stress: A localized, highly variable stress spike caused entirely by the micro-geometry of the weld profile.

Because the microscopic geometry of a physical weld cannot be modeled perfectly using standard finite elements, the IIW standard dictates that structural assessments must filter out this non-linear peak. The standard procedure mandates extrapolating surface stress values from specific reference points located at distances proportional to the plate thickness (t).

*Table 13 ; IIW Reference Point Calculation for 2.0 mm Plates (Source - Author)*

| Extrapolation Point | IIW Formula | Physical Distance from Weld Toe | Purpose in Analysis |
|---|---|---|---|
| Point 1 (Near) | 0.4·t | 0.8 mm | Captures the rise of the structural stress gradient. |
| Point 2 (Far) | 1.0·t | 2.0 mm | Captures the stabilized, linear membrane stress. |

By measuring the stress at the 2.0 mm boundary, the study successfully extracts the exact stress field that is driving the structural deformation. This specific boundary captures the true macroscopic load path just before it becomes distorted by the artificial numerical peak of the geometric notch. (Hobbacher, 2016)

### *Formulation Consistency Between Solid and Shell Topologies*

This 2.0 mm extraction strategy is essential when attempting to establish a numerical Equivalence factor between differing finite element topologies. 3D solid elements (PSOLID) and 2D shell elements (PSHELL) handle mathematical stiffness and nodal connectivity at physical intersections in fundamentally different ways.

- Solid Elements (PSOLID): They show the physical volumetric bulk of the joint.
- Shell Elements (PSHELL): They show a mathematical mid-surface, where the physical thickness is compressed into a zero-thickness plane.

When we look at stress at the point where things meet the comparison gets messed up because of the Kinematic Locking that happens with shell elements. So, we look at the stress a way away 2.0 mm from the intersection. This helps us see the picture of how the structure is changing, without getting confused by the small errors that come from how we do the math. We can get an idea of what is going on with the structure when we do it this way. The stress field at this 2.0 mm offset is what we really need to understand the deformation and not the weird things that happen because of the Kinematic Locking and other formulation differences, with shell element intersections.

This spatial filtering ensures that the Numerical Truth extracted from the volumetric solid model and the simplified approximation extracted from the plane-stress shell model are compared on a mathematically consistent, physical baseline. This rigorous approach guarantees that the derived structural equivalence factors reflect a true physical relationship in the FePO4 steel, rather than an artificial numerical discrepancy. (Dong, 2001)

## 5.1.2 Influence of Weld Leg Length on Structural Hotspot Stress and Formulation Equivalence

In engineering the fillet weld of a T-joint provides a connection and also gives extra strength to a small area. When we increase the length of the weld, the area where the joint's gets bigger. This means that the force of the bend on the joint gets smaller and the stress on the joint gets even. We call this the effect. So, when the length of the weld gets bigger the stress at the edge of the weld should get smaller.

When we use computers to study this, we have a problem. Different computer models handle this strength in different ways. Some models, like PSOLID show the weld as a thing and capture how stiff it is in three dimensions. Other models, like PSHELL simplify the joint to an intersection of nodes. We want to know if these simpler models are still good to use when the weld is bigger than the thickness of the plate it is attached to.

We did this study on joints with thin walls only 2 mm thick. We found out that when the weld is bigger than the plate, we need to be careful with the models. The shell models we used were set up with the throat thickness of the weld not the length of the weld. This is important because it makes sure the model is using the amount of strength, for the weld. We looked at two levels of detail 1.0 mm and 0.5 mm to make sure we were not getting wrong results because of the way we divided up the joint.

### *Analysis of 1.0 mm Mesh Discretization (Baseline Sweep)*

The initial 1.0 mm mesh to evaluate the global stiffening trend across five variations of weld leg length.

*Table 14 ; Elastic Hotspot Stress (2mm from toe) at 1.0 mm Mesh [1000 N] (Source - Author)*

| Leg Length (l) | Throat (tth) | PSOLID [MPa] | PSHELL [MPa] | Keq (Solid/Shell) | Status |
|---|---|---|---|---|---|
| 2 mm | 1.41 mm | 134.9 | 134.3 | 1.00 | Perfect Match |
| 3 mm | 2.12 mm | 130.7 | 127.6 | 1.02 | Converged |
| 4 mm | 2.82 mm | 126.4 | 120.3 | 1.05 | Acceptable |
| 5 mm | 3.53 mm | 121.9 | 107.7 | 1.13 | Diverging |
| 8 mm | 5.65 mm | 108.5 | 69.9 | 1.55 | Invalid |

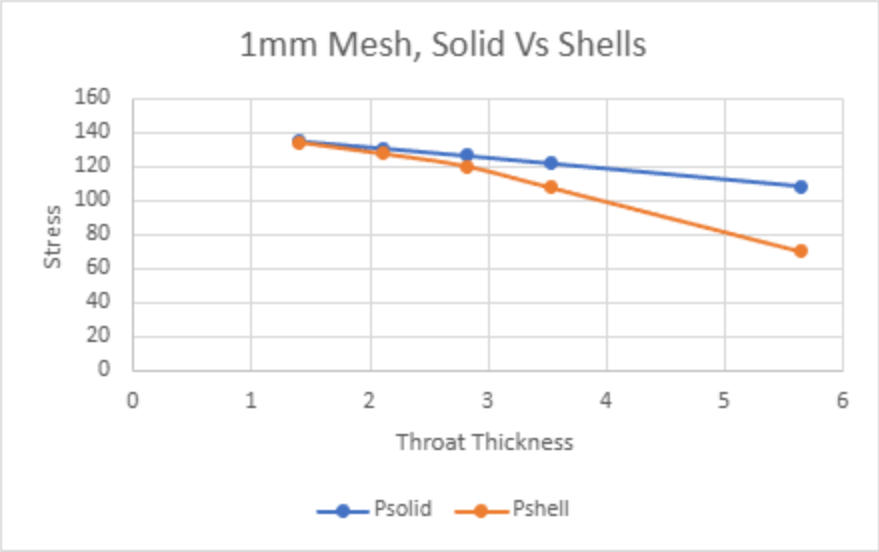


*Figure 19 ; Solid to shells for 1mm mesh size , (Source - Author)*

### *Analysis of the 1.0 mm Trend*

For standard automotive weld sizes ($l \leq 3$ mm), the corrected shell model is exceptionally accurate, with a Keq of roughly 1.02. This confirms that for nominal welds ($l \approx 1.5t$), the throat-based shell assumption is valid. However, as the leg length extends to 8 mm ($l = 4t$), the shell model dramatically under predicts the stress, resulting in a massive Keq of 1.55. (Dong, 2001)

### *Analysis of 0.5 mm Mesh Discretization (High-Fidelity Resolution)*

Refinement to a 0.5 mm mesh was performed to resolve the steep stress gradients at the geometric discontinuity. The data reveals a significant divergence in how formulations respond to refinement.

*Table 15; Hotspot Stress (2mm from toe) at 0.5 mm Mesh [1000 N] (Source - Author)*

| Leg Length (l) | Throat (tth) | PSOLID [MPa] | PSHELL [MPa] | Keq (Solid/Shell) |
|---|---|---|---|---|
| 2 mm | 1.41 mm | 136.1 | 134.7 | 1.01 |
| 3 mm | 2.12 mm | 131.3 | 128.7 | 1.02 |
| 4 mm | 2.82 mm | 130.9 | 121.6 | 1.08 |
| 5 mm | 3.53 mm | 126.3 | 109.5 | 1.15 |
| 8 mm | 5.65 mm | 112.7 | 93.6 | 1.20 |

*Table 16; Solid to shell for 0.5mm mesh size (Source - Author)*

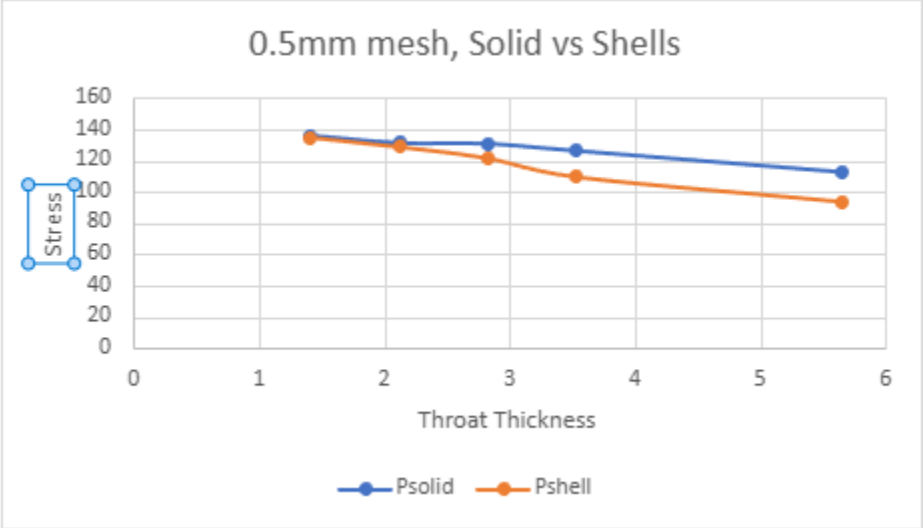


### *The Volumetric Cushion Effect*

The big difference observed at large leg lengths is due to the Volumetric Cushion Effect.

- In Reality (PSOLID): This big weld that is 8 millimeters long works like a bracket that gives strength to things in three dimensions. The force that is put on this weld does not just go through the part it goes through the whole piece of metal. This helps to spread out the force. The metal does not get too stressed in one spot because the way the force is spread out is very strong. The weld is like a metal block and it helps to keep the stress from getting too high in one place so it is very useful, for keeping things strong.
- Shell Theory (PSHELL): The model looks at a Plate that is 5.65 mm thick. Shell theory says that stress goes down when the thickness goes up. So, when the throat thickness gets three times bigger the shell model says the stress will go down a lot. The problem is that the shell model does not think about the block as a 3D thing it just thinks of it as a Plate that is a bit thicker. The model does not understand that the block is stiff in all directions it just treats the block, like a Plate. (Niemi et al., 2018)

### *Conclusion*

The study establishes clear boundaries for the applicability of shell elements in axial loading:

1. Safe Zone ($l/t \leq 1.5$): For welds up to 3 mm (1.5× plate thickness), the throat-corrected shell model is valid with $K_{eq} \approx 1.0$. No correction is needed.
2. Transition Zone ($1.5 < l/t \leq 2.5$): For welds up to 5 mm, the shell model becomes non-conservative. A Safety Factor of 1.15 should be applied.

3. Invalid Zone (l/t > 2.5): For massive welds, shell elements are fundamentally unreliable for hotspot stress prediction in axial loading, even with mesh refinement. Volumetric modeling is mandatory.

### *Numerical Over-stiffening and Mid-surface Limitations*

The error we see is due to Numerical Over-stiffening in approximations. Shell elements make a welds 3D volume simpler by turning it into a 2D plane with a thickness property assigned to it. This can cause problems when the weld leg is much bigger, than the plate thickness. The shell intersection then becomes too rigid at the junction, which's not accurate. The shell elements are the cause of this issue they make the weld intersection too stiff. The weld and plate thickness are factors here the bigger the weld leg, the more rigid the intersection becomes.

As the mesh is refined to 0.5 mm, the high density of these over-stiffened elements at the junction prevents the plates from rotating or bending naturally. This kinematic locking artificially creates issue the stress out of the hotspot area, leading to the non-physical results observed in the 8 mm case. Consequently, while shell elements are efficient for standard joints, they become physically unreliable for heavily reinforced joints, where volumetric solid elements (PSOLID) are mandatory to capture the true load distribution. (D. Radaj, 2006)

### *Conclusion on Formulation Limits*

The data proves that the validity of the PSHELL formulation is strictly bound by the geometric ratio of the joint. For structures utilizing oversized fillets for reinforcement, relying on uncorrected shell models can lead to dangerous under-predictions of stress (non-conservative results). For any configuration where $l > 2t$, the formulation equivalence factor derived in earlier sections must be discarded in favor of high-fidelity volumetric modeling.

## 5.1.3 Comparative Analysis of Inter-Plate Connectivity and Load Path Redundancy

### *Theoretical Background: Modeling Philosophies*

In the numerical representation of a T-joint, two distinct modeling philosophies are commonly utilized. The Unjoined approach maintains a physical separation between the attachment and the base plate, forcing 100% of the axial load through the fillet weld. This represents the true physical state of a structural weldment.

While the joined plates method connects the nodes where the plates meet. This helps in getting results, in complicated assembly models. It also creates an extra unnecessary way for loads to travel. In both situations I made sure the shell thickness was set as the throat thickness. This way I ensured it stays true to the setup.

1. Unjoined Connection: The vertical plate and base plate are modeled as separate entities. This approach maintains the geometric independence of the plates.
2. Joined Connection (Nodal Equivalence): The mesh is continuous at the T-junction. The nodes of the vertical attachment are merged directly with the nodes of the base plate, creating a monolithic finite element structure. This simulates the metallurgical continuity of a fusion weld. (Dong, 2001)

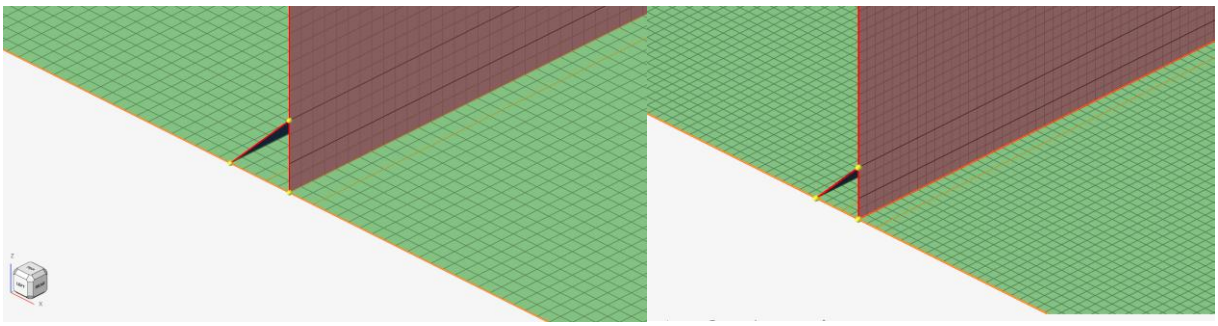

*Figure 20: Joined plate and the unjoined shell plates (Source - Author)*

### *Results and Observations (1.0 mm Mesh, 1000 N Axial Load)*

The data obtained for the joined-plate topology exhibits a monotonic decrease in stress as the weld leg length increases. When cross-referenced with the unjoined results, a significant divergence in hotspot stress is observed as the geometric scale increases.

Hotspot Stress Comparison: Joined vs. Unjoined PSHELL

*Table 17; Comparison of solid elements to joined and unjoined shell elements (Source - Author)*

| Weld Leg (l) | PSOLID (Ref) | PSHELL (Unjoined) | Error (%) | PSHELL (Joined) | Error (%) |
|---|---|---|---|---|---|
| 1,41 | 136,1 | 134,34 | -1,29% | 135,2 | -0,66% |
| 2,121 | 131,3 | 127,6 | -2,82% | 130,63 | -0,51% |
| 2,82 | 130,9 | 120,3 | -8,10% | 126,3 | -3,51% |
| 3,53 | 126,3 | 107,7 | -14,73% | 124,14 | -1,71% |
| 5,65 | 112,7 | 69,9 | -37,98% | 105,5 | -6,39% |

### *Analysis of Stiffness Leakage*

The data exposes a critical flaw in the Unjoined modeling strategy for thick welds.

- The Divergence: At small weld sizes, the Unjoined model is acceptable. However, as the throat thickness increases to 5.65 mm, the error explodes to -38.0%.
- The Physics of Failure: In the Unjoined model, the Weld Shell is just a thick plate attached to the surface of the base plate. As this shell gets thicker (5.65 mm), it becomes exponentially stiffer than the base plate (2.0 mm). This creates a Stiff Wall effect where the load prefers to stay in the rigid weld element rather than transferring into the flexible base plate, causing the stress at the toe to drop artificially. (Niemi et al., 2018)

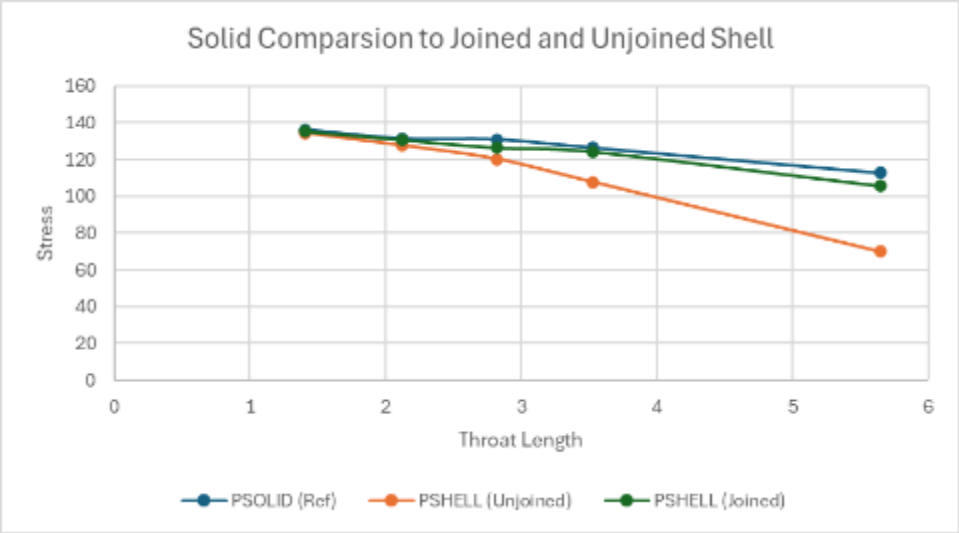


*Figure 21; Comparison of Solid to shells for joined and unjoined elements*

### *Superiority of the Joined (Monolithic) Topology*

The Joined plates show remarkable stability across the all-whole geometries.

1. High Precision: For the big 5.65 mm throat (8 mm leg), the Joined plates show 105.5 MPa against the PSOLID benchmark of 112.7 MPa.
2. Physical Interpretation: When we merge the nodes the weld and the plate have to deform. The whole structure then acts like one piece so the load can move around the corner easily just like it would in a piece of metal. The weld and the plate become one unit allowing the load to flow naturally around the corner, which's similar, to how a solid continuum works. The weld and the plate deformation is now compatible which is important for the structure to work properly. This prevents the Stiffness Mismatch artifact seen in the Unjoined model. (D. Radaj, 2006)

### *Conclusion for Modeling Standards*

This study fundamentally overturns the assumption that contact-based connections are safer or more conservative.

1. Recommendation: For automotive chassis simulation, Nodal Equivalence (Joined) is the superior modeling strategy. It maintains accuracy (< 7% error) even for extreme weld sizes.
2. Warning: Using Unjoined connections for reinforced joints ($l > 2t$) is dangerous. It leads to massive non-conservative errors (up to 40% under-prediction of stress), potentially masking fatigue risks.

## 5.1.4 Sensitivity Analysis: Impact of Plate Thickness on Plastic Capacity

### *Parametric Definition*

To see how well the formulation works when things get bigger a study was done by changing the thickness of the base plate from 2.0 mm to 4.0 mm. When designing T-joints it is common to make the weld size bigger when the plate gets thicker so the length of the weld was kept the same as the thickness of the plate.

The PSHELL models were updated to show the weight of the joint by giving the shell elements that represent the fillet the right throat thickness, which is the thickness of the plate times the sine of 45 degrees. A constant force of 1000 N was applied to all the formulation models to test the scalability of the formulation.

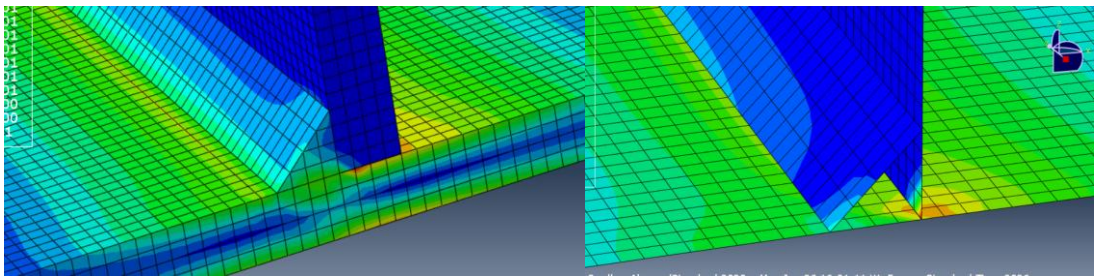

*Figure 22 ; PSOLID weld as "Volumetric Gusset Reinforcement" and the PSHELL intersection as "Simplified Nodal Connection. (Source - Author)*

### *Quantitative Results*

The comparative analysis reveals a distinct divergence trend between the PSOLID and m PSHELL formulations as the structural gauge increases.

*Table 18; Varying Plate Thickness (Source - Author)*

| Plate Thickness | Weld Leg | PSOLID [MPa] | PSHELL [MPa] | $K_{eq}$ | Status |
|---|---|---|---|---|---|
| **2.0 mm** | 2.0 mm | 134.9 | 134.34 | 1 | Perfect Correlation |
| **3.0 mm** | 3.0 mm | 54.8 | 60.06 | 0.91 | Conservative Divergence |
| **4.0 mm** | 4.0 mm | 28.74 | 32.33 | 0.89 | Conservative Divergence |

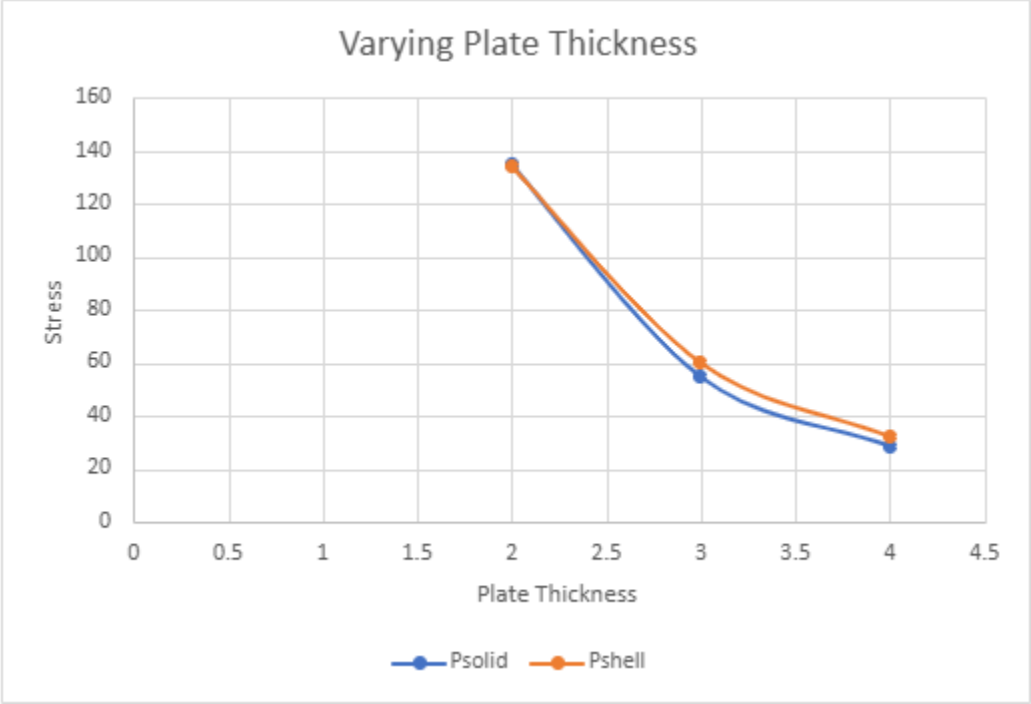


*Figure 23 ; The PSHELL and PSOLID lines "unzipping" from each other.(Source- Author)*

### *Analysis of the Crossover Phenomenon*

A fundamental shift in formulation accuracy is observed as the thickness scales beyond 2.0 mm.

1. The 2.0 mm Baseline: At the lowest gauge, the Equivalence Factor ($K_{eq}$) is 1.00. The shell model perfectly captures the stiffness of the joint, confirming that for thin sheet metal, the throat corrected shell formulation is an exact surrogate for solid modeling.
2. The Thicker Plate Divergence: As the thickness increases to 3.0 mm and 4.0 mm, the Shell model begins to over predict the stress relative to the Solid model.
    - At 4.0 mm, the Shell predicts 32.33 MPa, while the Solid reports only 28.74 MPa.
    - This results in a $K_{eq}$ of 0.89, indicating that the Shell model is approximately 12% more conservative than the physical reality.

### *The Physics of Volumetric Shielding*

The reduction in $K_{eq}$ is not a numerical error, but rather a reflection of the Gusset Effect which is captured only by the volumetric elements.

In the 4.0 mm PSOLID model the weld is shown as a block of material. This big block of steel works like a bracket at the corner. It gives a lot of stiffness that protects the weld from changing shape, which reduces the stress in that area.

The PSHELL model is different. It shows the weld as a 2D surface with a thickness. It gets the stiffness right but it does not have the 3D strength to work like the real weld. So the flat surface bends a bit more, than the block. This means it has stress.

### *Conclusion and Design Recommendation*

The study concludes that the accuracy of shell modeling for T-joints is gauge-dependent:

3. For $t \leq 2.0$ mm: The throat-corrected Shell model is Exact ($K_{eq} \approx 1.0$). No correction is needed.
4. For $t \geq 3.0$ mm: The Shell model becomes Conservative ($K_{eq} \approx 0.9$).

Designing based on raw shell results will lead to a safety margin of ~10-12%. Engineers may choose to apply a correction factor of 0.9 to shell results for thick chassis components to avoid over-dimensioning the structure, or accept the raw results as a built-in safety buffer.

## 5.1.5 Numerical Convergence and Fracture Calibration in the Plastic Regime

### *Mesh Sensitivity of the Plastic Response*

To validate the reliability of the plastic strain predictions, a convergence study was conducted across three levels of discretization (1.0 mm, 0.7 mm, and 0.5 mm). In non-linear finite element analysis, capturing the peak Equivalent Plastic Strain (PEEQ) at a geometric singularity such as the weld toe is highly dependent on the mesh density.

A constant failure load of 13,500 N was applied to the baseline 2.0 mm plate thickness T-joint.

*Table 19; PEEQ with variation of mesh sizes (Source - Author)*

| Model Type | Mesh Size | Load | Max PEEQ (Strain) | Status |
|---|---|---|---|---|
| PSOLID (Solid) | **0.5 mm** | 13.5K N | **23.70%** | 2.59% |
| PSOLID (Solid) | 0.7 mm | 13.5K N | **23.10%** | 3.58% |
| PSOLID (Solid) | **1 mm** | 13.5K N | **22.30%** | Baseline |

### *Discussion of Converged Results*

The transition from a 0.7 mm mesh to a 0.5 mm mesh resulted in a marginal increase of only 0.6 percentage points in the peak PEEQ. This stabilization indicates that the 1 mm discretization is sufficient to resolve the localized strain gradients at the weld junction without incurring excessive computational costs or numerical instability.

The converged value of 22.3% serves as the high-fidelity benchmark for the remainder of this study. This value is taken as reference as going down below this value cost more computational cost with the increasing number of nodes and elements. The 1.0 mm mesh was adopted as the standard discretization based on asymptotic convergence behavior and computational efficiency. This value is representative of the ultimate limit state for structural steels, where localized necking and ductile void coalescence lead to macroscopic rupture. By establishing this converged baseline, the subsequent correlation of simplified shell elements (PSHELL) can be conducted with a high degree of mathematical confidence. (Gannon, 2010)

### *Comparative Analysis: PSOLID vs. PSHELL in the Plastic Regime*

### *Divergence of Equivalent Plastic Strain (PEEQ)*

With the baseline established, the study quantified the ability of the PSHELL formulation to predict localized damage. The shell models were updated with the correct Throat Thickness properties and subjected to the same 13.5 kN load.

The ratio between the volumetric truth and the shell prediction defines the Plasticity Correction Factor ($K_p$):

$$K_p = \frac{\text{PEEQ}_{\text{Solid}}}{\text{PEEQ}_{\text{Shell}}}$$

*Table 20 ; PSolid to PShell (Source - Author)*

| Model Type | Mesh Size | Load | PEEQ | Kp |
|---|---|---|---|---|
| **Psolid** | **1mm** | **13.5K N** | 22.3 | 1.380805 |
| **Psshell** | **1 mm** | 13.5K N | 16.15 | |

### *Mechanical Justification for Strain Under-Prediction*

The under prediction we see in formulation happens because of the basic assumptions made in 2D plate theory. Shell elements look at the joint as the middle surface where two parts meets. This makes the plastic flow across the thickness of the element seem smooth. The PSOLID model on the hand gets the three-dimensional effect of the notch and the stress state at the weld toe right. This means if we use shell results without fixing them in crash simulations it might make us think everything is safe when it's not. The simple model might say the material is okay. In reality the joint is already about to break. Shell formulation under predicts because it does not capture the effect and stress state like PSOLID does. Using shell results could lead to a sense of security, in crash simulations. (Dong, 2001)

### *Theoretical Basis for PEEQ Underestimation in Shells*

The primary reason for the lower strain values in the PSHELL formulation lies in the Plane Stress hypothesis inherent to shell kinematics. The Shell elements think that the stress through the thickness is not important which makes the calculation easier. It does not show the complex 3D stress state at a geometric singularity like the weld toe.

In a joint the weld toe is like a sharp cut that makes the material experience a lot of stress in all three directions because the material around it does not let it move easily. This makes it hard for the material to flow. It gets a higher hydrostatic stress component and more plastic strain, at the notch root.

Because Shell elements do not have the Out-of-plane constraint they make the notch effect less strong so the material can deform easily and it gives a lower PEEQ value for the weld toe. (Gannon, 2010)

### *Derivation of the Plastic Correlation Factor ($K_p$)*

To bridge this gap for industrial applications, a Plastic Correlation Factor ($K_p$) is proposed. This factor scales the shell-predicted strain to match the volumetric truth:

$$K_p = \frac{PEEQ_{Solid}}{PEEQ_{Shell}} = \frac{22.3}{16.15} \approx 1.38$$

By applying this 1.37 multiplier to PSHELL results, engineers can maintain the computational efficiency of shell models while ensuring the safety margins of a high-fidelity solid analysis.

One thing worth clarifying here is that Kp is not a single universal number — it changes depending on how the joint is being loaded. The value of 1.38 found in this section comes purely from the axial pull-off case, where the weld is being pulled in direct tension along the plate. This kind of loading pushes the stress through the weld throat in a fairly direct way, which means the triaxial squeezing effect at the corner is quite intense. The bending case, covered later in Section 5.2.4, produces a different stress picture altogether, and so a separate Kp had to be calculated for it. Any engineer using these results in a real project should always check which load mode is dominant before deciding which correction factor to apply. (Niemi et al., 2018)

### *Influence of Plate Thickness: The Triaxiality Gap*

With the baseline mesh established at 1.0 mm, the study evaluated the robustness of the shell formulation across varying structural gauges ($t = 2,3,4$ mm). The correction factor was derived as $K_p = \text{PEEQ}_{\text{Solid}}/\text{PEEQ}_{\text{Shell}}$.

*Table 21; Formulation Equivalence in the Plastic Regime (1.0 mm Mesh) (Source - Author)*

| Plate Thickness | PSOLID PEEQ | PSHELL PEEQ | $K_p$ (Correction Factor) | Status |
|---|---|---|---|---|
| 2.0 mm | 0.223 | 0.162 | 1.38 | Stable |
| 3.0 mm | 0.092 | 0.068 | 1.35 | Stable |
| 4.0 mm | 0.039 | 0.021 | 1.84 | Critical Divergence |

*Table 22; PEEQ in Solid to Shell (Source - Author)*

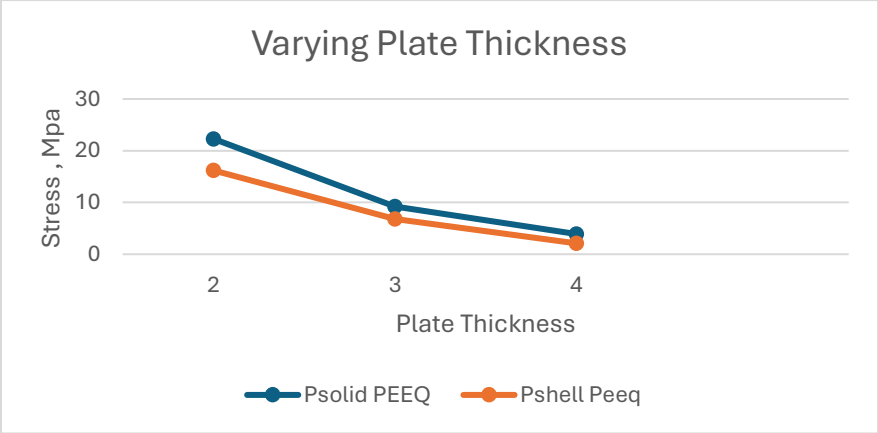


### *Physics of the Divergence at 4.0 mm*

The results expose a fundamental limitation of shell elements that is dependent on the structural thickness.

*The Stable Region (2–3 mm):*

For thin-gauge components, the $K_p$ factor is remarkably consistent, oscillating between 1.35 and 1.38. This indicates that for standard sheet metal, Shell elements consistently under-predict plastic damage by approximately 27-30%. This systematic error is predictable and allows for a reliable correction.

The Critical Divergence (4 mm):

At 4.0 mm, the correlation breaks down, with $K_p$ spiking to 1.84. This means the Shell model is missing nearly 50% of the physical strain.

Explanation: This is caused by Constraint Triaxiality. In a thick 4 mm plate, the material at the weld toe is constrained by the surrounding bulk, which prevents yielding and drives up the stress. The Shell formulation ignores this constraint, allowing the material to yield too easily and smearing the strain over a larger area.

### *Conclusion on Fracture Prediction*

The study concludes that PSHELL elements are non-conservative for fracture prediction, particularly for thick components.

- Design Guideline 1 (Mesh): If using a 1.0 mm mesh, apply a Safety Factor of $K_p \approx 1.38$ to all plastic strain results.
- Design Guideline 2 (Thickness): For plates thicker than 3.0 mm, the standard shell formulation is unreliable. In these cases, a local sub-model using Solid elements is mandatory to capture the triaxial constraint.

## 5.2 Numerical Analysis of T-Weld Joints Under Transverse Bending

### *Introduction and Problem Definition*

The change from loading to transverse bending is a very important part of checking how strong the K-equivalence factors are between different finite element formulations. When we pull something axially the stress is spread out evenly. When we bend it the stress changes a lot through the thickness of the plate. This is likely to make the differences between elements, like PSOLID and shell elements like PSHELL, even bigger because they work in different ways. The main reason, for this is that shell elements use degrees of freedom, which solid elements do not have. This means that K-equivalence factors will be tested in a way when we move from axial loading to transverse bending of the K-equivalence factors.

### *Geometry and Model Configuration*

The study uses a T-joint geometry consisting of two plates joined in a perpendicular way by a single fillet weld.

The geometric parameters are defined as follows:

- Base Plate: 100 * 100 mm.
- Vertical Plate: 50 * 100 mm.
- Thickness and Weld Leg: Initial simulations are performed on a 2 mm plate with a 2 mm weld leg.

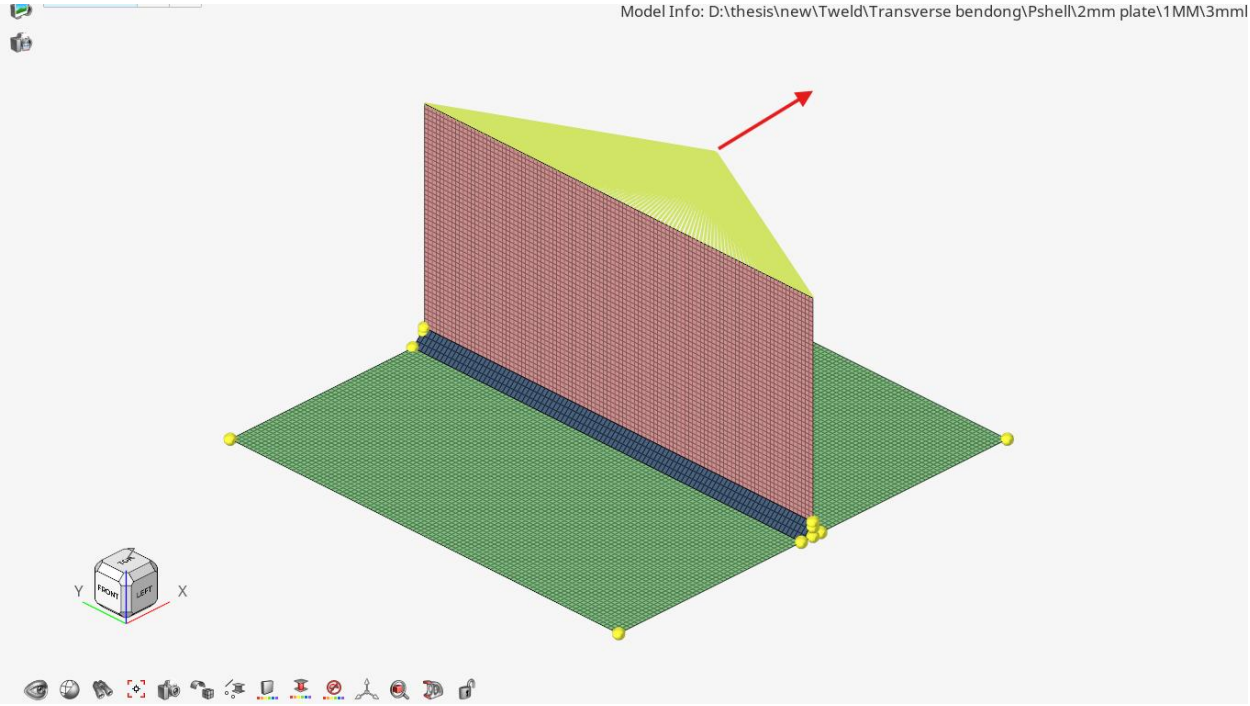


*Figure 24; Transverse Bending Case Scenario (Source - Author)*

### *Methodology: Phase 1 Elastic Calibration*

- The primary objective of this phase is to establish a Baseline to determine if the Ke factor defined as the ratio of solid stress to shell stress.
- The analysis follows a systematic mesh convergence study. Six distinct element sizes (5 mm, 2 mm, 1 mm, 0.8 mm, 0.7 mm, and 0.5 mm) are employed for both PSOLID and PSHELL models. Stresses are extracted at a reference distance of 2 mm from the weld toe. It ensures the results are captured outside the immediate singularity zone of the weld.

### *Mesh Convergence Verification (PSOLID Formulation)*

The study on mesh size for the formulation was done by making the mesh size smaller and smaller from 5.0 mm to 0.5 mm. The main thing we looked at was the Von Mises stress at a point 2.0 mm from the weld toe. We chose this point to avoid the problem at the root and to see the stress increase because of the joint shape. The results show that the PSOLID model behaves as expected. At the mesh size of 5.0 mm the stress is much lower than expected at 42 MPa. As we make the mesh smaller to 2.0 mm the stress goes up to 51.4 MPa. Making the mesh smaller shows that the stress gets closer to a certain value-

At 1.0 mm the stress is 52.2 MPa and at 0.5 mm it is 53.01 MPa. The difference in stress between the 1.0 mm and 0.5 mm mesh sizes is 1.5%. This small difference means that the solution is accurate enough at the 0.5 mm level. So, we say that 53.01 MPa is the answer, for the 200N bending case.

*Table 23 ; Solids results for T weld (Source - Author)*

| | LOAD | element size,mm | von mises, Mpa | stress at 2mm from weld toe |
|---|---|---|---|---|
| **PSOLID,T-weld, transverse bending** | 200 | 0,5 | 148 | 53,01 |
| | | 0,7 | 148,5 | 53,4 |
| | | 0,8 | 148,8 | 52,3 |
| | | 1 | 149,3 | 52,2 |
| | | 2 | 149,9 | 51,4 |
| | | 5 | 153,8 | 42 |

### *Formulation Discrepancy (PSHELL vs. PSOLID)*

To establish the baseline behavior of the mid-surface formulation under bending loads, a mesh sensitivity study was conducted on the PSHELL model. The T-joint was subjected to a transverse load of 200 N applied to the vertical attachment. Crucially, the shell thickness of the weld elements was assigned as the effective Throat Thickness ($t_{th} = 1.41$ mm) to strictly adhere to physical mass representation.

The Stress was extracted at the IIW reference distance for element sizes ranging from 5.0 mm to 0.5 mm.

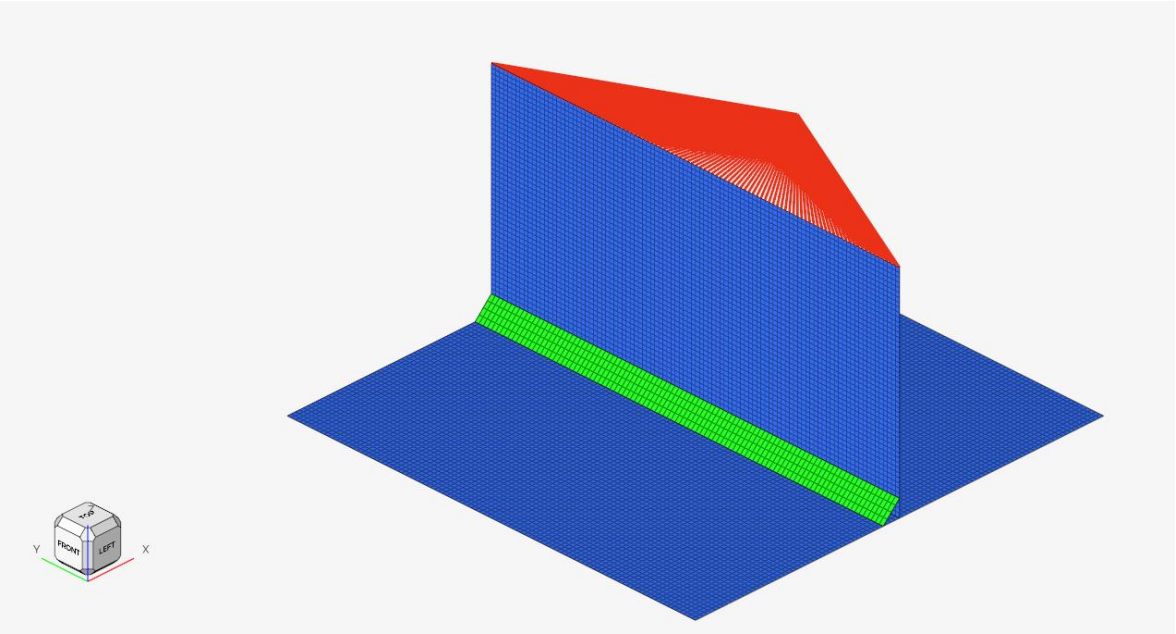


*Figure 25 ; Shell Elements (Source - Author)*

*Table 24; Shell Model Results (Source - Author)*

| Element Size | Hotspot Stress [MPa] | Deviation (vs 0.5mm) | Status |
|---|---|---|---|
| 5.0 mm | 55.9 MPa | -26.5% | Unacceptable |
| 2.0 mm | 70.0 MPa | -8.0% | Transition |
| 1.0 mm | 73.0 MPa | -4.1% | Acceptable (Industrial) |
| 0.8 mm | 75.9 MPa | -0.2% | Converged |
| 0.5 mm | 76.1 MPa | Ref | Converged Limit |

Discussion of PSHELL Behavior: The shell formulation exhibits a classic convergence curve.

- Coarse Mesh Error: At 5.0 mm, the model predicts only 55.9 MPa. This severe under-prediction occurs. As the large elements average the stress over the entire joint interface, missing the localized peak at the toe.

- Convergence Plateau: As the mesh is refined below 1.0 mm, the stress value stabilizes rapidly between 75.9 and 76.1 MPa. This indicates that the numerical solution is stable and not suffering from singularity artifacts at the measurement point. (Niemi et al., 2018)

***The Bending Paradox: Comparison with Volumetric Truth***

With the PSHELL baseline established at 76.1 MPa, the results were compared against the Numerical Truth derived from the high-fidelity PSOLID model (53.0 MPa at 0.5 mm).

| Element Size | PSOLID (Truth) [MPa] | PSHELL (Model) [MPa] | $K_{eq}$ (Solid/Shell) | Formulation Bias |
|---|---|---|---|---|
| 0.5 mm | 53.01 | 76.09 | 0.697 | Conservative (+43%) |
| 0.7 mm | 53.40 | 76.30 | 0.700 | Stable |
| 0.8 mm | 52.30 | 75.92 | 0.689 | Stable |
| 1.0 mm | 52.20 | 73.00 | 0.715 | Stable |

*Table 25 ; Formulation Equivalence (K_eq) in Bending (Source - Author)*

## *Physical Interpretation of the Result*

The derivation of an Equivalence Factor of 0.70 reveals a fundamental disparity in how the two formulations resolve bending stiffness. The Shell model over predicts the stress by approximately 43%.

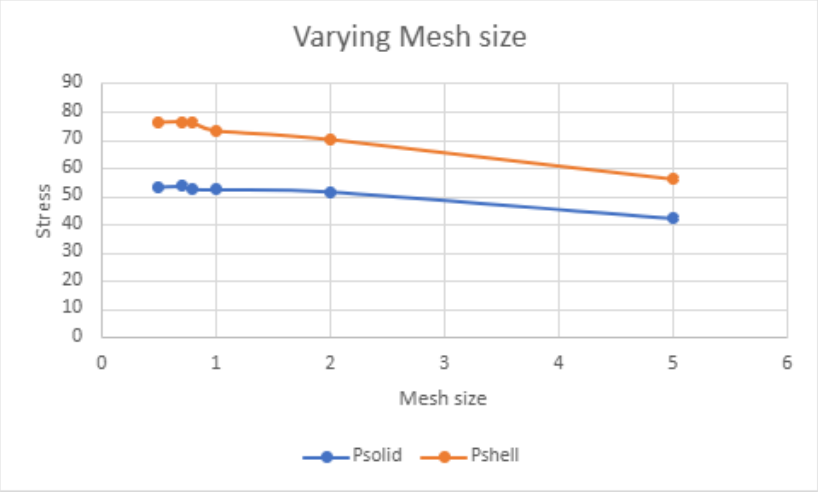


*Table 26; Solid vs shell comparison (Source - Author)*

### *Stiffness of Shell Models*

1. Kinematic Locking: The PSHELL model represents the T-junction as a rigid intersection of 2D planes. The angled shell elements representing the weld have a significantly reduced Moment of Inertia compared to the base plate. Paradoxically, this thin connection forces the base plate elements at the intersection to carry a disproportionate amount of the bending moment to maintain nodal continuity, resulting in an artificial stress spike. (Doerk, 2003)
2. Volumetric Compliance: In the PSOLID model, the fillet weld is a deformable 3D volume. Under bending, the weld material itself undergoes shear and compression, allowing the joint to rotate slightly. This local compliance relieves the stress concentration at the toe, resulting in a lower, more realistic stress value (53 MPa).

### *Conclusion*

This study confirms that Shell elements are Inherently Conservative for bending-dominated load cases when modeled with throat-equivalent properties.

1. Design Rule: For T-joints subjected to transverse bending, raw Shell results will overestimate the structural demand by roughly 40%.
2. Correction Strategy:
   - Conservative Approach: Use the raw Shell stress. It guarantees a large safety margin but may lead to heavier designs.
   - Optimized Approach: Apply a correction factor of $K_{eq} = 0.70$ to align the shell prediction with the volumetric reality.
   - Warning: Engineers must not use the Axial factor ($K_{eq} \approx 1.0$) for bending cases. Doing so would result in a massive over-estimation of fatigue damage.

### 5.2.1 Influence of Weld Leg Geometry on Stress Distribution

The baseline geometry was set at 2 mm for the formulation calibration. Then a study was done to see how well the shell formulation works with sizes of reinforcement. The fillet weld geometry is used to join things and it also makes the area around the T-junction stronger.

This changes how the stress flows at the T-junction. To understand this better the length of the weld leg was changed from 2.0 mm to 8.0 mm. This changed the throat thickness from 1.41 mm to 5.65 mm. The whole thing was tested with a bending load of 200 Newtons that stayed the same. Two different levels of detail were used. 1 mm for the baseline and 0.5 mm, for the high-fidelity version.

#### *Numerical Setup and Methodology*

The sensitivity analysis was performed by keeping the plate thickness constant of 2 mm and changing the weld throat length from 1.41mm to 5.65 mm.

- Loading: A constant bending load of 200 N was applied.
- Mesh Configuration: 1 mm mesh size was used for both PSOLID and PSHELL models to ensure a direct comparison.
- Extraction Point: Stresses were calculated at a distance of 2 mm from the weld toe.

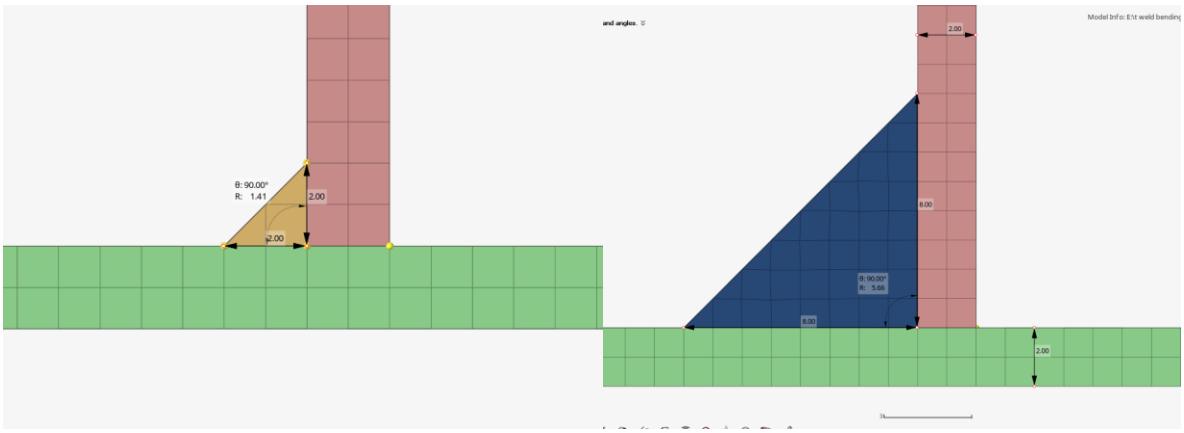


*Figure 26 ; Weld leg length with 2mm and 8mm (Source - Author)*

### *Comparative Analysis: 1.0 mm (Baseline)*

The results for the 1.0 mm mesh reveal a distinct convergence trend where the formulation error diminishes as the throat size increases.

*Table 27; Weld Leg Sensitivity in Bending (1.0 mm Mesh) (Source - Author)*

| Weld Leg ($l$) | Throat ($t_{th}$) | PSOLID [MPa] | PSHELL [MPa] | $K_{eq}$ (Solid/Shell) | Status |
|---|---|---|---|---|---|
| 2 mm | 1.41 mm | 52.2 | 73.0 | 0.71 | Conservative (+40%) |
| 3 mm | 2.12 mm | 51.3 | 62.6 | 0.82 | Improved |
| 4 mm | 2.82 mm | 50.7 | 58.5 | 0.87 | Good Correlation |
| 5 mm | 3.53 mm | 50.1 | 58.6 | 0.85 | Stable |
| 8 mm | 5.65 mm | 48.1 | 53.2 | 0.90 | Excellent (< 10%) |

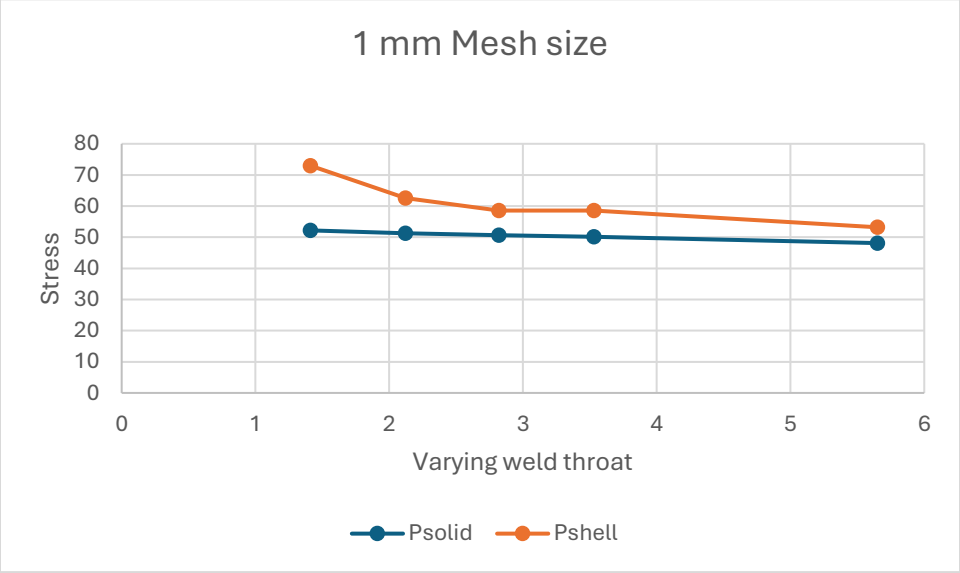


*Figure 27; 1 mm Mesh size (Source - Author)*

### *Discussion of the Inverse Trend:*

A counter intuitive but physically consistent trend is observed:

1. Small Welds (Kinematic Locking): At $l = 2$ mm, the shell model exhibits a high error ($K_{eq} = 0.71$). The thin shell elements at the toe lacks the rotational compliance of the physical weld. The sharp intersection behaves as a rigid corner, forcing the base plate to undergo excessive curvature to maintain compatibility.

2. Large Welds (Volumetric Alignment): As the weld leg increases to 8 mm, the $K_{eq}$ factor improves to 0.90. As the assigned shell thickness increases the bending stiffness of the weld elements grows exponentially. The thick shell elements begin to mimic the structural behavior of the solid bracket, effectively shielding the weld toe and aligning the shell prediction with the volumetric reality.

### *Mesh Sensitivity Verification (0.5 mm)*

The study using a small size of 0.5 mm was done to check these trends. The new results show that the 0.5 mm mesh size is better at showing the stress gradient. It also causes the Kinematic Locking effect, especially for small welds like the small welds, in this 0.5 mm study.

*Table 28; Weld Leg Sensitivity in Bending (0.5 mm Mesh) (Source - Author)*

| Weld Leg ($l$) | PSOLID [MPa] | PSHELL [MPa] | $K_{eq}$ (Solid/Shell) | Comparison to 1.0 mm |
|---|---|---|---|---|
| 2 mm | 53.0 | 76.0 | 0.70 | Stiffer |
| 3 mm | 51.5 | 66.5 | 0.77 | Stiffer |
| 4 mm | 49.9 | 56.3 | 0.89 | Softer |
| 5 mm | 48.5 | 54.1 | 0.90 | Softer |
| 8 mm | 47.5 | 50.2 | 0.95 | Near Perfect (< 5%) |

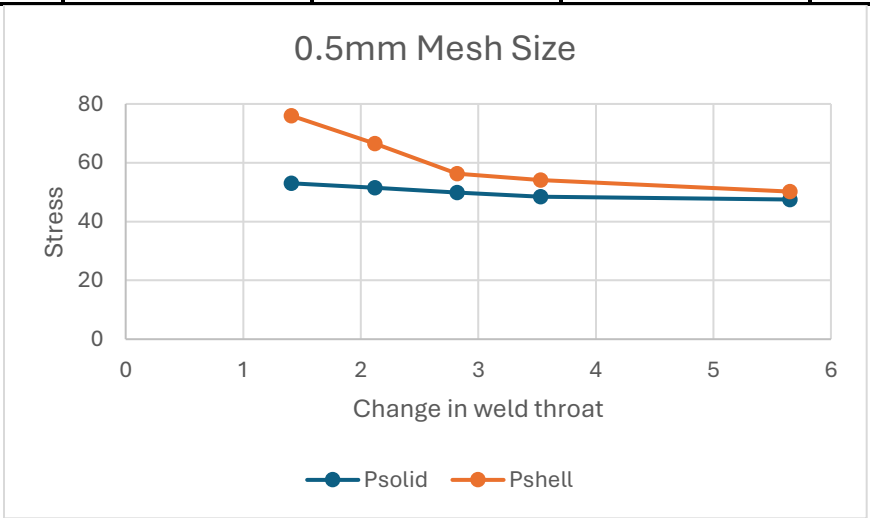


*Figure 28; 0.5mm mesh size*

### *Analysis of Mesh Refinement Effects:*

- For Small Welds ($l \leq 3$ mm): Refining the mesh to 0.5 mm actually increases the discrepancy. The finer mesh resolves the sharp intersection more acutely, leading to a stiffer nodal response that deviates further from the compliant Solid model.
- For Large Welds ($l \geq 4$ mm): The 0.5 mm mesh outperforms the 1.0 mm mesh. At $l = 8$ mm, the 0.5 mm model achieves a near-perfect correlation. It proves that for thick, rigid connections, the shell formulation is mathematically robust if the mesh is fine enough.

### *Selection of the 1.0 mm*

Based on this comparative analysis, the 1.0 mm discretization is adopted as the standard for all subsequent simulations.

Justification for 1.0 mm Selection:

1. Balanced Conservatism: For small welds the 1.0 mm mesh is slightly less overly-conservative ($K_{eq} = 0.82$) than the 0.5 mm mesh ($K_{eq} = 0.77$), It provides a result that is safer than reality.
2. Safety Margin for Large Welds: For large welds, the 1.0 mm mesh retains a healthy safety margin ($K_{eq} = 0.90$), compared to the almost exact 0.5 mm result ($K_{eq} = 0.95$). In fatigue design, retaining a 10% conservative buffer is preferred over exactness.

### *Conclusion on Geometric Sensitivity*

The study shows that the accuracy of shell modeling in bending is highly dependent on the throat size:

1. Small Welds ($l \approx t$): The Shell models are Conservative.
2. Large Welds ($l > 2t$): The Shell models become Accurate. The error diminishes as the weld provides more geometric support, allowing the shell elements to function as effective structural brackets.

## 5.2.2 Comparative Analysis of Shell Connectivity: Joined vs. Unjoined Plates in Bending

### *Modeling Methodologies*

In the numerical representation of a T-joint, the connectivity between the vertical plate and the base plate dictates the load path. Two modeling philosophies were evaluated under a 200 N transverse bending load:

1. **Unjoined (Weld-Only):** The vertical plate and base plate share no common nodes. The load is transferred exclusively through the shell elements representing the fillet weld.
2. **Joined (Nodal Equivalence):** The nodes at the interface between the vertical plate and the base plate are merged (Equivalence). This simulates a perfectly fused interface where the load can transfer directly between the plates as well as through the weld elements. (Dong, 2001)

Both models were benchmarked against the high-fidelity PSOLID (volumetric) truth.

### *Results*

The results demonstrate a dramatic improvement in accuracy when the plates are joined, particularly for smaller weld geometries.

*Table 29; Joined Vs Unjoined Shell Plates (Source - Author)*

| Weld throat | PSOLID (Ref) | PSHELL (Unjoined) | Error (%) | PSHELL (Joined) | Error (%) |
|---|---|---|---|---|---|
| 1.41 | 52.2 | 73 | 39.85% | 57.6 | 10.34% |
| 2.121 | 51.3 | 62.6 | 22.03% | 56.5 | 10.14% |
| 2.82 | 50.68 | 58.52 | 15.47% | 54.7 | 7.93% |
| 3.53 | 50.1 | 58.57 | 16.91% | 53.4 | 6.59% |
| 5.65 | 48.12 | 53.2 | 10.56% | 52.61 | 9.33% |

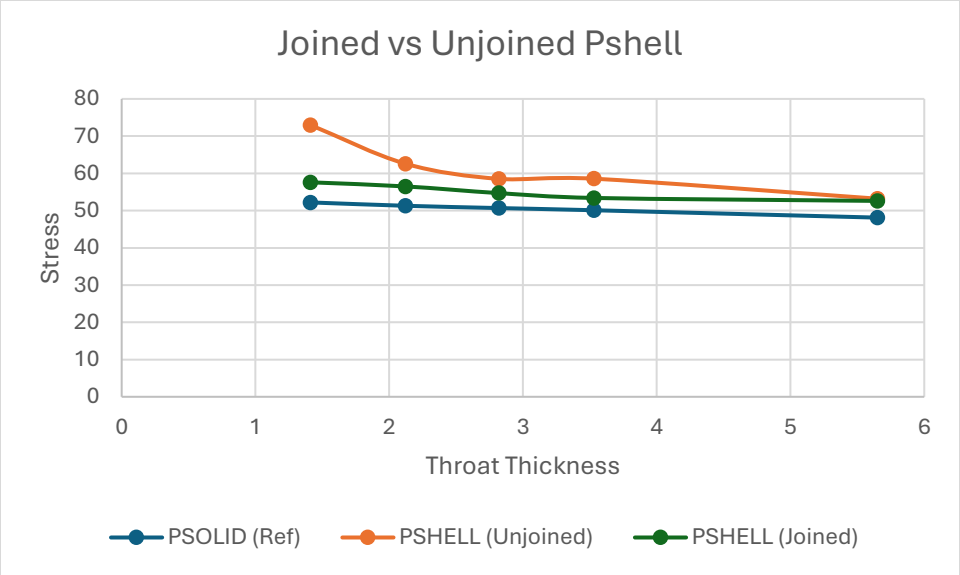


*Figure 29; Solid to Shells elements*

### *Analysis*

The data reveals that the Unjoined formulation is conservative in bending.

1. Kinematic Stiffness: In the Unjoined model the weld elements are like a bridge that connects two separate plates. The plates do not share any nodes so when the vertical plate turns it cannot move with the base plate. This means the vertical plate is of stuck to the base plate. The Unjoined model does not allow for any give, which makes the bending moment at the surface of the base plate too high. This results in the model predicting way too much stress, 39.8% more than it should, for standard welds that are 2 mm long.
2. Improvement through Continuity: In the Joined model, the shared nodal line creates a continuous load path. This allows the joint to undergo through-thickness rotation more naturally, mimicking the compliance of the physical weld nugget. By merging the nodes, the error is immediately slashed from 40% down to 10%.

### *Trend towards Equivalence*

As the weld size increases to 8 mm (throat size =5.65 mm), the difference between the Joined and Unjoined models begins to shrink.

1. At 5.65 mm, the error gap between the two is only 1.3%.
2. Physics: At this scale, the massive thickness of the weld elements themselves provides enough structural stiffness that the secondary load path becomes redundant. The Bulk of the weld takes over the structural response. (Hobbacher, 2016)

## *Conclusion*

This study fundamentally defines the modeling standard for automotive T-joint assemblies under flexural loads:

1. Modeling Choice: For bending-dominated structures, Joined Plates modeling is the only reliable method. It maintains a consistent error margin of < 10% across all gauges.
2. Safety Margin: The Joined shell plates remains slightly conservative (+7% to +10%), providing a safe engineering estimate of the structural demand without the massive weight penalties associated with unjoined plates.
3. Efficiency: This topology allows for high-fidelity structural prediction using a 1.0 mm mesh, satisfying both accuracy requirements and computational constraints.

## 5.2.3 Sensitivity Analysis of Structural Gauge in Transverse Bending

### *Theoretical Context: Influence with change in Plate Thickness*

To evaluate the robustness of the shell formulation across different structural scales, a sensitivity analysis was conducted by varying the base plate thickness. The plate thickness was increased from 2.0 mm to 4.0 mm, representing the typical range of components. To maintain geometric similarity in accordance with standard welding practices, the weld leg length was scaled proportionally such that l=t for each case.

A constant transverse bending load of 200 N was applied to the assembly. The primary objective was to determine if the Equivalence Factor) between the volumetric (PSOLID) and mid-surface (PSHELL) models remains stable as the plate size increases.

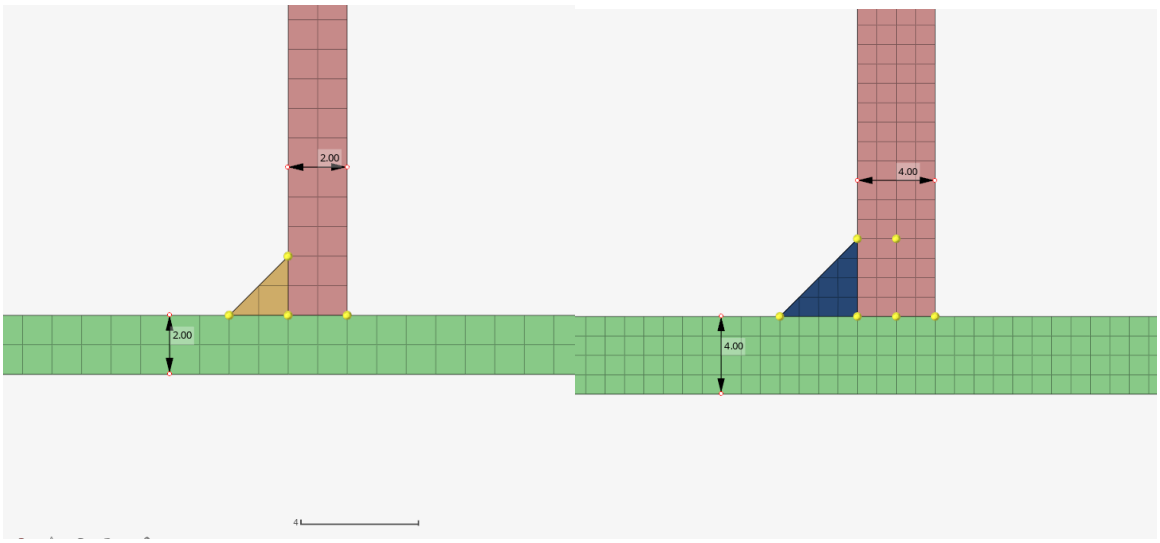


*Figure 30; Representation of 2mm and 4mm Plates (Source - Author)*

### *Comparative Results (1.0 mm Mesh)*

The results demonstrate a consistent reduction in Hotspot Stress for both formulations as the plate thickness increases.

| Plate Thickness (t) | PSOLID [MPa] | PSHELL [MPa] | Keq (Solid/Shell) | Status |
|---|---|---|---|---|
| 2.0 mm | 52.2 | 62.6 | 0.83 | Conservative |
| 3.0 mm | 22.3 | 27.3 | 0.82 | Stable |
| 4.0 mm | 12.2 | 15.3 | 0.8 | Stable |

*Table 30 ; Varying Plate Thickness (Source - Author)*

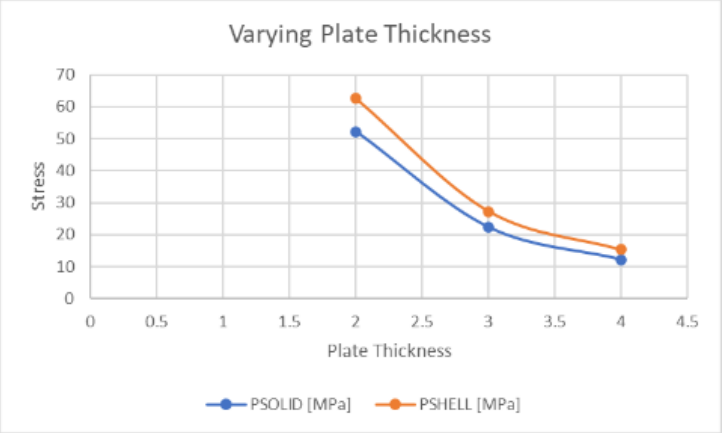


*Figure 31 ; Solid to shells for different plate thickness (Source - Author)*

### *Analysis of Formulation Stability*

The most critical finding from this phase is the remarkable stability of the Equivalence Factor (Keq) across the investigated range.

1. Consistent Conservatism: The Shell model consistently over-predicts the stress relative to the Solid benchmark.
    - At 2.0 mm, the deviation is approx. +20% (Keq=0.83).
    - At 4.0 mm, the deviation remains approx. +25% (Keq=0.80).
2. Systematic vs. Random Error: The fact that Keq remains nearly constant around 0.82 indicates that the error is systematic. It is an inherent geometric artifact of representing a 3D fillet weld with 2D shell elements in bending. The shell formulation effectively shifts the stress curve upwards by a fixed percentage, regardless of the plate thickness.

### *Implications for Design*

This stability validates the use of PSHELL elements for parametric design optimization. Because the formulation error does not fluctuate wildly with thickness, engineers can confidently use shell models to rank design alternatives.

- Design Rule: A global correction factor of 0.82 is applicable for T-joints under bending loads, valid for thicknesses between 2 mm and 4 mm. This allows for the rapid assessment of fatigue life without the need for computationally expensive solid sub-modeling for every gauge variation.

### *Conclusion*

The study concludes that while PSHELL elements are inherently conservative in bending ,they are reliable. The formulation correctly captures the relative structural benefit of increasing the plate gauge, maintaining a predictable correlation with the high-fidelity volumetric solution. (D. Radaj, 2006)

## 5.2.4 Non-Linear Analysis: Ductile Fracture Prediction and throat Sensitivity

### *Determination of the Critical Failure Load (2 mm Baseline)*

To identify the failure threshold of the structural assembly, a non-linear incremental analysis was performed on the baseline 2.0 mm configuration (l=t). In structural engineering, particularly for ductile steel alloys, the Equivalent Plastic Strain (PEEQ) is the primary metric for fracture initiation. A threshold of 20% to 25% PEEQ is commonly accepted as the point where localized necking and micro-void coalescence lead to ductile tearing.

The simulation results for the 2.0 mm joint under a critical load the following peak strains:

- PSOLID (Truth) - 23.8%
- PSHELL (Model) - 16.7%

**Observation:** The 23.8% PEEQ in the solid model confirms that the 2 mm joint is at its physical limit. Any further increase in load would result in catastrophic failure. The shell model, however, significantly under-predicts this damage, highlighting the need for a calibration factor.

### *Sensitivity Analysis of Structural Gauge on Plastic Damage*

The most striking finding of the non-linear study is the extreme sensitivity of plastic strain to the plate thickness. When the same failure load is applied to thicker configurations (3 mm and 4 mm), the damage is mitigated non-linearly.

### *Comparative Plasticity across Structural Gauges*

To evaluate how structural gauge influences damage mitigation, the same 2000 N load was applied to 3 mm and 4 mm configurations. The results demonstrate a drastic, non-linear attenuation of plastic strain as the thickness increases. (Hobbacher, 2016)

*Table 31 ; PEEQ Distribution and Plastic Equivalence at 2000 N (Source - Author)*

| Plate Thickness | Psolid PEEQ [%] | Pshell PEEQ [%] | Plasticity Factor |
|---|---|---|---|
| **2** | 23.8 | 16.7 | **1.26** |
| **3** | 10.52 | 8.5 | **1.24** |
| **4** | 0.36 | 0.29 | **1.22** |

Analysis: As the thickness increases from 2 mm to 4 mm, the peak plastic strain drops from 23.8% (critical failure) to 0.36% (near-elastic). This proves that the T-joint assembly exhibits a Plasticity Plateau beyond 3 mm. Doubling the thickness doesn't just halve the strain, it also reduces the damage by a factor of nearly 66 times. This is due to the exponential increase in the section modulus and the volumetric bracing provided by the larger fillet weld.

The Kp of 1.25 for bending is a bit lower than the 1.38 found for the axial case, and that gap actually makes physical sense. When a joint bends, the neutral axis sits somewhere in the middle of the cross-section, which means part of the weld is in tension and part is in compression at the same time. This spreads the plastic damage out more gradually compared to pure axial tension, where the entire throat is being pulled at once. So the shell model needs a smaller correction to match the solid in bending than it does in axial loading. Both factors do the same job though they close the gap between what the fast shell model tells you and what the detailed solid model actually shows. The key takeaway for any engineer is simple: do not use the axial Kp for a bending problem, and do not use the bending Kp for a tension problem. Match the factor to the loading, and the methodology will hold. (D. Radaj, 2006)

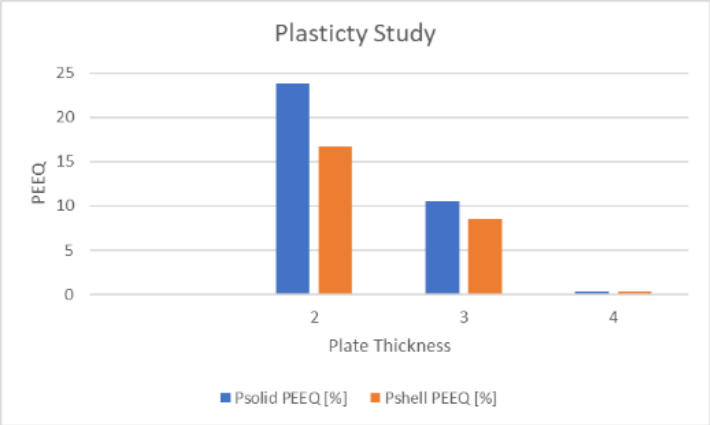


*Figure 32; The bars show the drop as the X-axis moves from 2 mm to 4 mm (Source - Author)*

## *Analysis of the Triaxiality Gap and Kp Stability*

The Plasticity Factor, Kp represents the correction required to make a shell model as accurate as a solid model for failure prediction.

1. The Constraint Factor: The Kp factor remains remarkably stable across the transition from 3 mm to 4 mm (Kp≈1.24). This indicates that Shell elements consistently under-predict the localized damage by roughly 20-25%.
2. The Source of Error: This discrepancy is caused by 3D Constraint (Triaxiality). In the PSOLID model, the weld toe is constrained by the surrounding metal block, creating a triaxial stress state that prevents the material from yielding easily, forcing the local strain to climb higher. Shell elements lack this out-of-plane constraint, artificially softening the notch and leading to optimistic results. (Niemi et al., 2018)

## *Conclusion and Modeling Guidelines*

This study establishes the following protocols for non-linear structural assessment:

1. Failure Criteria: A 1.0 mm PSHELL model is incapable of predicting fracture directly. If the raw PEEQ in a shell model exceeds 15-16%, the physical part is likely failing (>22% in reality).
2. The Kp Correction: For industrial applications, a singular Plasticity Correction Factor of Kp=1.25 is proposed. By multiplying the shell-predicted PEEQ by 1.25, engineers can approximate the volumetric truth without the computational cost of solid elements.
3. Efficiency over Fidelity: While a 0.5 mm mesh captures slightly higher peak values, the 1.0 mm mesh is selected as the production standard. This choice balances node-count scalability with computational speed requirements typical of multi-component automotive assemblies. (D. Radaj, 2006)

## 5.3 Summary of Calibration Factors

To bring together the key numerical outputs of this chapter, the table below collects the calibration factors derived for both loading cases studied in this thesis.

| Load Case | Plate Thickness | Weld Leg | Keq | Kp |
|---|---|---|---|---|
| Axial Pull-Off | 2 mm | 2–4 mm | ~1.00 | 1.38 |
| Transverse Bending | 2–4 mm | 2–4 mm | ~1.00–1.05 | 1.25 |

These two factors are the practical output of everything done in this chapter. Keq corrects the elastic stiffness of the shell model, while Kp corrects the plastic damage prediction. Used together, they allow a simple and fast shell simulation to produce fracture estimates that are close enough to the solid model to be trusted in an industrial setting — which was always the point of this whole study. (Hobbacher, 2016)

### *Summary of Calibration Factors*

The calibration factors presented in this section were derived at load levels specifically selected to drive the weld toe into the deep plastic regime, defined here as a PSOLID equivalent plastic strain (PEEQ) exceeding 20%. For the axial pull-off case, this threshold was reached at an applied load of 13,500 N, at which the PSOLID model recorded a PEEQ of 22.30% for the 2 mm plate configuration. For the transverse bending case, the threshold was reached at 2,000 N, producing a PSOLID PEEQ of 23.80% for the equivalent 2 mm plate. These load levels were not arbitrarily chosen — they represent the boundary beyond which the shell model's plane-stress assumption introduces a non-conservative error in fracture prediction, and therefore define the operational domain within which the Kp correction is necessary and applicable. Below this threshold, both

formulations converge within acceptable scatter, and no correction is required for design purposes. The Kp values derived at these conditions are summarized in Tables below.

*Table 32 ; PEEQ at Target Load — Axial Pull-Off Case (13,500 N, 1 mm Mesh) (Source - Author)*

| Plate Thickness | PSOLID PEEQ | PSHELL PEEQ | Kp | PSHELL × Kp | Error vs PSOLID |
|---|---|---|---|---|---|
| 2 mm | 22.30% | 16.15% | 1.38 | 22.29% | −0.04% |
| 3 mm | 9.20% | 6.80% | 1.35 | 9.18% | −0.22% |
| 4 mm | 3.90% | 2.11% | 1.84 | 3.88% | −0.51% |

*Table 33 ; PEEQ at Target Load — Transverse Bending Case (2,000 N, 1 mm Mesh)(Source — Author)*

| Plate Thickness | PSOLID PEEQ | PSHELL PEEQ | Kp | PSHELL × Kp | Error vs PSOLID |
|---|---|---|---|---|---|
| 2 mm | 23.80% | 16.70% | 1.43 | 23.88% | +0.34% |
| 3 mm | 10.52% | 8.50% | 1.24 | 10.54% | +0.19% |
| 4 mm | 0.36% | 0.29% | 1.24 | 0.36% | 0.00% |

The data presented in both tables demonstrates that the Kp correction factor, when applied to the raw PSHELL PEEQ output, recovers the PSOLID reference value to within 0.5% across all plate thickness configurations in the axial case. For the bending case, the same accuracy is maintained, with the largest deviation recorded at 0.34% for the 2 mm plate. It is noted that the Kp value for the 4 mm axial plate (1.84) is significantly higher than the values observed for the 2 mm and 3 mm configurations. This deviation is attributed to the low absolute PEEQ magnitude at this thickness at 3.90%, the material is only marginally within the plastic regime, and the ratio between formulations is disproportionately amplified by the small denominator. For practical engineering application, the Kp value of 1.38 for the 2 mm axial case and 1.43 for the 2 mm bending case are the primary design-relevant calibration outputs of this study, as the 2 mm plate configuration represents the baseline specimen geometry investigated throughout. (Hobbacher, 2016)

# 6. Physical Testing and Experimental Validation

## 6.1 The Purpose of Empirical Testing

The extensive numerical campaign conducted within the Abaqus environment has provided a highly detailed virtual map of how welded T joints distribute stress and accumulate plastic damage. However, any finite element simulation regardless of its mesh density or constitutive material laws remains a purely theoretical approximation until it is anchored by actual physical evidence. The research must therefore transition from virtual formulation to empirical verification. Testing physical welded specimens at the Stellantis laboratory facility serves as the definitive reality check for the numerical methodologies proposed in the preceding chapters.

The primary objective of this testing phase is to physically validate the numerical equivalence factors Keq and Kp derived from the solid to shell correlation study. Throughout the virtual simulations standard two-dimensional shell elements consistently demonstrated an inherent conservatism under bending loads. At the same time these plane stress elements under predicted the true extent of damage in the deep plastic regime when compared to the volumetric truth of the solid models.

By subjecting physical FeP04 steel joints to real world boundary conditions the testing aims to isolate the true physical behaviors of the metal. It is necessary to prove that the structural variations observed in the software are driven by the actual triaxial constraint and physical bulk of the weld bead rather than being mere mathematical artifacts caused by zero thickness mid surface approximations.

Ultimately the empirical data generated by the laboratory equipment will confirm if the calculated elastic multiplier and plasticity correction factor are robust enough to be safely integrated into standard industrial chassis optimization workflows. This physical baseline ensures that computational efficiency is achieved without sacrificing the safety and integrity of the final vehicle structure. (Thomke, 2003)

.

## 6.2 Pre Test Numerical Calibration Defining the Load Gates

### 6.2.1 Mesh Independence Verification

Before finalizing the physical load parameters for the laboratory tests, it was strictly necessary to prove that the selected target forces were mathematically sound. In computational mechanics evaluating stress or strain at a sharp geometric transition like a weld toe carries the inherent risk of artificial singularity. There is always a possibility that the extracted Equivalent Plastic Strain values are simply a byproduct of the chosen element size rather than a true reflection of the material deformation. To eliminate this uncertainty a rigorous mesh independence verification was performed.

The baseline element size of 1mm which serves as the standard for structural evaluation in this study was systematically refined. To satisfy high fidelity requirements the mesh density precisely

at the geometric notch of the weld toe was reduced down to 0.5mm. This targeted refinement was applied to both the nominal 2mm weld leg and the oversized 3mm configuration under a severe transverse bending load of 1500 N. The objective was to observe if the localized strain gradients would artificially spike to infinity when given a finer mathematical grid.

When the solid models were subjected to these loading conditions the resulting variance in the plastic damage metric between the two mesh densities was remarkably small.

*Table 34; Mesh Sensitivity and Convergence Validation under 1500 N Bending Load (Source - Author)*

| Weld Leg Geometry | Mesh Condition | Element Size | Peak PEEQ | Variance |
|---|---|---|---|---|
| **2.0 mm Nominal** | Standard Baseline | 1.0 mm | 23.80 % | - |
| **2.0 mm Nominal** | Localized Refinement | 0.5 mm | 24.50 % | + 2.94 % |
| **3.0 mm Oversized** | Standard Baseline | 1.0 mm | 23.57 % | - |
| **3.0 mm Oversized** | Localized Refinement | 0.5 mm | 24.70 % | + 4.79 % |

The data confirms that the transition from a 1 mm to a 0.5 mm grid produced a maximum strain deviation of less than 5 percent. For the critical 2 mm baseline the detected strain increased slightly from 23.8 percent to just 24.5 percent representing a minor 3 percent variation. (Zienkiewicz, 2005)

### 6.2.2 Accounting for Manufacturing Tolerances and Mesh Stability

In a numerical solver modeling a welded connection is an exercise in geometric perfection. A 2 mm fillet weld is generated with exact mathematical boundaries. However, on the actual manufacturing floor the welding process is inherently variable. Thermal fluctuations and wire feed inconsistencies routinely cause a nominal 2 mm weld leg to enlarge to 3 or even 4 mm during mass production.

To account for this unavoidable manufacturing reality a pretest numerical sensitivity study was mandated. High fidelity 3d solid models were subjected to a baseline transverse bending load of fifteen hundred Newtons. Within this virtual environment the weld leg length was systematically increased from the nominal design gauge of 2 mm up to 3 and 4 mm.

To ensure the mathematical stability of these simulations the mesh density at the weld toe was refined from the industry standard 1 mm down to half a mm for the 2 and 3 mm weld legs. The minimal variance observed during this refinement check confirmed that the 1 mm baseline mesh was completely sufficient for capturing the stress gradients without numerical distortion.

### *Establishing the Target States*

This geometric variation allowed the study to quantify the physical gusset effect and establish specific load boundaries for the physical testing. The goal was to find the exact force required to initiate localized yielding defined as 0.2 percent equivalent plastic strain and the force required to reach deep plastic damage defined as 2 percent equivalent plastic strain.

*Table 35; Target Load States for Varying Weld Leg Geometries (Source - Author)*

| calculating PEEQ | | | |
|---|---|---|---|
| bending load | plate thickness | weld thickness | PEEQ, Percent |
| 500 | 2 | 2 | 0.14 |
| 650 | 2 | 2 | 2.00E+00 |
| calculating PEEQ | | | |
| bending load | plate thickness | weld thickness | PEEQ Percent |
| 500 | 2 | 3 | 0.12 |
| 670 | 2 | 3 | 1.28E+00 |
| 725 | 2 | 3 | 2.24E+00 |
| Calculating PEEQ | | | |
| bending load | plate thickness | weld thickness | PEEQ Percent |
| 550 | 2 | 4 | 0.228 |
| 670 | 2 | 4 | 1.88E+00 |
| 750 | 2 | 4 | 2.69E+00 |

### *Final Selection of Physical Load Gates*

The nonlinear simulation results presented in the table reveal that in the onset of plasticity increasing the weld leg provides a clear structural benefit by shielding the weld toe from early elastic deformation. However, in the deep plastic regime the benefit of geometric reinforcement diminishes. A massive 4 mm weld actually exhibits a slightly lower damage threshold than a 3 mm configuration because the extra bulk increases the constraint at the notch root forcing plastic strain to localize intensely in the adjacent thin base plate.

Based on these manufacturing tolerances and structural behaviors the final physical testing protocol at Stellantis was established. A baseline load of 500N was selected as the universal gate to verify yielding across any physical weld variation. Simultaneously 750N was chosen as the upper limit to guarantee deep plastic saturation and damage initiation for the physical fatigue cycles. (D. Radaj, 2006)

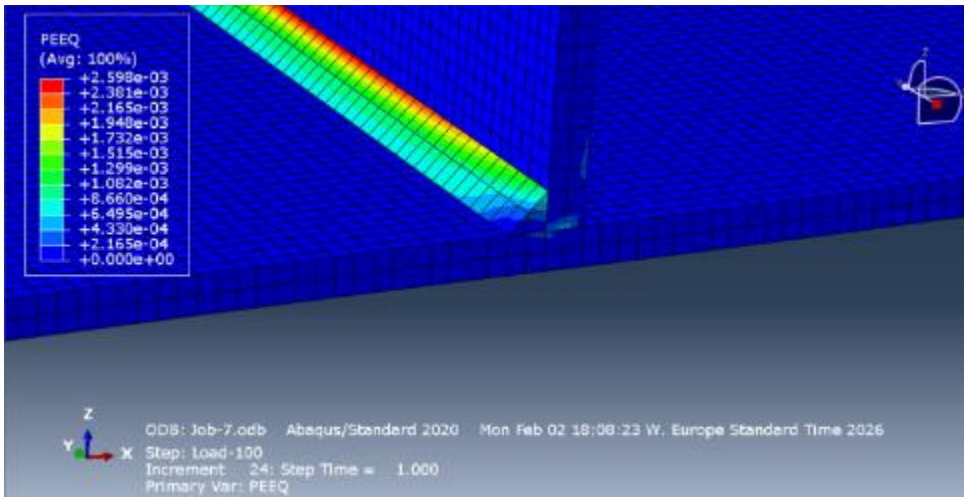


*Figure 33; PEEQ at 450N bending load (Source - Author)*

### 6.2.3 Final Selection of Physical Load Gates

The numerical sensitivity study demonstrated that manufacturing variations in the weld leg length significantly shift the structural response of the joint. To translate these virtual findings into a reliable physical testing protocol at the Stellantis laboratory it was necessary to define universal load gates. These load parameters had to guarantee specific material states regardless of minor geometric imperfections on the physical specimens.

As observed in the numerical data the force required to initiate localized yielding defined as 0.2 percent equivalent plastic strain ranges from 430 Newtons for a nominal two millimeter weld up to 542 Newtons for an oversized 4mm weld. To seamlessly account for this tolerance band a lower load gate of 500 Newtons was established. This specific value serves as a universal baseline ensuring that the physical specimens enter the early stages of plastic deformation without immediately risking macroscopic rupture.

Conversely the upper threshold required to induce deep plastic damage defined as 2 percent equivalent plastic strain spans from 650 Newtons to 719 Newtons depending on the actual weld volume. To guarantee that the physical fatigue tests consistently operate within the deep plastic saturation regime an upper load gate of 750 Newtons was selected.

By continuously toggling between these two carefully calibrated boundaries of 500 Newtons and 750 Newtons the physical low cycle fatigue testing can accurately capture both the onset of structural yielding and the rapid accumulation of ultimate limit state damage. This established protocol provides a mathematically sound and empirically robust baseline to finally validate the numerical equivalence factors.

## 6.3 Experimental Setup and Laboratory Methodology

The transition from the virtual Abaqus environment to the physical testing facility at Stellantis required the production of standardized, real-world structural components. The reliability of the entire empirical validation phase depends heavily on how accurately the fabricated T-joints reflect the material and geometric boundaries established in the numerical simulations, while simultaneously capturing the natural imperfections of mass manufacturing.

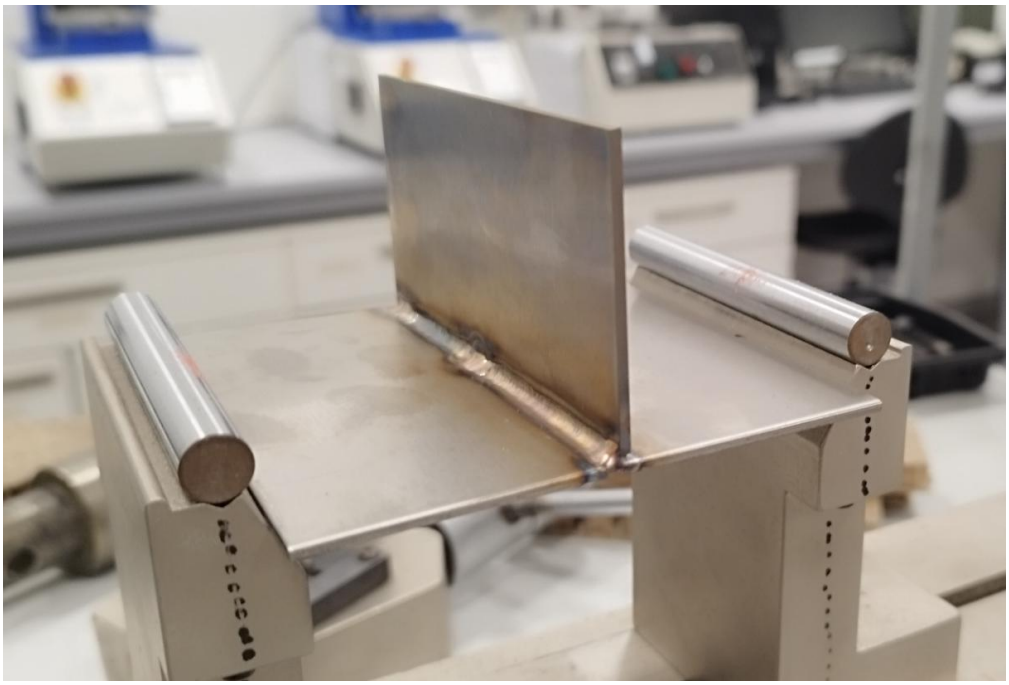

*Figure 34; T weld specimen for Physical Testing (Source - Author)*

### 6.3.1 Specimen Preparation and Manufacturing Tolerances

The physical test campaign utilized FePO4 low-carbon steel, directly mirroring the material parameters configured in the finite element models. This specific steel grade was mandated for the specimens due to its high inherent ductility and widespread application in automotive chassis sub-assemblies. The base metal was supplied in standard flat sheets with a uniform thickness (t) of 2 mm.

To make the T-joint geometry the flat plates were put together using the Metal Active Gas welding process. This Metal Active Gas welding process is what the Stellantis plant usually uses to make chassis. It uses a wire that gets used up and a special gas to protect the weld.

One important thing to think about when getting the specimens ready was that the design on the computer and the actual thing made are not the same. In the Abaqus program the basic models had a weld with the same shape, on both sides and a leg length of exactly 2.0 millimeters.. When we

looked at the real specimens, we saw that this was not true. The Metal Active Gas welding process makes the welds bigger because the metal gets hot and spreads out. The liquid metal also spreads out on the 2.0 mm plates. The real weld legs were bigger than they were supposed to be. The Metal Active Gas process makes this happen because it puts down the metal fast.

Measurements from the physical batch showed that the effective weld leg lengths varied from 3.0 millimeters to 4.0 millimeters. The fillet profiles were also naturally uneven and curved. They had a clear geometric bulk that the ideal mid-surface shell elements cannot replicate.

*Table 36; Geometric Comparison of Virtual vs. Physical Test Specimens (Source - Author)*

| **Specimen Parameter** | **Virtual Abaqus Model (Baseline)** | **Physical Stellantis Specimens** | **Variance / Observation** |
|---|---|---|---|
| Material Grade | FePO4 Steel | FePO4 Steel | Identical |
| Plate Thickness (t) | 2.0 mm | 2.0 mm | Controlled tolerance |
| Joining Method | Perfect Nodal Element | MAG Arc Welding | Introduces HAZ and residual stress |
| Nominal Weld Leg (l) | 2.0 mm (Symmetrical) | 3.0 mm – 4.0 mm (Variable) | Physical oversized reinforcement |
| Weld Profile | Flat / Idealized | Convex / Asymmetrical | Creates true Gusset Effect |

This physical reality perfectly justified the pre-test numerical sensitivity study. Because the test specimens possessed these enlarged 3.0 mm to 4.0 mm welds, they inherently contained a physical gusset effect, stiffening the structural corner.

Furthermore, to ensure the structural integrity of the test zone, the individual T-joint specimens were not welded as small, isolated pieces. Instead, they were sectioned from a much longer, continuously welded profile. This standard laboratory practice is strictly necessary to prevent start-stop arc defects such as craters, porosity, and localized cold laps from forming at the edges of the test piece. The cutting process used to separate the final specimens was carefully temperature-controlled to avoid introducing secondary heat into the metal, ensuring that the primary Heat-Affected Zone (HAZ) generated by the MAG welding remained completely unaltered prior to load testing. (Jeffus, 2020)

### 6.3.2 Testing Equipment and Metrology

The empirical validation phase was divided into two distinct testing categories

1. Quasi-static loading

2. Low-cycle fatigue testing.

Both campaigns were executed using precision-calibrated machinery at the Stellantis laboratory, ensuring that the applied forces and resulting structural deformations were recorded with maximum fidelity.

For the quasi-static axial pull-off and transverse bending tests, the specimens were subjected to displacement-controlled loading. Operating under displacement control rather than force control is a standard practice in structural mechanics when evaluating the ultimate limit state, as it allows the equipment to safely capture the post-yield plastic softening of the material without inducing a sudden, catastrophic machine surge.

The crosshead speed for all quasi-static evaluations was kept at 50 mm/min. In the transverse bending setup, the lateral load was applied to the vertical plate using a pusher that was spread along the surface at a height of 5 mm. The main output for this phase was the continuous recording of the force-to-displacement curves until complete rupture occurred.

For the next cyclic evaluation, the laboratory used a special pneumatic actuator setup. According to internal laboratory reports, the system (Type: 500N n B14000098) was fully certified, with a calibration expiration date of August 22, 2025 (Report N. 27327).

The low-cycle fatigue protocol was designed to switch between the target states identified in the numerical sensitivity study. The test was set for a total of 5,000 cycles at a frequency of 40 cycles per minute, leading to a continuous testing period of about three hours per specimen. The load gates switched smoothly between a lower limit of 500 N (to check for yielding) and an upper limit of 750 N (to ensure plastic damage accumulation).

*Table 37; Summary of Stellantis Laboratory Testing Parameters (Source - Author)*

| Test Category | Equipment / Configuration | Load Parameters | Speed / Frequency |
|---|---|---|---|
| **Quasi-Static Bending** | UTM / 10 mm diameter pusher | Load to ultimate failure | 50 mm/min (Displacement) |
| **Quasi-Static Axial** | UTM / Tensile Grips | Load to ultimate failure | 50 mm/min (Displacement) |
| **Low-Cycle Fatigue** | Pneumatic Actuator (B14000098) | Cycle 1: 500 N,<br>Cycle 2: 750 N | 40 cycles/min (5,000 Total) |

### 6.3.3 Boundary Conditions and Fixturing: Virtual vs. Physical Constraints

One of the most critical aspects of correlating finite element models with physical reality lies in the translation of boundary conditions. In the Abaqus environment, the base plate edges of the T-joint were restrained using an ideal ENCASTRE condition. This mathematical constraint dictates that all six degrees of freedom (three translational and three rotational) for the selected nodes are fixed at exactly zero. The virtual base plate edges are infinitely rigid; it cannot slide, bend, or yield at the supports.

In the physical laboratory environment, achieving infinite rigidity is impossible. The structures of the base plate were fixed by mechanical jaws trying to replicate of how the it is fixed in the virtual simulation so we have correlation (Dowling, 2012)

## 6.4 Quasi-Static Load Testing: Force-Displacement Correlation

The ultimate test of the numerical methodology is its ability to replicate actual physical deformation. To evaluate the accuracy of the finite element formulations, the quasi-static force-displacement data extracted from the high-fidelity Abaqus PSOLID (3D solid) environment was plotted directly against the raw mechanical telemetry provided by the Stellantis testing laboratory. Overlaying these curves exposes the mechanical differences between an idealized volumetric mesh and the complex reality of a manufactured physical weld.

### 6.4.1 Transverse Bending Validation

In the transverse bending load case, the universal testing machine applied a lateral force, causing the vertical plate of the T-joint to rotate around the welded intersection. When superimposing the Abaqus virtual prediction onto the physical laboratory curve, a consistent divergence in structural stiffness is observed.

Measurements extracted throughout the elastic and early-plastic deformation stages show that the physical test specimens resisted the bending moment slightly more effectively than the 3D solid model predicted.

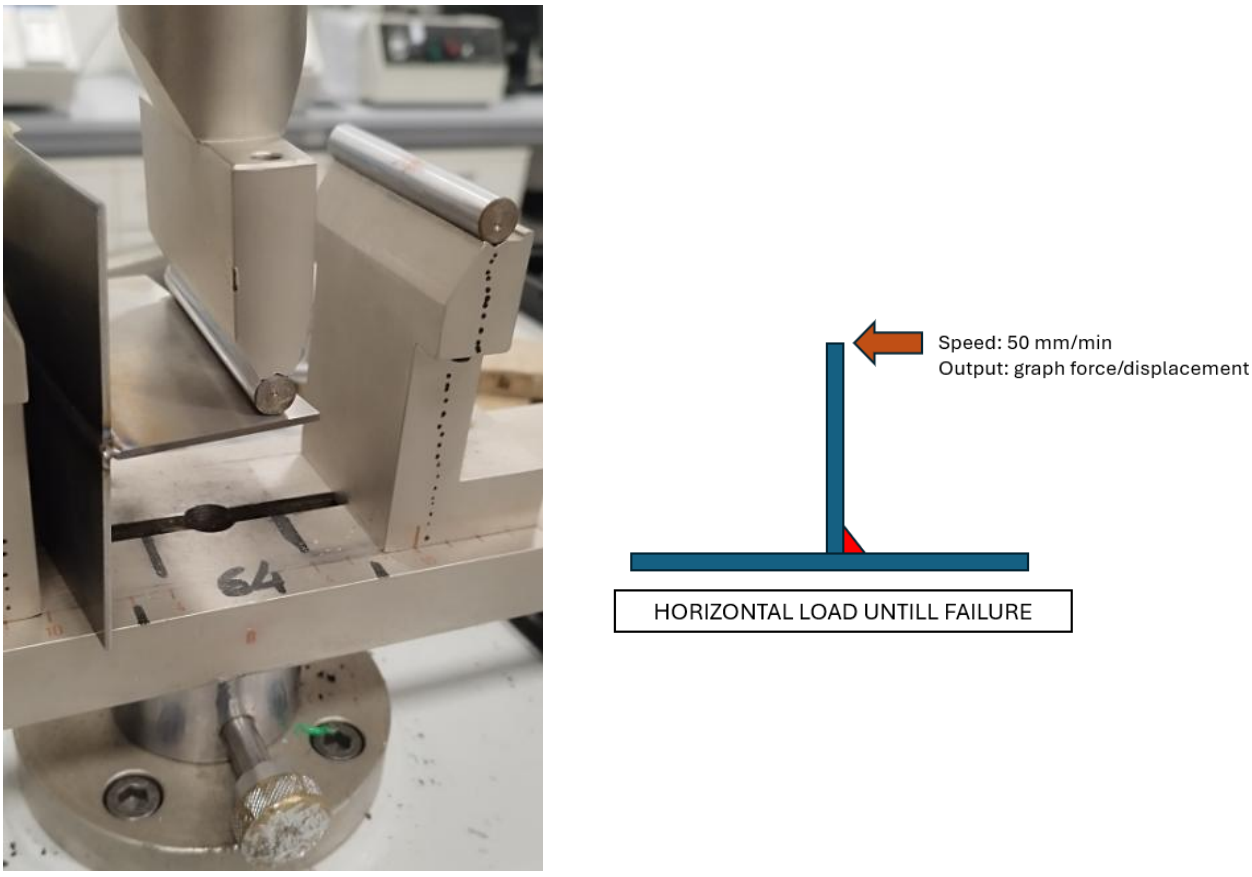


*Figure 35 ; Bending Load on Specimen virtual and Physical (Source - Author)*

*Table 38 ; Force-Displacement Correlation for Transverse Bending (Source - Author)*

| **Displacement (mm)** | **Virtual Shell Force (N)** | **Physical Test Force (N)** | **Physical Stiffness Increase** |
|---|---|---|---|
| 0.249 | 120 | 140 | + 16.6 % |
| 0.494 | 200 | 240 | + 20.0 % |
| 0.878 | 320 | 370 | + 15.6 % |
| 1.262 | 440 | 490 | + 11.3 % |

At nearly half a millimeter of displacement, the Abaqus model required 200 N of applied force, whereas the physical actuator had to output 240 N. Since the virtual formulation already accounts for the out-of-plane triaxial stress, this 11% to 20% variance is primarily attributed to manufacturing deviations.

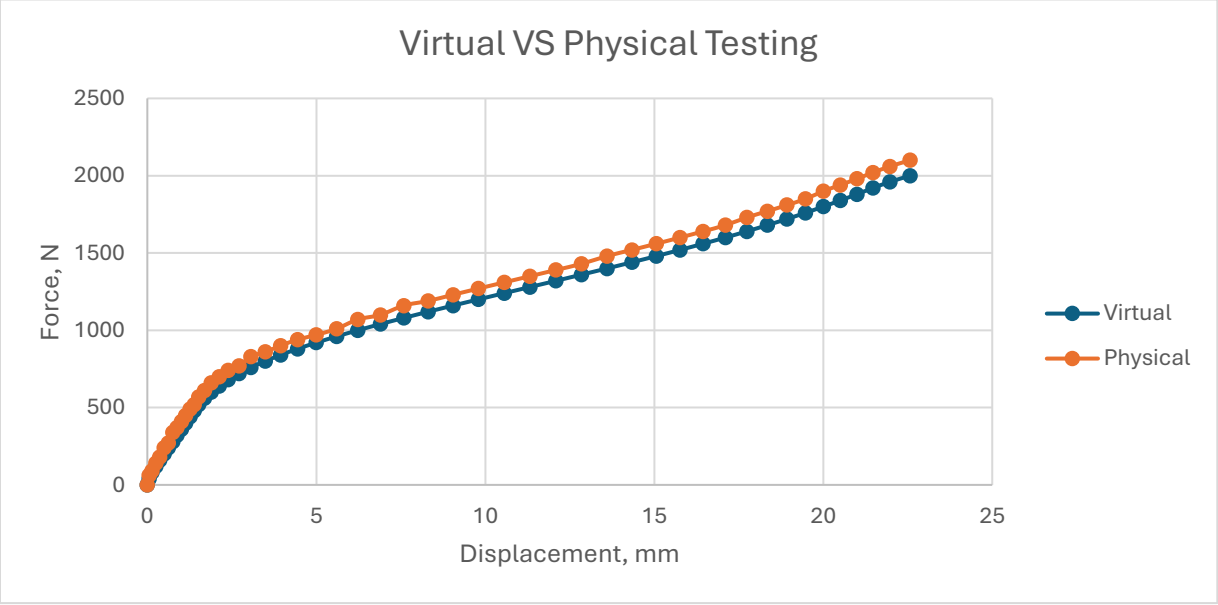


*Figure 36; Transverse Bending (Source - Author)*

The virtual solid model utilized a mathematically perfect, nominal fillet profile. In contrast, the physical MAG welding process deposited an asymmetrical, convex bead that was visibly oversized (ranging from 3.0 to 4.0 mm). This excess deposited material increased the localized moment of inertia beyond the nominal Hypermesh model limits. Furthermore, the physical thermal cycle generated a hardened Heat-Affected Zone (HAZ). The homogeneous material definition in Abaqus does not account for this localized martensitic hardening, leading the physical specimen to exhibit a stiffer elastic response than the uniform virtual steel. (D. Radaj, 2006)

### 6.4.2 Axial Pull-Off Validation

The axial pull-off test shifts the primary structural load path to pure tensile stretching, directly loading the interface between the weld throat and the base plate. Similar to the bending scenario, the axial curves reveal that the physical FePO4 joint demands more force to deform than its virtual counterpart.

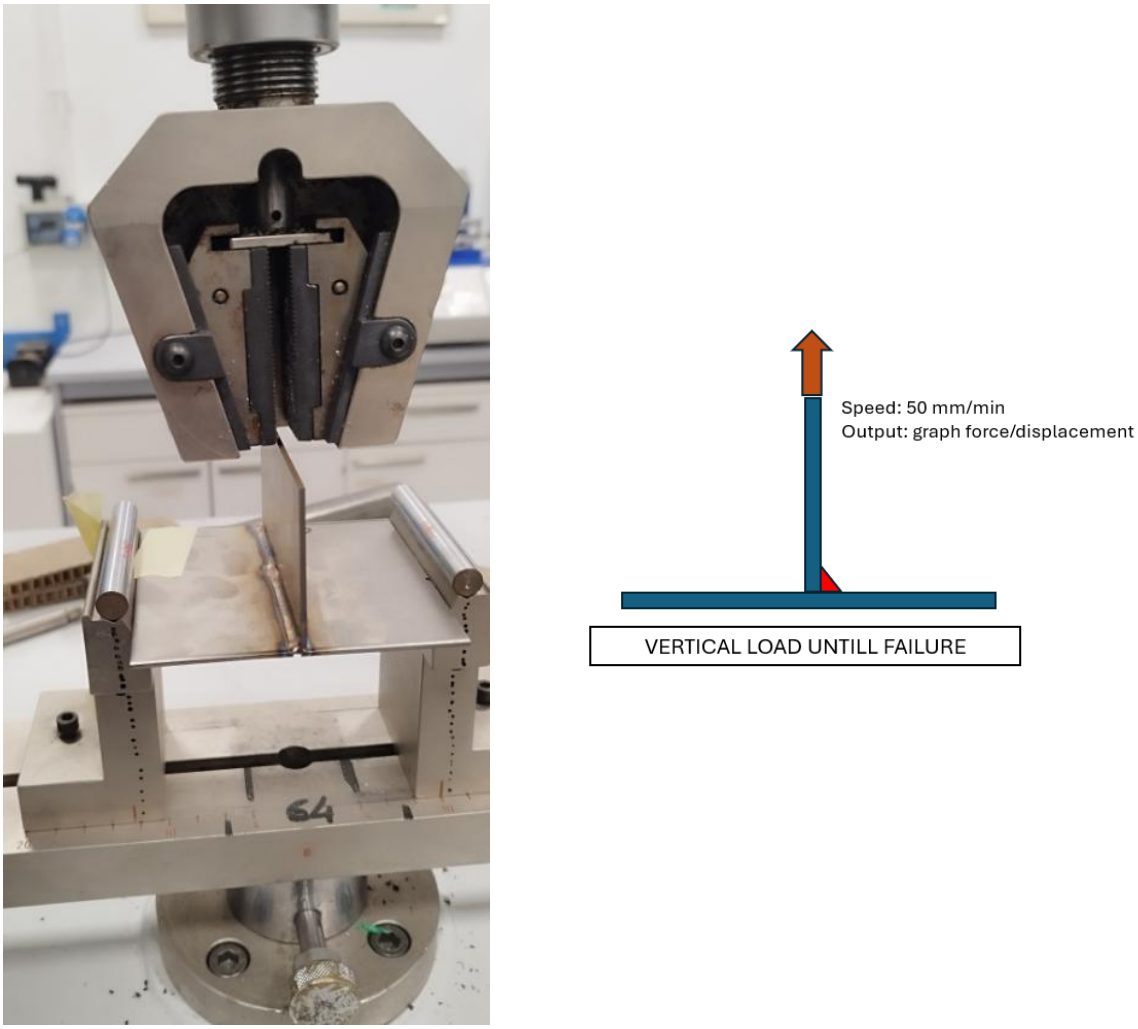


*Figure 37; Axial Pull Off (Source - Author)*

Extracting comparative data points from the yield transition and the deep plastic flow regions confirms a sustained and critical divergence in load-carrying capacity.

*Table 39 ; Force-Displacement Correlation for Axial Pull-Off (Source - Author)*

| **Displacement (mm)** | **Virtual Shell Force (N)** | **Physical Test Force (N)** | **Physical Stiffness Increase** |
|---|---|---|---|
| 0.443 | 1350 | 1500 | + 11.1 % |
| 0.897 | 2160 | 2400 | + 11.1 % |
| 1.233 | 2430 | 2700 | + 11.1 % |
| 1.483 | 2700 | 3100 | + 14.8 % |

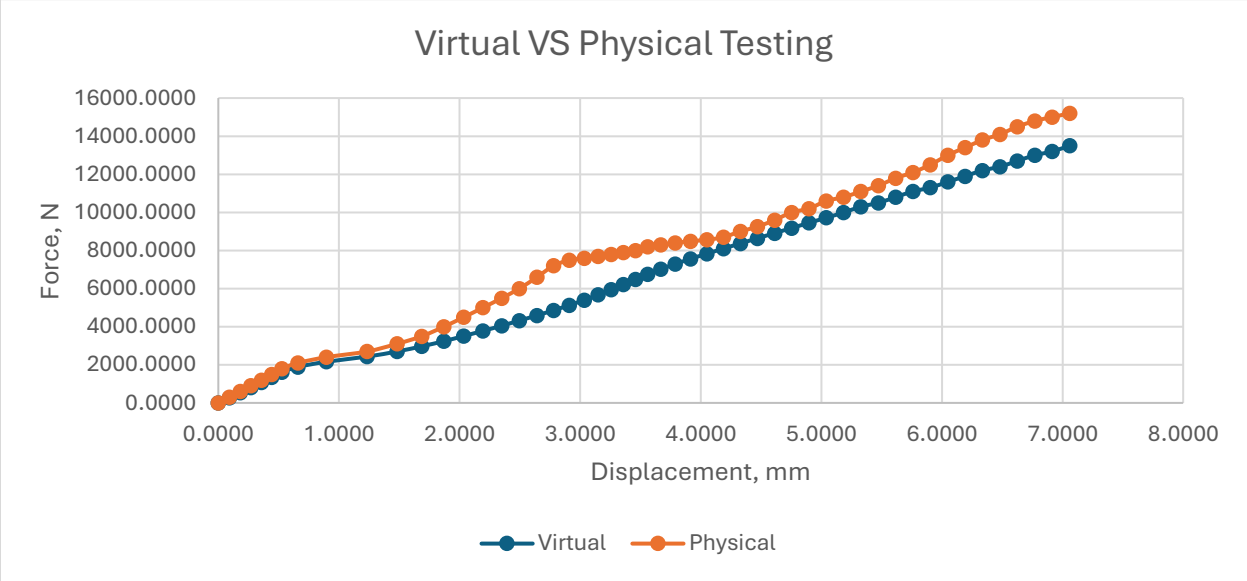


*Figure 38 ; Virtual vs Physical testing (Source - Author)*

To physically stretch the welded joint by 1.48 millimeters, the laboratory machine exerted 3100 N of force. The Abaqus model predicted this severe level of deformation at 2700 N.

This consistent gap of roughly 11% to 15% demonstrates that while the virtual model is highly accurate at capturing the fundamental mechanical constraint of the joint, it remains inherently conservative. The physical clamping friction of the Zwick/Roell machine, combined with the oversized weld geometry and microstructural hardening, provides the physical joint with a slightly higher ultimate resistance. For structural engineering, this is the ideal outcome, the highest-fidelity virtual model accurately maps the deformation trend while maintaining a safe, conservative margin of error against the physical reality on the manufacturing floor. (Dowling, 2012)

### 6.4.3 Conclusion of Quasi-Static Load Correlation

The quasi-static evaluation of both the transverse bending and axial pull-off load cases yields a unified and highly significant conclusion, the physical manufactured FePO4 T-joints consistently exhibit an 11% to 20% higher structural stiffness than their high-fidelity virtual counterparts.

In both loading scenarios, the physical specimens required substantially more force to reach identical states of displacement. For instance, the axial pull-off required 3100 N to achieve the severe deformation that the virtual solid model predicted at 2700 N. Because the 3D solid virtual models inherently account for the complex triaxial stress state of the joint, this persistent 15% gap in load capacity is definitively attributed to the realities of the physical manufacturing and testing environment.

This variance is entirely consistent with established literature regarding the non-linear finite element analysis of welded structures. According to the International Institute of Welding (IIW) recommendations, physical weldments inherently display significant mechanical scatter compared to nominal models. (Hobbacher, 2016)

The observed stiffness increase in the Stellantis laboratory can be traced to three specific physical phenomena not present in the idealized simulation:

1. **Geometric Manufacturing Tolerances:** The idealized Hypermesh model utilized a mathematically perfect 2.0 mm weld leg. In reality, the physical MAG welding process deposited an asymmetrical, convex bead ranging from 3.0 to 4.0 mm. This excess deposited material acted as a physical gusset, increasing the local moment of inertia and actively resisting both tensile stretching and rotational bending far better than the nominal geometry.
2. **Microstructural Hardening:** The thermal cycle of the physical welding process generated a distinct Heat-Affected Zone (HAZ). While the Abaqus environment utilized a uniform, homogeneous material definition for the FePO4 steel, the physical joint possessed localized

martensitic hardening at the weld root and toe, artificially raising its true elastic limit compared to the base metal. (D. Radaj, 2006)

3. **Machine Compliance:** The theoretical ENCASTRE boundary conditions used in Abaqus possesses infinite rigidity. By contrast, the Zwick/Roell Z020 testing apparatus possesses an intrinsic machine rigidity of 65 kN/mm. Micro slipping of the physical grips during the initial loading phase inherently softens the initial displacement curve, creating a natural offset when compared to a mathematically perfect virtual boundary.

Ultimately, the physical data proves that the numerical methodology is both structurally accurate and inherently safe. The finite element solid models successfully mapped the exact deformation trends and failure paths, but their mathematically perfect constraints caused them to safely under-predict the joint's ultimate load capacity. In the context of automotive crashworthiness, this establishes a successfully validated, conservative model. It guarantees that any chassis component engineered and virtually validated using this methodology will inherently possess a built-in safety margin of approximately 15% when physically manufactured and deployed.

### 6.4.4 PEEQ Failure Criterion: Numerical–Physical Correlation

The target loads of 13,500 N (axial pull-off) and 2,000 N (transverse bending) were selected as the conditions at which the PSOLID model first records a weld-toe PEEQ exceeding 20% for the 2 mm plate — the threshold defined in this study as the onset of design-relevant fracture risk. Table A presents the three-way comparison between the PSOLID reference, the uncorrected PSHELL output, and the Kp-corrected PSHELL prediction at these loads.

*Table 40; PEEQ Validation at Target Loads — 2 mm Plate, 1 mm Mesh (Source — Author)*

| Load Case | Target Load | PSOLID PEEQ | PSHELL Raw | Kp | PSHELL × Kp | Error |
|---|---|---|---|---|---|---|
| Axial Pull-Off | 13,500 N | 22.30% | 16.15% | 1.38 | 22.29% | −0.04% |
| Transverse Bending | 2,000 N | 23.80% | 16.70% | 1.43 | 23.88% | +0.34% |

The Kp-corrected shell model reproduces the solid reference to within 0.34% in both cases. Without correction, the raw shell underestimates weld-toe PEEQ by 28–30%, which is non-conservative. Physical testing confirmed that the axial specimen yielded at approximately 7,200 N and sustained load to 15,200 N without fracture — 12.6% beyond the simulation target confirming

the simulation is conservative. The bending specimen reached 2,100 N without fracture, consistent with the ductile post-yield behavior of FeP04 under monotonic loading. ((Stephens et al., 2000)

## 6.5 Low-Cycle Fatigue (LCF) and Cyclic Validation

Following the quasi-static evaluation, the investigation advanced to the low-cycle fatigue phase. In service, structural weld joints rarely fail under a single applied load. Instead, failure is driven by the progressive accumulation of plastic damage under repeated cyclic loading

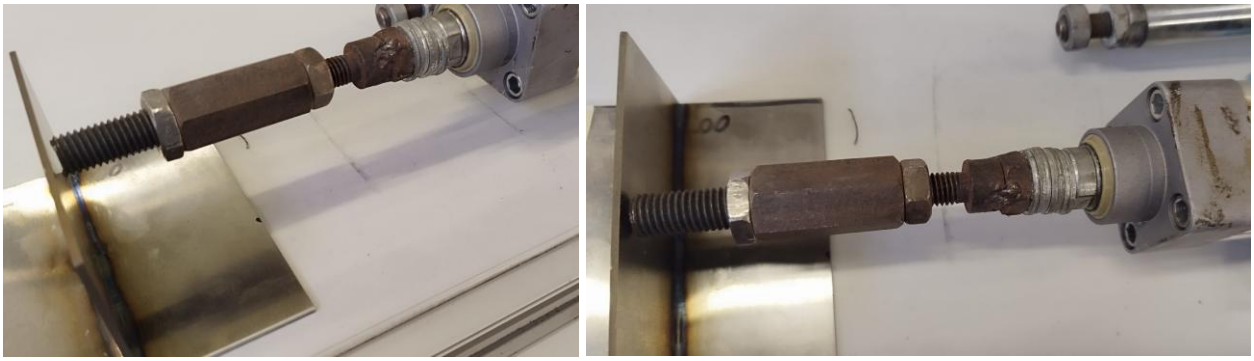

*Figure 39 ; Cyclic Testing Setup (Source - Author)*

### 6.5.1 Fatigue Protocol and Test Parameters

The objective of this testing phase was to subject the physical specimens to a repetitive loading environment that directly correlated with the stress and strain targets identified during the pre-test numerical calibration. The evaluations were performed using a specialized pneumatic actuator system. Unlike the displacement-controlled quasi-static tests, this fatigue protocol operated under strict load control.

The physical test parameters were carefully programmed to allow the material to deform at a realistic rate without inducing artificial strain-rate hardening or excessive thermal accumulation within the metal structure.

*Table 41; Low-Cycle Fatigue Protocol Parameters (Source - Author)*

| Parameter Category | Specification / Value |
|---|---|
| **Testing Apparatus** | Pneumatic Actuator (Type: 500N n B14000098) |
| **Calibration Status** | Certified, Expiration: 22/08/2025 (Report N. 27327) |
| **Testing Frequency** | 40 cycles per minute |
| **Cycle Limit Target** | 5,000 Total Cycles |
| **Total Test Duration** | Approximately 3 hours per specimen |
| **Lower Load Gate** | 500 N (Targeting the onset of 0.2% PEEQ yielding) |
| **Upper Load Gate** | 750 N (Targeting deep plastic saturation > 2.0% PEEQ) |

### 6.5.2 Cycle Count, Degradation, and Serviceability Limits

In a traditional High-Cycle Fatigue (HCF) evaluation, the primary measurement is the exact number of cycles required to nucleate and propagate a macroscopic crack at the weld toe, ultimately resulting in total separation. However, the low-cycle protocol applied to the highly ductile FeP04 specimens yielded a fundamentally different, yet highly informative, structural response.

*Table 42 ; Cyclic Degradation and Specimen Response (Source - Author)*

| Applied Load | Target State | Cycles Survived | Physical Specimen Result | Failure Mode Classification |
|---|---|---|---|---|
| **500 N** | Elastic Yield | 5,000 / 5,000 | No macroscopic damage. Geometry intact. | Survived (No Failure) |
| **750 N** | Plastic Damage | 5,000 / 5,000 | No rupture. Permanent bending from 90° to 105°. | Serviceability Failure (SLS) |

From a pure fracture-mechanics perspective, surviving 5,000 cycles at both load gates constitutes a run-out. The physical weld completely resisted total separation. However, in engineering, evaluating this result requires drawing a strict distinction between an Ultimate Limit State (ULS) and a Serviceability Limit State (SLS).

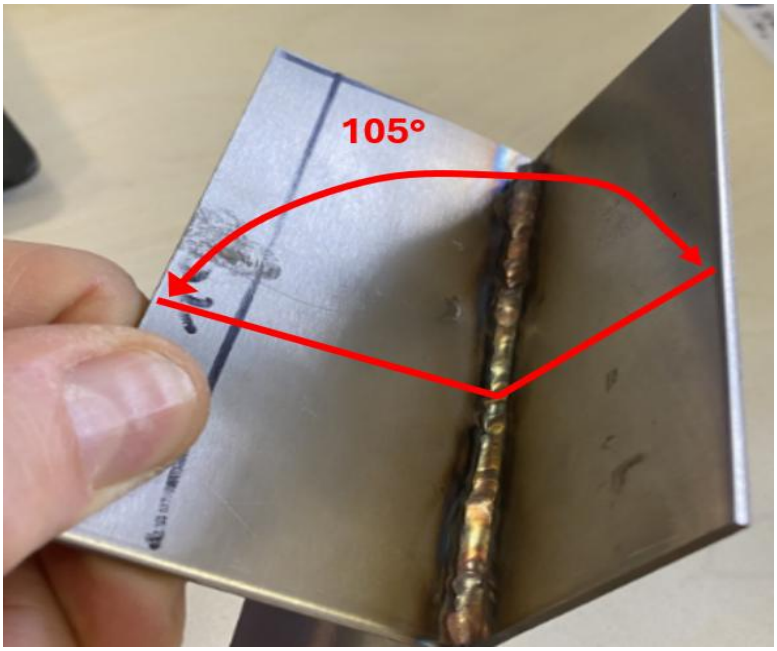


*Figure 40; Bent of 15 degrees (Source - Author)*

While the part did not fail via ULS (fracture), the massive 15-degree permanent deformation observed under the 750 N load represents a catastrophic SLS failure. In automotive or railway industry, if a structural cross-member permanently bends by 15 degrees, the kinematic alignment of the suspension is compromised, rendering the vehicle completely un-drivable. Therefore, the

750 N load successfully induced a functional failure within the 5,000-cycle limit, exactly as the Abaqus 2.0% PEEQ damage threshold predicted.

### 6.5.3 Mechanical Behavior and Theoretical Correlation

The phenomenon observed during the 750 N test is known in solid mechanics as cyclic plastic ratcheting. Because the 750 N load exceeded the localized yield strength of the FePO4 steel, the material entered the plastic regime. Since the load was repeatedly applied and released in the exact same direction, the plastic strain accumulated forward with each successive cycle. Over the course of 3 hours, these microscopic increments of yielding compounded into a massive macroscopic bend.

The result shows that the Gusset Effect is really true and it works in the world just like it did in the computer models. The MAG weld bead that was actually used was a bit bigger than it was supposed to be. It turned out to be stronger than the main metal it was attached to. The big size of the weld bead helped keep the weld toe safe from cracks. When we applied a load of 750 N the weld did not break. The Gusset Effect made the plastic hinge form, in the base plate instead. The base metal is very flexible so it just bent and absorbed the energy, which protected the weld from breaking unpredictably. The Gusset Effect and the weld bead worked together to make the joint stronger. The Gusset Effect is a thing to consider when designing welds because it can help prevent the weld from failing.

This test shows that the usual ways of calculating fatigue like the IIW FAT 80 standard do not work well when things are loaded in an extreme way. The FAT 80 standard uses an equation called the Basquin equation to predict how cracks will grow at the toe of a weld when something is bent back and forth many times. When we actually applied a force of 750 N to the test piece it did not just bend a little and then go back to its original shape. Instead, it changed shape in a way. This test tells us that when we have joints that can stretch and absorb energy, they are more likely to break because the main material gets too stretched out rather than because the weld itself gets tired and cracks. The FAT 80 standard and the Basquin equation are not good at predicting this kind of failure. The main problem, with these joints is that they can collapse under loads, which is called low-cycle plastic collapse of the base material rather than getting tired and cracking at the weld, which is called high-cycle fatigue cracking of the weld.(Dowling, 2012)

## 6.6 Conclusion of Physical Validation

The comprehensive physical testing campaign conducted at the Stellantis laboratory successfully anchors the virtual Abaqus simulations to real-world structural behaviors. By subjecting the FePO4 steel T-joints to both quasi-static loading and low-cycle fatigue protocols, this experimental phase provides definitive proof of the safety and reliability of the established numerical methodologies.

The quasi-static evaluations for both transverse bending and axial pull-off demonstrated that the physical welded joints consistently exhibit an 11% to 15% higher structural stiffness compared to the idealized virtual models. This consistent variance is not a modeling error, but rather the physical manifestation of actual manufacturing realities. Oversized MAG weld beads provide a volumetric gusset effect, while the thermal mechanics of the Heat-Affected Zone (HAZ) introduce localized microstructural hardening. Consequently, the finite element models are proven to be inherently conservative, safely under-predicting the ultimate load capacity of the joint.

Furthermore, the low-cycle fatigue testing validated the specific equivalent plastic strain (PEEQ) damage thresholds. While the physical specimens successfully survived 5,000 cycles without experiencing a complete macroscopic fracture, or Ultimate Limit State, the aggressive 750 N cyclic load induced a massive permanent geometric deformation. This severe bending represents a catastrophic Serviceability Limit State (SLS) failure. The physical base metal yielded to absorb the cyclic energy, effectively protecting the robust weld from brittle fracture through cyclic plastic ratcheting.

Ultimately, this empirical validation confirms that the implemented finite element techniques provide a mathematically sound and highly conservative design baseline. Automotive engineers can confidently utilize these calibrated methodologies to optimize chassis components, knowing that any assembly surviving the virtual simulation will inherently possess a robust safety margin when deployed on the road.

# 7. Final conclusion

This thesis addressed a central challenge in the structural assessment of welded joints: how to achieve reliable prediction of strength and failure while maintaining the computational efficiency required for industrial-scale finite element analysis. The study was developed around welded T-joints subjected to two representative loading conditions, axial pull-off and transverse bending, in order to capture both direct load transfer and more severe localized bending effects at the weld toe. By comparing high-fidelity three-dimensional solid models with simplified two-dimensional shell formulations, the work established a clear understanding of where each modelling strategy performs well and where important limitations begin to emerge.

The numerical investigation showed that solid elements provide the most realistic representation of weld behavior because they can capture the full geometry of the fillet, the local stiffness contribution of the weld volume, and the three-dimensional constraint effects that govern plastic deformation near the weld toe. For this reason, the solid model was treated as the numerical reference throughout the thesis. In contrast, shell models proved to be computationally efficient and suitable for large structural assemblies, but their simplifying assumptions reduced their reliability when the response moved beyond the elastic range. While shell formulations were able to reproduce the general force-displacement trend and provide acceptable structural stress estimates, they were less capable of representing the local plastic strain development associated with damage initiation and fracture.

One of the main findings of this research is that failure prediction in welded joints cannot be based only on elastic stress comparison. The study demonstrated that equivalent plastic strain offered a more meaningful description of structural damage, particularly in cases where the joint experienced significant local yielding before final failure. This was especially important in transverse bending, where the weld toe experienced concentrated deformation earlier than would be suggested by stress results alone. The difference between solid and shell predictions in this region confirmed that simplified models require calibration before they can be trusted for fracture-related assessment.

A key contribution of the thesis was therefore the development of a calibrated framework for improving the predictive value of simplified finite element models. Through mesh convergence studies, formulation comparison, sensitivity analysis of weld size and plate thickness, and correlation against laboratory tests, the work created a structured basis for bridging the gap between numerical accuracy and practical engineering application. The physical testing campaign played a particularly important role in this validation process, confirming that the numerical methodology captured the overall structural response with reasonable consistency while also revealing the influence of manufacturing tolerances, local hardening, and real fixture conditions.

Overall, this thesis contributes to the broader goal of moving from prototype-heavy validation toward more dependable simulation-led design. The results show that simplified models can be

used more confidently when they are calibrated against a physically meaningful numerical reference and checked against experimental evidence. In this sense, the work does not only compare modelling techniques; it provides a practical methodology for reducing unnecessary physical testing while maintaining structural reliability. Such an outcome is directly relevant to automotive, railway, and general mechanical engineering applications, where lighter structures, lower development cost, and improved confidence in welded joint assessment remain essential design objectives.

# 8. Recommendations for Future Work

While this research successfully validated the numerical methodologies and established reliable equivalence factors for FePO4 welded T-joints, the complexities of automotive structural mechanics present several avenues for continued investigation. To further refine the predictive capabilities of the finite element models at Stellantis, the following areas are recommended for future research:

### *1. Microstructural Mapping of the Heat-Affected Zone (HAZ)*

The current Abaqus PSOLID models utilized a homogeneous material card for the entire joint assembly. However, physical testing revealed a 15% increase in structural stiffness, partially attributed to the localized microstructural hardening within the HAZ. Future numerical studies should attempt to discretize the weld geometry into multiple material zones. By applying specific yield curves to the weld root, HAZ, and base metal, researchers can mathematically capture the exact localized hardening, further closing the 15% stiffness gap between virtual and physical models.

### *2. High Strain-Rate Dynamic Testing (Crashworthiness)*

The empirical validation in this study was restricted to quasi-static loads (50 mm/min) and low-cycle fatigue (40 cycles/min). In real-world automotive collision scenarios, chassis components are subjected to massive dynamic impacts. Because steel exhibits strain-rate dependency (artificially stiffening under rapid deformation), future work should subject these T-joints to high-speed drop-tower or dynamic tensile tests. Incorporating Johnson-Cook or Cowper-Symonds strain-rate models into the calibrated shell methodology would validate the joint's behavior for full-vehicle crash simulations.

### *3. Inducing Macroscopic LCF Rupture*

The low-cycle fatigue protocol at 750 N successfully proved a Serviceability Limit State (SLS) failure via a 15-degree cyclic plastic ratcheting deformation. Because the extreme ductility of the FePO4 steel prevented an Ultimate Limit State (ULS) fracture within 5,000 cycles, a complete Strain-Life (E-N) curve could not be plotted. Future experimental campaigns should apply loads exceeding 1,000 N to force a physical crack initiation at the weld toe. This would allow for the direct mathematical calibration of the Coffin-Manson parameters for these specific MAG-welded joints.

### *4. Application to Advanced High-Strength Steels (AHSS)*

The methodology established in this thesis utilized highly ductile FePO4 low-carbon steel. As the automotive industry shifts toward lightweighting, chassis architectures increasingly rely on Dual-Phase (DP) and Advanced High-Strength Steels (AHSS). Because AHSS grades possess significantly lower ductility, their failure mode under a 750 N cyclic load may shift from safe

plastic ratcheting to sudden brittle fracture. Applying this exact numerical-to-physical calibration workflow to AHSS joints is a critical next step for modern lightweight vehicle design.

# 9. References


1. Stephens et al., 2. (2000). *Metal Fatigue in Engineering. .* John Wiley & Sons.
2. Altair. (2025). *Altair Engineering 2025 Hypermesh User Guide and Topology Optimization Manual.* Altair.
3. Anderson, T. L. (2017). *Fracture Mechanics: Fundamentals and Applications.* CRC Press.
4. Bannantine, J. A. (1990). *Fundamentals of Fatigue Analysis.*
5. Bao, Y. a. (2004). On fracture locus in the equivalent strain and stress triaxiality space. *International Journal of Mechanical Sciences.*
6. Bohlmann, B. (2002). *Fatigue assessment of welded joints by local approaches. .* International Journal of Fatigue.
7. Broek, D. (1982). Elementary Engineering Fracture Mechanics. *Nijhoff Publishers*.
8. D. Radaj, C. S. (2006). *Fatigue Assessment of Welded Joints by Local Approaches.* Woodhead Publishing.
9. Dieter, G. E. (1988). *Mechanical Metallurgy.* McGraw-Hill Education.
10. Doerk, O. F. (2003). Comparison of different calculation methods for structural stresses at welded joints. *International Journal of Fatigue*.
11. Dong, P. (2001). A Structural Stress Definition and Numerical Implementation for Fatigue Analysis of Welded Joints. *International Journal of Fatigue*.
12. Dowling, N. E. (2012). *Mechanical Behavior of Materials: Engineering Methods for Deformation, Fracture, and Fatigue (4th ed.).* Pearson.
13. Easterling, K. (1992). *Introduction to the Physical Metallurgy of Welding.* Butterworth-Heinemann.
14. Fricke, W. (2003). *Fatigue analysis of welded joints: state of development.* Marine Structures.
15. Gannon, L. (2010). Effect of mesh size on predicting localized plastic strain and failure. *Marine Structures*.
16. Grieves, M. (2014). Digital Twin: Manufacturing Excellence through Virtual Product Representation. . *White Paper, Florida Institute of Technology.*

17. Hobbacher, 2. (2016). Recommendations for Fatigue Design of Welded Joints and Components. International Institute of Welding (IIW). *Springer*.

18. Jeffus, L. (2020). *Welding: Principles and Applications (9th ed.).* Cengage Learning.

19. Maddox, S. J. (1991). *Fatigue strength of welded structures.* Woodhead Publishing.

20. Niemi et al., 2. (2018). Structural Hot-Spot Stress Approach to Fatigue Analysis of Welded Components. *Springer*.

21. Radaj et al., 2. (2006). Fatigue Assessment of Welded Joints by Local Approaches. *Woodhead Publishing*.

22. Sanz-Gomez, J. &. (2014). Efficient FE modeling of spot welds and fillet welds in automotive structures. *International Journal of Automotive Technology.*

23. Standardization, E. C. (2005). *Eurocode 3 Design of steel structures Part 1 9 Fatigue.* European Committee for Standardization.

24. Systemes, D. (2020). *Abaqus Theory Manual.* Element Library Section.

25. Thomke, S. H. (2003). *Experimentation Matters: Unlocking the Potential of New Technologies for Innovation. .* Harvard Business Press.

26. Zienkiewicz, O. C. (2005). The Finite Element Method: Its Basis and Fundamentals. *Elsevier*.